



Review article

Understanding the cellular dynamics, engineering perspectives and translation prospects in bioprinting epithelial tissues

Irem Deniz Derman^{a,b,1}, Joseph Christakiran Moses^{a,b,1}, Taino Rivera^c,
Ibrahim T. Ozbolat^{a,b,c,d,e,f,g,*}

^a Engineering Science and Mechanics Department, Penn State University, University Park, PA, 16802, USA

^b The Huck Institutes of the Life Sciences, Penn State University, University Park, PA, 16802, USA

^c Biomedical Engineering Department, Penn State University, University Park, PA, 16802, USA

^d Materials Research Institute, Penn State University, University Park, PA, 16802, USA

^e Cancer Institute, Penn State University, University Park, PA, 16802, USA

^f Neurosurgery Department, Penn State University, University Park, PA, 16802, USA

^g Department of Medical Oncology, Cukurova University, Adana, 01330, Turkey

ARTICLE INFO

Keywords:

3D bioprinting

3D *in vitro* models

Engineered epithelium

In vitro disease modeling

ABSTRACT

The epithelium is one of the important tissues in the body as it plays a crucial barrier role serving as a gateway into and out of the body. Most organs in the body contain an epithelial tissue component, where the tightly connected, organ-specific epithelial cells organize into cysts, invaginations, or tubules, thereby performing distinct to endocrine or exocrine secretory functions. Despite the significance of epithelium, engineering functional epithelium *in vitro* has remained a challenge due to its special architecture, heterotypic composition of epithelial tissues, and most importantly, difficulty in attaining the apico-basal and planar polarity of epithelial cells. Bioprinting has brought a paradigm shift in fabricating such apico-basal polarized tissues. In this review, we provide an overview of epithelial tissues and provide insights on recapitulating their cellular arrangement and polarization to achieve epithelial function. We describe the different bioprinting techniques that have been successful in engineering polarized epithelium, which can serve as *in vitro* models for understanding homeostasis and studying diseased conditions. We also discuss the different attempts that have been investigated to study these 3D bioprinted engineered epithelium for preclinical use. Finally, we highlight the challenges and the opportunities that need to be addressed for translation of 3D bioprinted epithelial tissues towards paving way for personalized healthcare in the future.

1. Introduction

The epithelium plays a crucial role in maintaining the structural integrity and physiological equilibrium of various organs in the human body. In addition to its barrier function, epithelium also executes endocrine and exocrine functions. For example, squamous epithelial cells aid in diffusion and transport processes in tissues such as the skin (Fig. 1Ai), blood vessels, and cornea (Fig. 1Aii) [1–5]. Columnar epithelial cells form the endometrial epithelium (Fig. 1B), which is crucial for embryo implantation and pregnancy maintenance by creating a receptive environment within the uterine lining [6]. These cells also

line the gastrointestinal (GI) tract, where they contribute to nutrient absorption and fluid secretion (Fig. 1C) [7–10]. Cuboidal epithelial cells in glandular tissues and kidney tubules are involved in secretion, absorption, and filtration (Fig. 1D) [11–13]. Pseudostratified epithelial cells, commonly found in the respiratory tract, assist in mucociliary clearance and pathogen defense (Fig. 1E) [14–17]. The unique morphological features and molecular characteristics of these epithelial cell types are closely related to their specific functions. Typically, epithelium is observed as an organized single, stratified, or multiple layers of cells over a basement membrane and a specific orientation or polarity is essential for its function. The basement membrane is formed

Peer review under responsibility of KeAi Communications Co., Ltd.

* Corresponding author. Engineering Science and Mechanics Department, Penn State University, University Park, PA, 16802, USA.

E-mail address: ito1@psu.edu (I.T. Ozbolat).

¹ Authors contributed equally.

<https://doi.org/10.1016/j.bioactmat.2024.09.025>

Received 15 July 2024; Received in revised form 4 September 2024; Accepted 18 September 2024

2452-199X/© 2024 The Authors. Publishing services by Elsevier B.V. on behalf of KeAi Communications Co. Ltd. This is an open access article under the CC BY-NC-ND license (<http://creativecommons.org/licenses/by-nc-nd/4.0/>).

by maturing epithelia, which is an acellular connective scaffolding on which the epithelial cells rest on an apical-basal polarity [18]. The basement membrane also aids in selective filtering of nutrients and waste. In multi-layered epithelia, the types of apical cells—like columnar in the GI and cuboidal in the kidney—are specialized for absorption or secretion, whereas squamous cells in the respiratory tract are adapted for diffusion and filtration [19]. Pseudostratified epithelial cells

with ciliated surfaces maintain respiratory health by clearing mucus and debris from airways [14,20]. Therefore, it is essential to understand epithelial cell biology and its diverse functions, as well as the specialized roles of squamous, cuboidal, columnar, and pseudostratified epithelial cells in supporting tissue homeostasis and physiological functions of various organs to reconstitute this tissue specific epithelium.

Bioprinting has emerged as a revolutionary technology in tissue

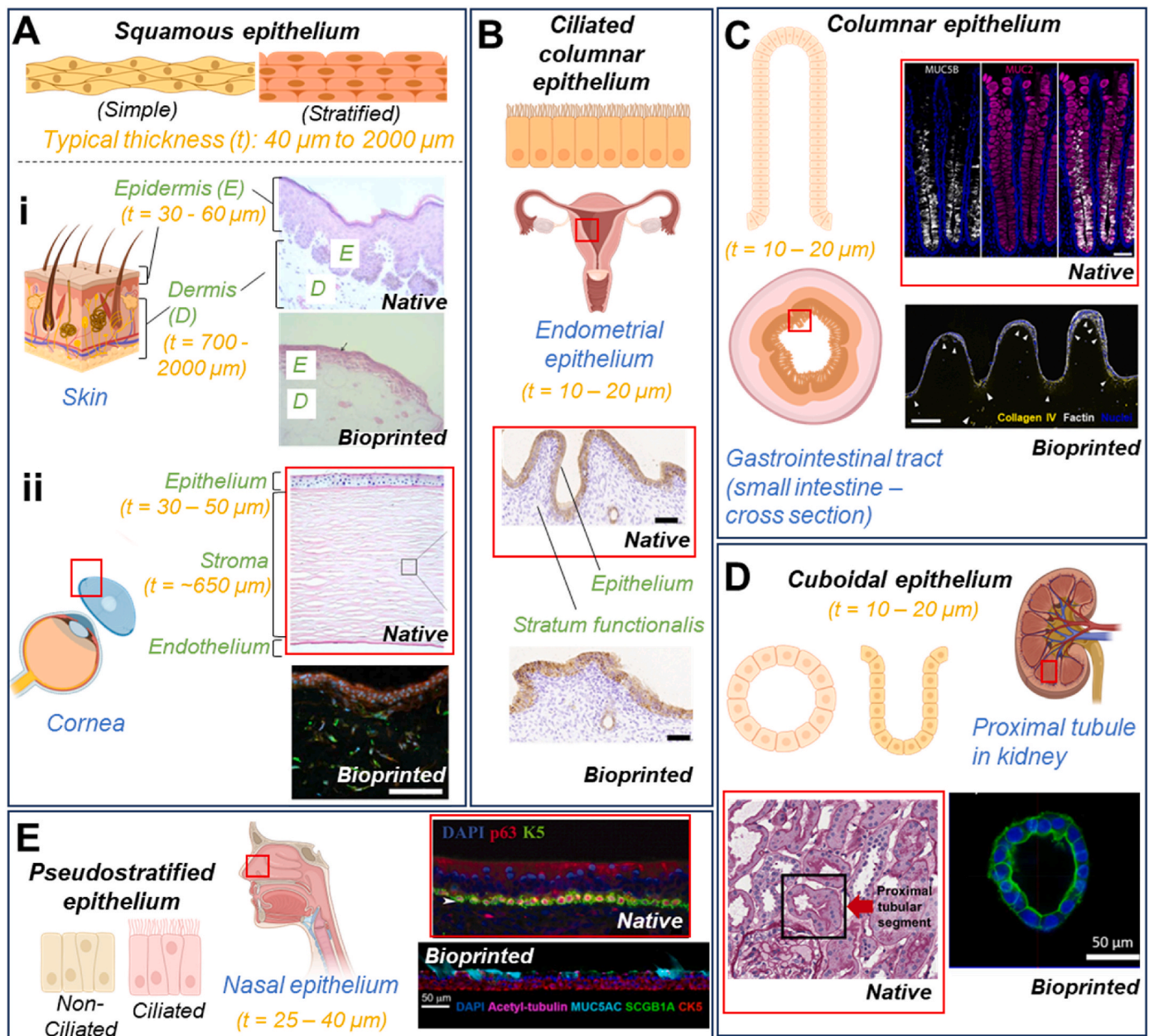


Fig. 1. Overview of the different types of epithelia with their typical thickness (t) and their associated organs which they make up, in reference to the native human epithelial architecture as compared to the 3D bioprinted epithelium. **A)** Squamous epithelium (simple or stratified), which make up the integumentary epithelium noticed in the i) skin, comprising of the epidermis and dermis as seen in the native skin and bioprinted skin (reproduced with permission from Ref. [4] 2024 Informa UK Limited), ii) cornea, comprising of the epithelium, stroma in the native cornea (reproduced with permission from Ref. [3] 2020 MDPI), and bioprinted corneal epithelium (reproduced with permission from Ref. [5] 2024 IOP Publishing). **B)** Ciliated columnar epithelium noticed in urothelium, here shown in reference to endometrial lining consisting of ciliated epithelia and underlying stratum functionalis in the native and bioprinted endometrium (reproduced with permission from Ref. [6] 2024 Elsevier). **C)** Columnar epithelium noticed in the inner lining of the native gastrointestinal tract (reproduced with permission from Ref. [9] 2024 Elsevier) and the bioprinted counterpart (reproduced with permission from Ref. [10] 2024 Elsevier). **D)** cuboidal epithelium noticed in native proximal tubule in kidney cortex (reproduced with permission from Ref. [13] 2024 Elsevier) and bioprinted proximal tubule in kidney cortex (reproduced with permission from Ref. [12] 2024 IOP Publishing). **E)** Pseudostratified epithelium noticed in the upper airway tract, as seen in the native and bioprinted nasal epithelium (images reproduced with permission from Ref. [16] 1999–2024 John Wiley and [17] 2024 IOP Publishing, respectively). Illustrations were prepared using Biorender.com.

engineering and regenerative medicine, offering unprecedented opportunities to fabricate physiologically and anatomically relevant tissues and organs [21,22]. The ability to precisely deposit cells, biomaterials, and bioactive factors in a layer-by-layer manner has opened new avenues for the creation of intricate structures that mimic native tissues. This technology holds immense promise for the development of epithelial tissues, offering researchers the possibility to replicate the microarchitecture and functionality of various epithelial structures. Bioprinting techniques can be classified into four major modalities, including extrusion-based bioprinting (EBB), droplet-based bioprinting (DBB), laser-assisted bioprinting (LaBB), and light-based bioprinting (LiBB), each offer unique advantages and distinct challenges, especially when applied to the reconstitution of epithelial tissues [23–25]. EBB employs extrusion forces to precisely deposit bioinks containing living cells onto a substrate, making it particularly valuable in tissue engineering (Fig. 2A.) This modality uses a mechanical or a pneumatic system to expel a bioink through a nozzle, forming continuous filaments that can be precisely layered [23]. EBB is capable of depositing multiple bioinks within a single construct, allowing for varied compositions (i.e. cell types, densities, and signaling molecules), which is essential for mimicking the complex architecture of epithelial tissues [26]. EBB's unique advantages include: i) the ability to bioprint in high-cell density; ii) feasibility to use multi-material and multiple cell types by virtues of its modularity with multiple nozzle systems. Furthermore, EBB's scalability makes it feasible to produce large tissue constructs necessary for functional replacements, such as full-thickness skin grafts or large organ linings [27]. However, the shear stress experienced by cells during the extrusion process can impair their viability and function [28]. In this regard, hydrogels utilizing specialized chemistry to minimize shear stress on cells have been explored. Recent innovations in EBB have introduced nanoengineered granular bioinks (NGB) that preserve interconnected microporosity during extrusion, which significantly reduces shear stress-induced damage to cells [29]. The use of NGBs helps to impart interconnected microporosity during extrusion, which reduces shear-stress induced damage to cells. These NGB bioinks leverage dynamic bonding between microgels, enabling smoother extrusion and maintaining cell viability by minimizing the mechanical stress exerted during the process. This approach overcomes a significant limitation in traditional EBB, where increased viscosity often leads to high shear stress and lower cell viability [30,31]. By maintaining the porous structure during and after extrusion, NGBs also enhance nutrient and oxygen diffusion, which is critical for sustaining cell viability in densely packed tissues [29]. Moreover, the use of shear-thinning materials and optimized nozzle designs in EBB further reduces the mechanical forces acting on cells [32,33]. Studies have shown that using nozzles with specific inner diameters and tapering profiles can decrease the extrusion pressure required, thereby lowering the shear stress experienced by cells [29,34,35]. Additionally, innovations such as the introduction of sacrificial materials or support baths during bioprinting have further mitigated the risks of cell damage by providing mechanical support to the printed structures, thereby reducing the extrusion force needed and enhancing cell viability [36,37]. However, the shear stress experienced by cells during the extrusion process can impair their viability and function [28]. This challenge is being addressed not only through advancements in nozzle design and extrusion techniques but also by the development of hydrogels with shear-thinning properties [38]. These hydrogels, such as those incorporating dual-cross-linking strategies, enable a reduction in viscosity during extrusion while rapidly recovering mechanical integrity after deposition, thereby minimizing cellular damage [39]. Additionally, shear-thinning hydrogels like those based on hyaluronic acid, which exhibit both guest-host and covalent cross-linking, further enhance the bioprinting process by maintaining high cell viability and allowing for the fabrication of stable, multi-layered structures [40]. Despite its limitations, EBB remains accessible and user-friendly, making it suitable for beginners and experts alike, thus playing a crucial role in advancing tissue engineering

applications.

DBB utilizes gravity, atmospheric pressure, and fluid mechanics to produce bioink droplets (Fig. 2B) [41]. This modality can be divided into continuous inkjet and drop-on-demand methods. Continuous inkjet bioprinting generates droplets continuously, regardless of a need, which requires a recovery device to minimize material waste [42]. However, this recovery process can introduce contamination, making continuous inkjet less suitable for high precision bioprinting applications. In contrast, drop-on-demand bioprinting releases bioink droplets only when needed, offering precise control over the bioink delivery. This method involves the use of thermal, piezoelectric, or electrostatic actuators to create pressure pulses that expel droplets from the nozzle when the bioink overcomes surface tension [43]. DBB reduces shear stress on cells, improving their viability and function, which is crucial for maintaining the integrity of delicate epithelial cells [44,45]. Other factors which influence the cell deposition and viability in DBB are droplet impact velocity, droplet volume, and bioink properties [46,47]. Studies have shown that higher droplet impact velocities can cause significant cell deformation and reduced cell viability [47]. However, increasing the viscosity and viscoelasticity of the bioink can mitigate these effects by providing a cushioning effect during droplet impact as the polymer component of the bioink helps to dissipate energy more effectively [46,48]. Additionally, optimizing droplet volume is crucial for maintaining cell viability, as smaller droplets are prone to evaporation, leading to a hypertonic environment that can induce cell apoptosis [49,50]. A minimum volume of 20 nL per droplet has been recommended to minimize evaporation-induced damage and maintain high cell viability during bioprinting [47]. Additionally, DBB's high-throughput capabilities enable quick development and iteration of tissue constructs, accelerating the biofabrication process. Its versatility with different bioinks and cell types enhances its applicability across various bioprinting needs, making it a valuable tool for both research and translational applications.

LaBB uses a pulsed laser to deposit the bioink onto a substrate with exceptional precision (Fig. 2C) [54]. This technique involves a laser-induced forward transfer process, where a focused laser pulse propels a small volume of the bioink from a donor ribbon to a receiver substrate [55]. LaBB's precision allows for the placement of a single cell per droplet, which is beneficial for constructing complex tissue structures that require high-precision cellular arrangements. The non-contact nature of this method minimizes the risk of contamination and cell damage, ensuring high-quality tissue constructs. However, LaBB faces significant challenges, including high costs, stability, and scalability [56]. These challenges stem from the need for sophisticated laser systems and precise control mechanisms, which can be expensive and complex to maintain. Despite these drawbacks, integrating LaBB with other biofabrication approaches could expand its applications, making it a promising tool (i.e., two-photon polymerization [57]) in bioprinting. For example, combining LaBB with other methods can enhance the precision and scalability of tissue constructs, potentially leading to breakthroughs in regenerative medicine.

LiBB employs light to selectively solidify a bioink, utilizing techniques such as stereolithography (SLA), digital light processing (DLP), and volumetric bioprinting (VBP) [58–60]. These methods use ultraviolet (UV) or alternative light sources to initiate the polymerization of the bioink based on computer-aided designs, enabling the creation of highly detailed and complex 3D structures (Fig. 2D) [61,62]. SLA involves using a laser beam to cure an the photosensitive bioink layer by layer, offering significant flexibility for applications like insulin delivery devices or intricate tissue scaffolds [62]. DLP, on the other hand, uses a digital light projector to cure entire layer at once, providing high resolution and rapid curing capabilities that are ideal for tissue regeneration [63]. The photocurable polymer usually consist of end-functionalized groups (such as acrylate, methacrylate, thiol or vinyl ether), which undergo free-radical chain extension or photo-click or photo-mediated redox or photodimerization reactions in the presence of radical

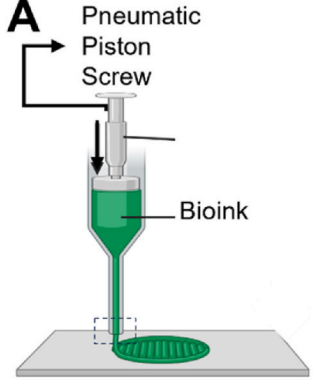
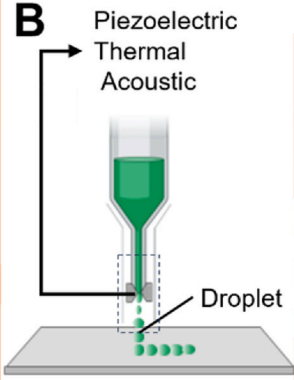
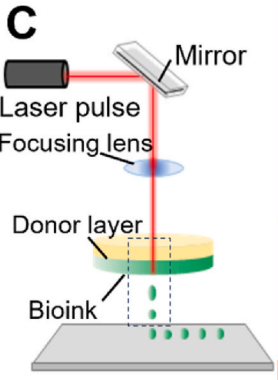
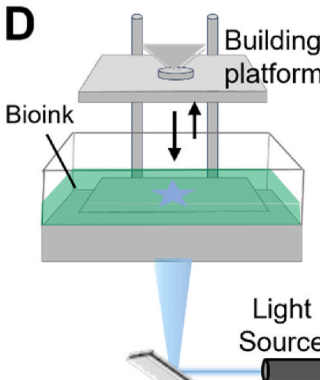
EBB	DBB	LaBB	LiBB
<p>A</p>  <p>Pneumatic Piston Screw</p> <p>Bioink</p> <p>Extruded filaments With low cell density</p> <p>With high cell density</p>	<p>B</p>  <p>Piezoelectric Thermal Acoustic</p> <p>Droplet</p> <p>Piezoelectric actuation</p> <p>Ejected droplet</p>	<p>C</p>  <p>Mirror</p> <p>Laser pulse Focusing lens</p> <p>Donor layer</p> <p>Bioink</p> <p>Laser pulse</p> <p>Energy absorbing layer</p> <p>Bioink with cells</p> <p>Droplet</p>	<p>D</p>  <p>Building platform</p> <p>Bioink</p> <p>Light Source</p> <p>Photo-crosslinked gel with cells</p> <p>Projected light</p> <p>Uncrosslinked bioink with cells</p>
<p>Resolution</p> <p>100 – 500 μm</p> <p>Resolution depends upon bioink properties and nozzle diameter</p>	<p>20 – 50 μm</p> <p>Resolution depends upon bioink properties and nozzle diameter</p>	<p>10 – 50 μm</p> <p>Resolution depends upon laser spot size, bioink properties, substrate (donor layer) properties and laser parameters</p>	<p>10 – 100 μm</p> <p>Resolution depends upon photo-curable polymer, photo-initiator system, photo-absorber and light curing modality</p>
<p>Spatial organization</p> <p>Can support multimaterial/multiple bioink (multiple printheads) with different cell types encapsulated to fabricate thicker tissues</p>	<p>Higher precision to control cell density and different cell types placement</p>	<p>Capable of achieving near single cell level precision and precise control of cell density and organization</p>	<p>Capable of creating complex structures; however, not feasible to incorporate multiple cell types within bioprinted constructs</p>
<p>Barrier quality</p> <p>Well suited for fabricating thicker epithelial tissues (skin, corneal epithelium). Bioprinted constructs need to mature in vitro before cell-cell interaction is achieved to form an intact barrier</p>	<p>Epithelial tissues fabricated using DBB or LaBB bioprinters, generally exhibit good barrier quality (functional – with selective permeability). Better precision and spatial organization enables rapid tight junction formation. Examples include the bioprinted upper respiratory tract epithelium</p>		<p>Although capable of replicating intricate designs, achieving uniform cell density within photocured polymer network is difficult and hence needs maturation in vitro for barrier integrity. Examples include the intestinal epithelium.</p>

Fig. 2. Different bioprinting techniques that have been explored for fabricating epithelial tissues: A) EBB, B) DBB, C) LaBB, and D) LiBB, with schematics depicting cells within bioinks. A few key aspects, such as resolution, spatial organization and barrier integrity, which are crucial in bioprinted epithelium are also compared among different bioprinting techniques [51–53]. Illustrations were prepared using Biorender.com.

photo-initiators, namely Norrish type-I or type II. Type I radical photo-initiators are cleavable, and some examples are benzoin and acetophenone derivatives, while type-II radical photo-initiators are hydrogen abstractable and some examples are benzophenone, 2-isopropylthioxanthone and 4-methylbenzophenone [64,65]. The choice of photo-initiators (PIs) and their concentration are crucial factors that influence the efficiency of the polymerization process and the viability of embedded cells [66]. For instance, water-soluble PIs like Irgacure 2959 and lithium phenyl-2,4,6-trimethylbenzoylphosphinate (LAP) are commonly used in VBP due to their high efficiency under hydrophilic conditions and relatively low cytotoxicity [25,67]. The concentration of these PIs must be carefully optimized; too low a concentration can result in insufficient cross-linking, while too high a concentration can lead to excessive free radical formation, which can damage cells [66,68,69]. UV wavelength and intensity used in SLA can also have a significant impact on cell viability [70]. Shorter wavelengths (e.g., UVB: 280–320 nm, UVC: 200–280 nm) possess higher energy, which can cause severe DNA damage [71,72]. Therefore, longer wavelengths in the UVA range (320–400 nm) or even visible light (around 405 nm) are often preferred to reduce cellular damage while still achieving effective polymerization [73]. Additionally, the intensity and exposure time of the light source must be optimized to balance efficient curing with cell viability [74]. Excessive exposure or high intensity can lead to overheating and cell death, while insufficient light energy can result in incomplete curing and weak structural integrity of bioprinted constructs [75,76]. In this context, the rapid curing process of VBP, combined with the use of visible light, has been shown to maintain higher cell viability compared to UV-based methods, further highlighting the importance of selecting appropriate light sources and conditions for bioprinting [25,61]. VBP builds constructs within seconds using visible light, demonstrating high biocompatibility and the potential for creating large-scale tissue constructs in a short time frame [58]. Overall, LiBB's advantages include its precision, versatility, and high resolution, allowing for the meticulous reconstruction of complex 3D structures [77]. However, challenges such as potential cell damage from prolonged light exposure and a limited selection of bioinks responsive to photopolymerization must be addressed [76]. Additionally, achieving scalability for larger tissues and organs remains a significant hurdle. Ongoing research focuses on refining LiBB techniques, developing new photopolymerizable bioinks, and improving light delivery systems to enhance cell viability and overall bioprinting efficiency.

In the context of epithelial tissue bioprinting, EBB is particularly effective for fabricating large-scale epithelial tissue constructs, developing organ-on-a-chip systems, and modeling tissue environments for drug testing and toxicity screening. Its compatibility with a wide range of bioinks allows for scaffold-free bioprinting (i.e., with the use of tissue spheroids) and facilitates vascularization. However, EBB can cause substantial cell damage due to shear stress, has limited resolution, and is not ideal for high-throughput models. DBB excels in high-speed bioprinting and high resolution, making it ideal for creating high-throughput epithelial cell arrays, detailed microarrays for drug testing, and organ-on-a-chip models for *in vitro* studies. Its challenges include droplet size inconsistency, difficulty in single-cell encapsulation, nozzle clogging at high cell densities, and cross-contamination risks with multiple bioinks. LaBB is known for its high resolution and minimal cell damage, making it suitable for creating high precision, intricate epithelial tissue models, engineering detailed tissue structures for regenerative medicine, and developing complex tissue constructs with minimal cell damage. Despite these advantages, LaBB is labor-intensive, time-consuming, costly, and has limited commercial availability, making it impractical for heterocellular models. LiBB offers extremely high resolution and rapid bioprinting, especially for large constructs. It is useful for fabricating detailed and complex epithelial tissue architectures, developing high-resolution tissue models for *in vitro* testing, and maintaining cell viability in intricate constructs. However, LiBB is limited to photo-crosslinkable bioinks, poses UV light exposure risks to

cells, and involves expensive equipment and materials. Each bioprinting method, with its unique strengths and limitations, plays a crucial role in advancing the field of epithelial tissue engineering.

Together, these bioprinting modalities offer a comprehensive toolkit for advancing tissue engineering, particularly in developing functional epithelial tissues. EBB's scalability and versatility, DBB's precision and high-throughput capability, LaBB's accuracy and non-contact benefits, and LiBB's high resolution and customizability, each contribute unique strengths (with limitations) to the bioprinting field (Table 1). By addressing their respective challenges through continuous research and technological advancements, these methods can be refined and integrated to overcome the complexities of creating complex epithelial structures. This holistic approach to bioprinting holds the potential to revolutionize regenerative medicine, enabling the production of functional epithelial tissues for transplantation, drug testing, and disease modeling, ultimately improving patient outcomes and advancing medical science. Table 2 lists a diverse range of epithelial tissues with the key aspects highlighted enabled by bioprinting.

2. Need for 3D bioprinting of epithelial tissues

Epithelial tissues consist of polarized epithelial cells on a basement membrane, providing physical support and acting as a barrier between epithelial and stromal compartments [91]. The epithelium is composed of tightly bound cells, which are laid out as sheets forming physical barriers lining cavities. The epithelial makeup of each organ is different and so is the thickness of each epithelial tissue type, ranging from single cell sheet thick as noticed in ciliated or non-ciliated columnar or cuboidal epithelium of urothelium and digestive tract (10–20 μm) (Fig. 1) to few cell layers thick as seen in the upper respiratory tract's pseudostratified epithelium (25–40 μm) to millimeter thick as noticed in skin or corneal epithelium (40–2000 μm) [92–94]. Proper apical-basal polarization is crucial for epithelial function, as seen with cilia on the apical surface of airways. Polarization is essential for the barrier function and its disruption is linked to diseases like cancer or cystic fibrosis, where it serves as a non-cell autonomous tumor-suppressor mechanism. Pathogens must bypass the polarized epithelial barrier to infect the host, with intercellular junctions and the apical surface's molecular composition preventing penetration [95,96].

Polarization in epithelial cells is driven by molecular changes in response to environmental and internal signals. This process involves the formation of tight junctions at cell-cell contacts, which create a barrier between the apical and basolateral plasma membrane domains [97–99]. During polarization, the membrane segment facing the lumen becomes distinct from the segment in contact with the basement membrane and extracellular matrix (ECM) [99]. Both cell-cell interaction and interactions (Fig. 3Ai) with the basement membrane (cell-matrix interaction) are essential for establishing the apical-basal polarity [100]. Indicators of polarization include the expression of Zonula Occludens-1 (ZO-1) and the formation of cilia on the apical surface (in case of ciliated epithelium) [100]. In addition to this, in epithelial tissues where gas-liquid interfacial exchange is needed, certain specific transmembrane proteins, such as claudins, are also present. Claudin 4 and 7 are ubiquitously expressed in upper and lower airway epithelia, whereas Claudin18 is expressed in alveolar epithelium, which help in modulating this specialized tight junction permeability [101]. The association of these junction proteins guides the cell polarity (planar as well as apico-basal) from local to global level, which is needed for formation of continuous epithelial sheets or lumens as noted in glandular tissues. Additionally, the association of epithelial cells with the mesenchyme also gives the necessary biological cues (growth factors) to aid in the apico-basolateral polarity [18].

2.1. Controlling cell-cell interactions through bioprinting

Through conventional tissue engineering strategies, it is difficult to

Table 1
Bioprinting modalities and their effectiveness in fabricating epithelial tissues.

Modality	Background & Working Mechanism	Key strengths	Major Limitations	Typical Applications in Epithelial Cell Biofabrication	Printable Bioink Viscosity	Cell density	Cell Viability	References
EBB	Introduced in the early 2000s. Uses pneumatic or mechanical forces to extrude bioinks as filaments.	<ul style="list-style-type: none"> - Broad compatibility with bioink properties and viscosities. - Enables scaffold-free bioprinting of tissue spheroids. - Facilitates vascularization. - Moderate cost and commercially available. 	<ul style="list-style-type: none"> - High shear stress can damage cells. - Limited resolution and control over cell interactions. - Not ideal for high-throughput models. 	Fabricating large-scale epithelial tissue constructs, developing organ-on-a-chip systems, and modeling tissue environments for drug testing and toxicity screening.	30 to >6 × 10 ⁷ mPa/s	1x10 ⁶ to 1x10 ⁸	Moderate to high (70–95 %) depending on the shear stress	[78–80]
DBB	Introduced in the early 2000s. Utilizes thermal, piezoelectric, or acoustic forces to print liquid droplets.	<ul style="list-style-type: none"> - High speed (1–10,000 droplets/s), high resolution (1–300 pl in volume). - Compatible with many biological materials (cells, DNA, RNA). - Affordable and commercially available. 	<ul style="list-style-type: none"> - Droplet size inconsistency. - Difficulty in encapsulating single cells. - Nozzle clogging at high cell densities. - Risk of cross-contamination with multiple bioinks. 	Creating high-throughput epithelial cell layers, developing detailed microarrays for drug testing, and constructing organ-on-a-chip models for <i>in vitro</i> studies.	1–40 mPa/s	1x10 ⁶ to 2x10 ⁷	High (80–98 %) but can vary with nozzle clogging	[81–83]
LaBB	Introduced in 1999. Uses pulsed laser beams for precise cell deposition.	<ul style="list-style-type: none"> - High resolution. - Minimal cell damage. - Nozzle-free, suitable for high-density cell deposition. 	<ul style="list-style-type: none"> - Labor-intensive and time-consuming. - High cost. - Limited commercial availability. - Not practical for heterocellular models. 	Creating high-resolution, intricate epithelial tissue models, engineering detailed tissue structures for regenerative medicine, and developing complex tissue constructs with minimal cell damage.	Not applicable	5x10 ⁵ to 5x10 ⁶	High (85–99 %)	[84,85]
LiBB	Utilizes DLP, SLA and VBP to photopolymerize bioinks.	<ul style="list-style-type: none"> - High resolution. - Rapid bioprinting, especially for large constructs. - Capable of complex, multi-material structures. 	<ul style="list-style-type: none"> - Limited to photocrosslinkable bioinks. - UV light exposure risks affecting cell viability. - Expensive equipment and materials. 	Fabricating detailed and complex epithelial tissue architectures, developing high-resolution tissue models for <i>in vitro</i> testing, and maintaining cell viability in complex constructs	1–5000 mPa/s	1x10 ⁶ to 2x10 ⁷	Moderate to high (60–90 %), depending on the photoinitiator used	[61,86]

control cell-cell interactions. However, with the aid of 3D bioprinting, a more precise control on cell density and layer thickness can be achieved. The relevance of this is helpful in controlling molecular mechanisms pertaining to cell-cell contacts being established through adherens and tight junctions (Fig. 3Aii) through cadherins, occludins and claudins. This establishes the Hippo signaling pathway, which phosphorylates YAP/TAZ through TAOK and MAP4K kinases. It has also been noticed that Hippo signaling pathway is triggered by mechanical tension, surrounding ECM stiffness and cell density [102,103]. For instance, in higher cell densities, the Hippo signaling cascade is switched on leading to phosphorylation of YAP and subsequently the transcription of key markers pertaining to epithelial cell maturity and inhibition of cell proliferation [104]. While lower cell densities do not trigger Hippo signaling, which leads to its co-localization with TEAD into the nucleus and promote cell proliferation [103]. Meanwhile, filamentous actin (F-actin), which dynamically responds to mechanical changes, is a crucial regulatory factor in the Hippo signaling pathway [102].

In vitro culture systems are indispensable for investigating the physiological characteristics to model homeostatic conditions and disease mechanisms of epithelial tissues [105]. Among various approaches, the filter insert culture system stands out, where cells are cultivated on a permeable membrane within a dual-compartment structure. This setup facilitates distinct exposure of cells to different conditions at their apical and basal surfaces, crucial for inducing directional polarization [106]. It

results in fully differentiated epithelial cells, allowing the exploration of tissue properties like vectorial transport and pathogen infection. Typically, this system employs serum-free medium or an air–liquid interface (ALI) to enhance polarization, creating an environment that more closely mirrors *in vivo* conditions compared to conventional plastic or glass substrates [107]. Additionally, co-culturing with stromal cells further promotes the differentiation of epithelial cells in these setups. Cells are grown as a 2D or 3D sheet on a filter insert membrane, with nutrients supplied from below. Cells are initially fed from both compartments, then matured by removing serum-containing medium from the top. Full polarization takes 7–21 days, depending on the cell type [108–111]. Altering culture conditions by supplementing different growth factors also positively influences the polarization potential of these epithelial cells. For instance, ALI (with bronchial epithelial differentiation medium) cultures do not form columnar epithelium and do not present with mucociliary characteristics; on the contrary, culturing hBECs in Pneumacult™ media (under ALI) facilitates the formation of physiologically relevant pseudostratified morphology as noticed in the upper airway epithelium [112].

2.2. Controlling cell-matrix interaction through bioprinting

In addition to the use of growth factors and soluble factors in culture media, providing physical cues to epithelia is essential to aid in their

Table 2

Examples of various epithelial tissues fabricated using different 3D bioprinting modalities and the advantages of such modalities.

Modality	Cells	Results	Aspect	Advantages of 3D Bioprinting	Application	References
EBB	Fibroblasts, human umbilical vein endothelial cells (HUVECs), dermal papilla cells (DPCs), epidermal cells (EPCs)	Bioprinted scaffolds demonstrated suitable cytocompatibility and increased DPC proliferation (1.2-fold). They facilitated self-aggregation of DPCs into spheroids and restored DPC genes associated with hair induction. Compared to manually seeded scaffolds, the bioprinted constructs showed higher cell viability, better spatial organization, and enhanced hair follicle formation <i>in vivo</i> .	Long-term Stability	Ensures sustained functionality for long-term applications	Regenerative medicine	Kang et al. [87]
EBB	Autologous nasal epithelial cells, auricular chondrocytes	The bioprinted artificial trachea was transplanted into rabbits. In the experimental group, 13 out of 15 animals survived, showing regeneration of epithelial cells and formation of immature cartilage at 6 and 12 months. Compared to the control group, where 3 out of 6 rabbits survived and showed no epithelial regeneration and significant narrowing due to granulation tissue, the bioprinted group demonstrated better tracheal patency and histological outcomes, closely resembling normal tracheal structure.	<i>In vivo</i> Integration	Improves success rates of tissue grafts and implants	Regenerative medicine	Park et al. [88]
DBB	Human nasal epithelial progenitor cells (hNECs)	Bioprinted hNECs showed higher degree of differentiation into multiple cell types, including ciliated and goblet cells, compared to manually seeded ones. The bioprinted tissue formed a more uniform pseudostratified columnar epithelial architecture and demonstrated better barrier function, mucus secretion, and beating cilia.	Spatial Organization	Mimics natural tissue architecture, improving functionality	Regenerative medicine and disease modelling	Derman et al. [17]
DBB	A549, EA.hy926	Successful engineering of a human air-blood barrier analogue. Bioprinted constructs showed improved cell organization and barrier function compared to manual methods.	Barrier Quality	Achieves higher physiological relevance in tissue models	Disease modelling	Horvarth et al. [89]
LaBB	Human embryonic stem cell derived limbal epithelial stem cells (hESC-LESCs), human adipose tissue derived stem (hASCs)	Bioprinted hESC-LESCs maintained viability, exhibited epithelial morphology, and expressed key markers. Compared to manually seeded cells, bioprinted hESC-LESCs formed a more uniform stratified epithelium with apical CK3 and basal p63a and p40 expression.	Tissue Architecture	Enables creation of more realistic and functional tissue models	Regenerative medicine	Sorkio et al. [90]
LiBB	NIH-3T3 fibroblasts, Caco-2 epithelial cells	Bioprinted intestinal stromal cells supported the growth of epithelial monolayer, creating a functional 3D model of the intestinal mucosa. The epithelial cells formed a continuous monolayer with improved barrier properties compared to cell-free hydrogels. Compared to manually seeded hydrogels, the bioprinted structures showed higher cell viability, better spatial organization, and enhanced barrier function.	Functional Properties	Achieves higher physiological relevance in tissue models	Disease modelling	Torras et al. [10]

polarization. This stems from the developmental biology aspect that basement membrane proteins dictate the differentiation of cells, and epithelial cells, which encounter these basement membrane proteins, orient and maintain their apico-basolateral polarity (Fig. 3Bi). When β -integrin receptors on an unpolarized epithelial cell encounter a basement membrane protein (like collagen or laminin), they trigger integrin-mediated signaling. This signaling involves the activation of Rho-family GTPases, which helps the unpolarized cell establish the apical side opposite to the surface in contact with the basement protein (Fig. 3Bii) [110,111]. Thus, it is a common phenomenon observed in epithelia, which requires the formation of lumens that are formed inwards to basal surfaces docked to an ECM [113]. This led to the prevalent practice of embedding epithelial cells in cell-instructive hydrogels for cultivating polarized epithelium, offering a 3D environment to study tissue architecture and differentiation more deeply [114,115]. Two primary types of hydrogels are used: those derived from ECM components like collagen, laminin, and fibronectin, and those reconstituted basement membrane hydrogels such as MatrigelTM and Cultrex^R basement membrane extract, often sourced from tumors due to their rich basement membrane content [116–119]. These hydrogels are thermoresponsive,

shifting from a liquid state at 4 °C to a gel state at 37 °C, enabling cells to be embedded in them for formation of complex 3D structures like hollow cysts with polarized epithelium. These structures can be cultured either attached to a dish or floating in a medium, with the possibility of micropatterning cells to create specific architectures. However, variability in manual seeding techniques do not offer the control of maintaining cell density to facilitate optimal cell-cell interaction, which complicate experimental reproducibility and comparisons across studies [120]. Additionally, controlling the physical and biological properties of these hydrogels is limited through conventional cell culture techniques, prompting the need for new biofabrication strategies to manipulate these hydrogels that replicate natural biological cues while offering tunable properties [121,122]. Despite these challenges, 3D hydrogel systems are widely used to explore epithelial cyst differentiation, tissue architecture, physiology, and disease mechanisms, particularly in cancer research [123,124].

3D Bioprinting is crucial for advancing epithelial tissue research and applications, offering significant advantages over traditional culture methods. For successful recapitulation of epithelial tissue architectures, it is critical to form a continuous apical barrier, where neighboring cells

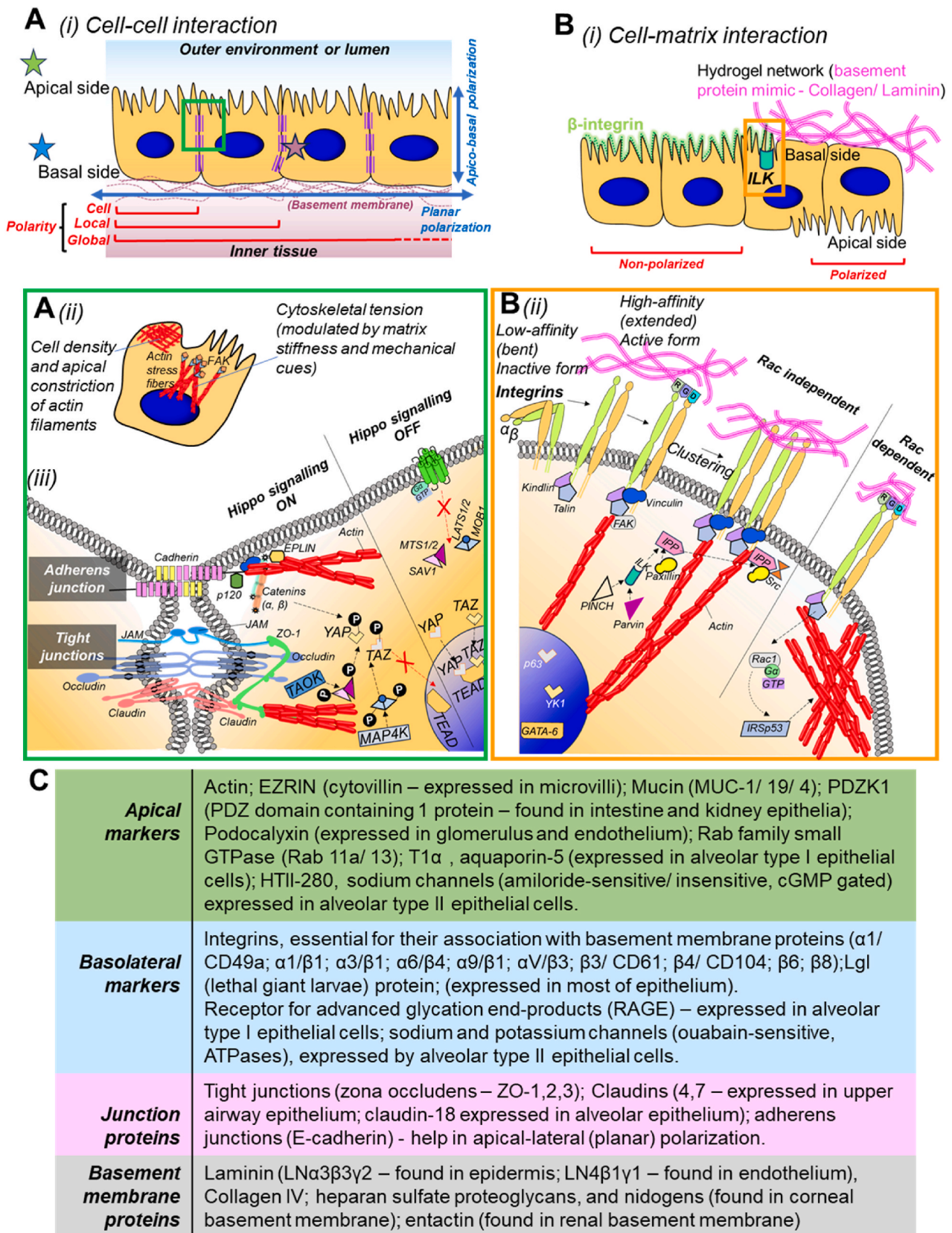


Fig. 3. Polarization of epithelial cells is orchestrated by cellular events, which are governed by A) cell-cell interactions that guide the apical-basal polarity and also the apico-lateral (planar polarization) by the association of one cell with its neighbor; thereby, establishing local and global polarity through epithelial fusion, B) cell-matrix interactions, wherein the basement membrane protein polarizes an unpolarized cell by virtue of integrin-binding and activation of integrin-linked kinases (ILK); and C) few of the common apical, basal, junctional markers and basement membrane proteins, which are seen in the epithelium. Illustrations were prepared using Biorender.com.

dock their apico-basal axes to maintain a global tissue-level polarity. This phenomenon, termed ‘epithelial fusion,’ is essential for forming continuous epithelial sheets or tubes at the embryonic stage and remains to be the major mechanism to heal epithelial wounds during repair [125]. Few important markers (apical and basal) noted after the apico-basal polarity is established were listed in Fig. 3C. Bioprinting offers the precision to control this cell-cell contact, which is difficult to achieve through conventional manual seeding techniques.

Bioprinting enables multi-material and hetero-cellular patterning, thus enabling researchers to create spatially compartmentalized cellular niches thereby mimicking mesenchyme-epithelium cell-cell interactions towards the apico-basolateral polarity establishment. Moreover, cell-matrix interactions can also be controlled through the proper choice of biomaterial to be used as a bioink. With the advent of new technologies, such as the adaptive nozzle printing, lumens with variable diameter, as noted in renal epithelium or bronchiolar epithelium branching, could be printed [126]. Additionally, bioprinting offers the advantages of enhancing the reproducibility and reliability in generating these tissues in a high-throughput manner. In terms of research and development endeavors, bioprinted disease models hold promise in attaining microtissues that can be easily integrated into microfabricated disease-on-chip platforms. Such platforms also use automated control systems for introducing infectious agents, which minimize the risk of exposure to users/researchers as opposed to conventional manual techniques while ensuring safe monitoring of these disease-on-chip models [127,128].

3. 3D bioprinted epithelial tissues

Engineering the functional epithelium *in vitro* has remained challenging due to the distinct architecture, the heterotypic nature of some epithelial tissues, and most importantly, difficulty in attaining the apico-basal and planar polarity of epithelial cells. Recapitulating the barrier integrity and polarization of the epithelium is crucial for the success of restoring function of many engineered organs, such as trachea, esophagus, skin and bladder. In this section, we highlight the recent advancements in bioprinting of a wide range of epithelia present in various

human body systems and organs, such as respiratory system, cornea, skin, digestive, urinary and female reproductive system (Table 3).

3.1. Respiratory epithelium

The development of 3D bioprinting techniques for the respiratory epithelium holds promise for advancing our understanding of respiratory diseases for drug discovery. Primary airway epithelial cells can be listed as nasal epithelial cells (NECs), bronchial epithelial cells (BECs), tracheal epithelial cells (TECs), and small airway epithelial cells (SAECs). Particularly, NECs obtained non-invasively from the middle turbinate of nostrils, serve as vital tools for studying molecular and functional aspects of virus infection [108]. These cells are integral to the construction of well-differentiated cell cultures, a significant advancement in modeling the upper respiratory tract. Epithelial cells, including ciliated, club, and goblet cells, are the predominant cell types in lungs, with distinct roles in maintaining respiratory function. The thickness of a healthy epithelium ranges from 25 to 40 μm in the upper respiratory tract, decreasing along airways [155].

Basal cells in the respiratory epithelium form a single layer along the basement membrane, contributing to its pseudostratified appearance. They have large nuclei and ribosome-rich cytoplasm and are anchored by hemidesmosomes [156]. They can repopulate major epithelial cell types, acting as stem cells in upper airways [157]. Basal and parabasal cells make up 51 % and 33 % of the proliferating cell population, respectively, indicating their role as progenitor cells [158]. Ciliated cells are columnar, attaching to the basal lamina via desmosomes and reaching the luminal surface, connected by tight junctions. They have numerous mitochondria, and 200–300 cilia interspersed with microvilli [159]. Ciliated cells are crucial for airway repair and exhibit significant plasticity [160]. Goblet cells in the respiratory epithelium have dense cytoplasm with numerous mucous granules and a basal nucleus [161]. They secrete mucous glycoproteins, aiding in particle removal and epithelial protection [162]. Clara cells are primarily found in the distal conducting airways and bronchioles of large animals, while in smaller animals, they are distributed throughout airways, sharing similar features [163]. Biofabrication of such cellular complexities through

Table 3
Summary of 3D bioprinting approaches for epithelial tissue fabrication.

Epithelial Tissue Type	Key Cell Types	3D Bioprinting Techniques	Most Common Bioink Compositions	Notable Outcomes	Applications	References
Respiratory Epithelium	Nasal epithelial cells (NECs), tracheal epithelial cells (TECs), bronchial epithelial cells (BECs)	EBB, DBB	Alginate, atelocollagen, PCL	Successful regeneration of respiratory epithelium; improved differentiation, and structural integrity; enhanced cilia and mucus production.	Airway disease modeling; tracheal replacements; high throughput bioprinting of the nasal epithelium	[17,88, 129–131, 132]
Cornea	Limbal stem cells, corneal stromal keratocytes	LaBB, DBB, LiBB	Human recombinant laminin, collagen, methacrylated gelatin, hyaluronic acid	High cell viability; transparency; successful replication of corneal layers.	Corneal tissue engineering; transplantation	[133–135]
Integumentary Epithelium	Keratinocytes, fibroblasts, melanocytes	EBB, DBB	GelMA, collagen, fibrin, alginate	>90 % cell viability; precise cell organization; successful dermo-epidermal junction formation; HF and SG regeneration	Skin replacement therapies: hair follicle and sweat gland integration	[136–138]
Digestive Epithelium	Intestinal epithelial cells, goblet cells, paneth cells, enterocytes	EBB, DBB, LiBB	Collagen, decellularized small intestine submucosa, GelMA	Improved barrier function; enhanced cell viability; successful crypt-villus architecture	Intestinal disease modeling; drug absorption studies	[139–141, 142,143, 144,145]
Urothelium	Umbrella cells, basal cells, intermediate cells	EBB, DBB, LiBB	PCL, PLCL, GelMA, alginate	High cell viability; smooth muscle differentiation; multilayered urethral constructs	Bladder tissue engineering; urethral reconstruction	[146, 147–149]
Female Reproductive Epithelium	Endometrial epithelial cells, endometrial stromal cells, mammary epithelial cells. Myoepithelial cells	EBB, DBB, Magnetic Bioprinting	Alginate, collagen, hyaluronic acid, gelatin	Restoration of endometrial morphology; improved reproductive outcomes; functional uterine models; control over mammary epithelial structure; resistance to paclitaxel	Uterine and vaginal reconstruction; fertility restoration; breast cancer research	[150,151, 152–154]

conventional cell culture practices is tedious in contrast with the help of 3D bioprinting, coupled with the robustness of the ALI culture system, offers valuable tools for studying airway disease mechanisms owing to their physiological relevance and structural fidelity.

3.1.1. Upper respiratory system

Ciliated, goblet, club, and basal cells constitute the upper respiratory epithelium, which serves a crucial protective role by acting as a physical barrier against pathogens and foreign particles while humidifying the inhaled air. Moreover, its innate immune functions enable the detection of pathogens through pattern recognition receptors, contributing to overall respiratory health [164,165]. Through innovative 3D bioprinting techniques, researchers aim to recreate this complex epithelial architecture, offering new avenues for disease modeling, drug testing, and personalized medicine in respiratory research. Park et al. (2019) utilized EBB to create tracheal replacements. They demonstrated the feasibility of using a bioink composed of alginate loaded with autologous NECs and chondrocytes [88]. The artificial trachea, transplanted into rabbits (in a ventral tracheal defect – semi-cylindrical 1.5 cm × 1.5 cm), showed successful regeneration of respiratory epithelium but limited cartilage regeneration. The study highlights the potential of NECs in tissue engineering for tracheal defects. This study paved the way for follow-up studies, where Park et al. (2021) developed a two-step 3D bioprinting method (on a rotating mandrel) for trachea-mimetic constructs, reducing bioprinting time significantly compared to traditional methods [129]. Utilizing an atelo-collagen-based bioink, chondrocytes and human nasal turbinate stem cells were bioprinted on the rotating mandrel technique comprising design features for separate cartilage rings and epithelial lining. *In vitro* analysis confirmed successful cartilaginous ECM formation complete with tracheal mucosal epithelial markers (mucin, keratin 14, and β -tubulin) on the luminal side of the bioprinted construct's bellows framework, which dictated the maturation of mucosal epithelial rings due to topographical cues. Constructs were bioprinted and then implanted into mice to assess biocompatibility and functionality. Meanwhile, Torsello et al. (2022) investigated bioprinting's potential for creating laryngotracheal scaffolds using polycaprolactone (PCL) in ovine models [130]. While some animals showed successful scaffold integration with respiratory epithelium growth, challenges like respiratory distress and poor integration were observed in others. Histological analysis revealed a cylindrical pseudostratified ciliated epithelium covering integrated scaffolds. Despite PCL's biocompatibility, its stiffness did not align with the ovine costal cartilage. Future research aims to develop more flexible scaffolds, possibly using collagen with crosslinking agents. More recently, Derman et al. (2023) developed a method for high-throughput bioprinting of nasal epithelium via DBB using patient-derived nasal cells using (bio-material-free) cell medium as the bioink solution (Fig. 4A) [17]. Histology images revealed that bioprinted hNECs achieved a higher degree of differentiation, forming pseudostratified columnar epithelial architecture with cilia and tight junctions more effectively than manually seeded cells. Single-cell RNA sequencing identified five major epithelial cell populations, showing a more uniform distribution in bioprinted tissues. Compared to manual seeding, DBB allowed for lower initial cell densities while maintaining high differentiation efficiency. Tight junction formation, indicated by ZO-1 staining, was more consistent in bioprinted samples. Cilia and mucus production was also enhanced, with bioprinted tissues showing higher densities of ciliated cells and more mucus production. Functional assays demonstrated that bioprinted tissues had slightly higher transepithelial electrical resistance (TEER) values and lower permeability, indicating a tighter barrier. Both methods produced tissues permissive to respiratory virus infection, but bioprinted tissues exhibited a higher percentage of infected cells due to their more uniform and differentiated structure. Overall, DBB offers advantages over manual seeding, including lower cell density requirements, higher differentiation efficiency, more uniform cell distribution, and better functional properties, making it a promising approach

for high-throughput and high-precision tissue engineering applications.

Despite the differences in their specific focuses, these studies collectively highlight the collaborative nature of 3D bioprinting (using different modalities) alongside bioengineering principles to cultivate the biofabricated upper airway epithelium in a more robust manner.

3.1.2. Lower respiratory system

The lower respiratory system is a vital part of the human body, as it provides the blood-air interface that allows the exchange of O₂ and CO₂ in and out of the bloodstream, respectively [166]. Comprising structures such as the bronchi, bronchioles, and alveoli, it plays a vital role in respiratory function [167]. The epithelial structure of the lower respiratory tract is essential for its function and susceptibility to diseases. Airway epithelial cells in the lower respiratory tract act as a barrier against pathogens and environmental insults [167]. Disruption of this barrier function can contribute to the pathogenesis and prognosis of respiratory diseases from infancy to adulthood [167]. Lymphatic tissue within this system assists in combating pathogens and foreign debris, underscoring its significance in maintaining overall health [168]. Given its importance, there is a growing need to develop accessible, reliable, and replicable models of lower respiratory systems. Such models offer numerous benefits, including the reduction of reliance on animal testing, enhanced understanding of drug responses, and the ability to study the impact of pathogens on cellular systems. The lower airway (2° to 2⁵) branching epithelium is lined up with ciliated, secretory, undifferentiated columnar, and basal cells, while further branching down (in small airways, 2⁶ to 2²³ order of branching) epithelium is lined up with undifferentiated columnar, relatively more ciliated cells and secretory cells shift to club cell type. Beyond the 2²³ branching, the lower airway epithelium merges with the alveolar epithelium, which is composed of alveolar type I (ATI) and type II (ATII) epithelial cells [169].

3.1.2.1. Lower airway epithelium. The lower airway epithelium comprises diverse cell types, such as ciliated and secretory cells, and is intricately structured to efficiently perform its functions [170,171]. Among the secretory cells, ATI and ATII cells are the major cells, which constitute alveolar sacs. ATI cells in the respiratory epithelium are large and flat and serve as thin, gas-permeable membranes. They are sensitive to injury from agents such as ozone and bleomycin and rely on ATII cells for repopulation [172,173]. ATI cells cannot divide and rely on the mitosis and differentiation of ATII cells for repopulation. ATII cells are small, cuboidal, and makeup about 15 % of the alveolar epithelium [174,175]. These cells are polarized with tight junctions dividing them into apical and basolateral domains [176]. They synthesize and secrete surfactants, reducing surface tension and preventing alveolar collapse. These surfactants are rich in dipalmitoylphosphatidylcholine and phosphatidylglycerol and include surfactant proteins (SP), such as SP-A, SP-B, SP-C, and SP-D. They can proliferate and differentiate into ATI cells, repopulating the epithelium after injury or infection [177].

To achieve successful bioprinting of the lower airway epithelium, it is crucial to consider the design and bioprinting strategies to ensure successful bioprinting of cells [178]. In addition, stem cell differentiation through bioprinting can be tailored to be neutral or stimulatory, offering flexibility in tissue engineering applications [179]. De Santis et al. (2021) showed a promising proof-of-concept for bioprinting human airways using a hybrid bioink composed of alginate reinforced with decellularized ECM (dECM) [180]. The inclusion of dECM in the bioink favored the maturation of murine and lung epithelial cells (MLE12 and A549, respectively), which was confirmed by phenotypic markers such as for ciliated cells (*FOXJ1*), club cells (*CC10*), and goblet cells (*MUC5AC* and *MUC5B*) that were absent in the alginate-alone groups. This emphasizes the need for the selection of a suitable bioink, which is akin to the native tissue to help regulate the differentiation and maintenance of progenitor cells towards different epithelial cell lineages.

Creating a functional lung tissue model via bioprinting poses challenges, particularly in terms of vascularization to support gas exchange within biomimetic structures [181]. In this regard, researchers have successfully replicated the lower airway epithelium using bioprinting, providing a platform to investigate infections, such as SARS-CoV-2, and potential antiviral treatments [182]. Berg et al. (2021) developed a multi-layered distal lung model consisting of a base layer containing lung fibroblasts and macrophage-like THP-1 cells, overlaid with a top layer of alveolar epithelial A549 cells. This stratified arrangement allowed the model to replicate the physiological interactions between different cell types, crucial for studying complex tissue responses. The multi-layered structures provide a supportive environment for the epithelial cells, enabling them to form organized clusters and maintain their functional characteristics over an extended culture period. This biomimetic tissue construct demonstrated the capability of bioprinting to produce tissues with high structural and functional fidelity, offering a valuable platform for studying viral infections and testing antiviral drugs in a setting that closely resembles human lung tissue (Fig. 4B) [131]. Park et al. (2019) utilized EBB to create an airway-on-a-chip

model that mimicked lung epithelial–blood vessel interactions [183]. Porcine tracheal-mucosa derived dECM based bioink was used to encapsulate endothelial cells within a PCL frame. Primary human tracheal epithelial cells (hTEpCs) were seeded on Transwell inserts and matured using ALI culture and then assembled on top of the vascular platform to obtain an airway-on-chip model. By treating the airway-on-chip model with interleukin 13 (IL-13), hTEpCs replicated asthmatic conditions and exhibited features, such as goblet cell hyperplasia and inflammation. Nevertheless, due to limitations in the spatial resolution of current bioprinters, challenges remain in accurately reproducing the lower airway epithelium and vascularization [184].

The bronchi are an important structure of lungs as they are the main pathway that begins the distribution of ambient air toward the alveoli [34]. The bronchi are vital to disease research and physiological response since they are lined with cilia, which produce mucus and trap pathogens. The benefits of being able to produce and utilize a bronchial epithelial model would allow researchers to investigate the cellular response to common respiratory illnesses, such as influenza and bronchitis. A study done by Estermann et al. (2020) had the main goal of

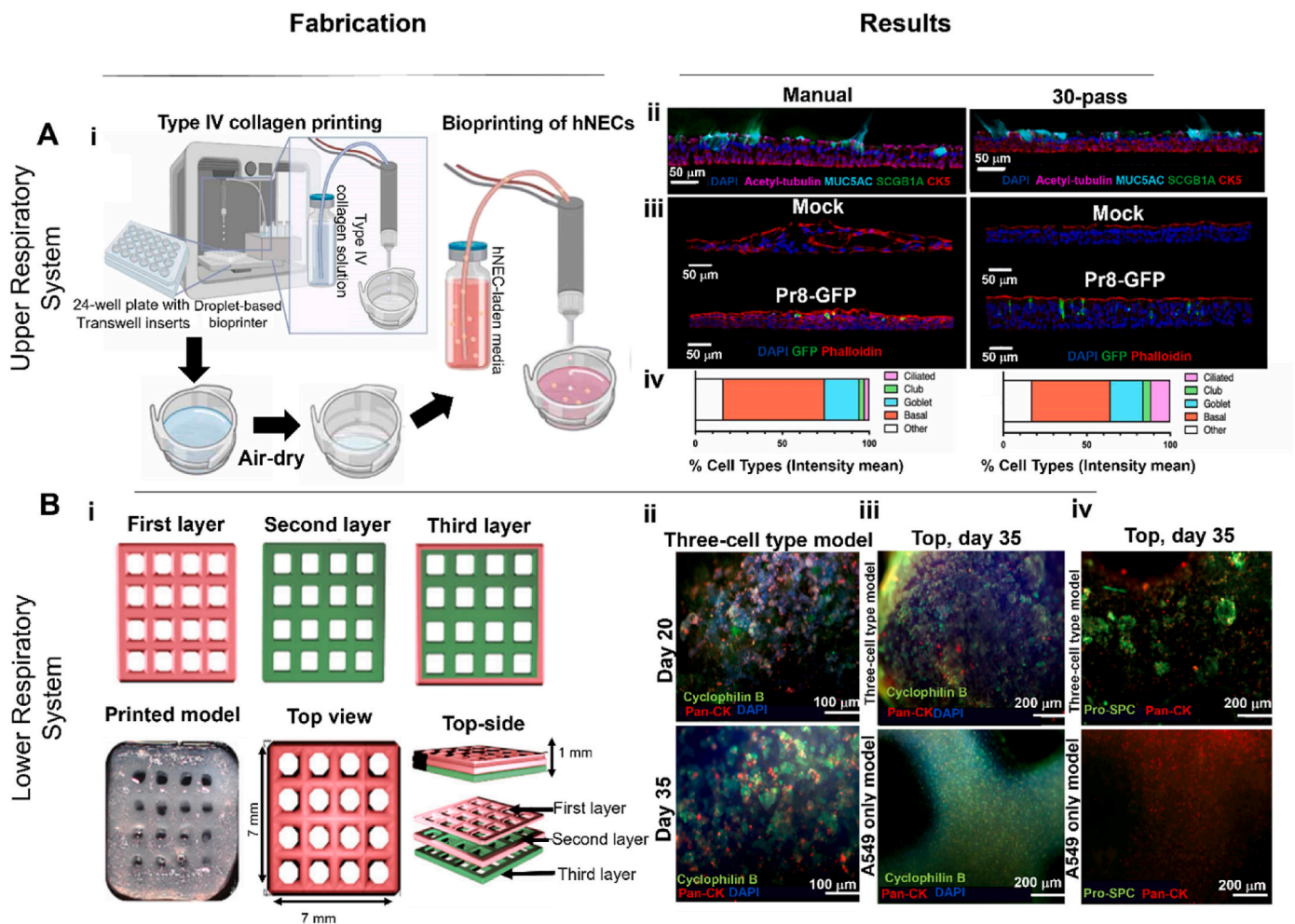


Fig. 4. (A) i) A schematic illustration of DBB for the nasal tissue model, ii) cellular comparison between manually seeded and bioprinted nasal epithelium. Figures illustrate representative immunofluorescent (IF) images of differentiated hNECs distinguished by major epithelial cell markers: basal (CK5, red), goblet (MUC5AC, cyan), club (SCGB1A1, green), and ciliated cells (acetylated α -tubulin, magenta), alongside nuclei (DAPI, blue), iii) primary hNECs ALI cultures susceptible to Puerto Rico 8 (PR8)- green fluorescent protein (GFP) influenza infection. Representative IF images of nasal ALI from manual seeding and bioprinting (30-pass (where a bioprinted single layer was referred to as a ‘pass’)) after 24 h of exposure to uninfected control (Mock) or influenza virus (2.5×10^5 pfu PR8-GFP). Nuclei are shown with DAPI (blue), actin filaments with phalloidin (red), and GFP-expressing influenza virus indicating effective viral replication (GFP, green), iv) quantitative analysis of epithelial cell types in nasal ALI cultures using histocytometry (reproduced with permission from Ref. [17], 2024 IOP Publishing). (B) i) Illustration of the multi-layer structure of the bioprinted model, ii) comparison of protein expression and morphology in different bioprinted cells. Bioprinted models with either A549 cells, THP-1 cells, and human lung fibroblasts or models with only A549 cells were cultured for specified time periods, then fixed, immunohistochemically labeled, cleared, and examined using fluorescence microscopy (reproduced with permission from Ref. [131], 1996–2024 MDPI (Basel, Switzerland)).

improving testing methods used to test respiratory medications and chemical interactions with lungs. Most current testing methods rely on animal testing to assess adverse and/or beneficial effects of medications, which poses ethical and physiological issues, as humans and animals differ in metabolic processes and disease progression [132]. The model relating to epithelial bronchial cells was made with the 16HBE14o-cell line and is suitable for recapitulating properties of the human bronchial epithelium. The model was bioprinted into Transwell inserts coated with collagen type I as a substrate [132]. The viability of the model as assessed by lactate dehydrogenase (LDH) assay revealed that cells were viable for one week and the integrity of the barrier function was also affirmed by TEER measurements. Although the initial results of the model were promising, its standardization and reproducibility should be improved. Overall, lower airway epithelial models hold promise for screening of drugs and airway toxins and testing their dosage response evaluation.

3.1.2.2. Alveolar epithelium. Alveoli are small air sacs located at the end of bronchioles and are the location of gas exchange between the bloodstream and lungs [185]. They are the smallest structure of lung tissue, which interacts with other systems in the body, such as the circulatory and lymphatic systems. Since alveoli is a vital part of lungs, it is extremely important to have a reproducible model to be able to study the effects of medications and diseases on alveoli.

In a model of alveolus, it is pertinent to have some form of an air-blood barrier to better replicate the interaction and metabolization of medications between alveolar cells and the bloodstream. Although there were many models of the alveolar air-blood barrier developed, most of them could not effectively replicate the minimal distance of the barrier (around 1.6 μm). Horváth et al. (2015) aimed to combat this issue with the utilization of DBB and then compared the results of the bioprinted model with a manually seeded model. The bioprinted model was composed of a layer of Matrigel™ followed by a layer of EA.hy926 endothelial cells suspended in a culture medium and then left to incubate for 2 days [89]. Then another layer of Matrigel™ was added, followed by a layer of A549 human epithelial cells suspended in the medium. The results of the bioprinted model displayed uniform monolayers of each cell type, while the manually seeded model had cells that tend to grow in uneven multilayered clusters. The even layers of the bioprinted model allowed more intracellular and intercellular interactions, which better represent the native air-blood barrier. Both models showed a viability of over 95 %, which proves that bioprinting had no adverse effect on the survival of cells. Moreover, the barrier integrity was assessed by the diffusion of Dextran from the apical to the basolateral side, where the bioprinted model exhibited lesser leakage of the dye. This model pioneered the first steps towards the bioprinted functional lung tissue by improving upon existing models, using bioprinting for increased precision in layering cells.

Alveolar models frequently struggle to survive longer than 3 days post-fabrication due to several critical factors [186–188]. One major issue is the limited diffusion of nutrients and O_2 within the dense or thick constructs, leading to nutrient deprivation and hypoxia, which ultimately causes cell death. Additionally, maintaining the structural integrity of the fabricated construct is challenging as the mechanical properties of the scaffold material and its ability to support cell attachment and growth can degrade over time, resulting in collapse or deformation. It is crucial for them to last longer as it makes it easier to study the long-term effects of pathogens on them. In this regard, Ng et al. (2021) created a model, which utilized MRC-5 lung fibroblasts in tandem with A549 epithelial and EA.hy926 endothelial cells using DBB [189]. The addition of fibroblasts allows for increased longevity of the model and a more accurate representation of the environment within the human body. Cells were bioprinted in droplets in several layers with polyvinylpyrrolidone (PVP)-based formulations as suspensions, with collagen type I separating each layer. The initial viability test with

bioprinted versus non-bioprinted cells showed that the bioprinting process did not impair cell viability. The bioprinted model lasted at least 14 days, allowing ample time for pathogenic tests to be conducted. The model was reproducible, scalable, and could be extended to incorporate primary human alveolar cells for respiratory-related toxicological studies.

3.2. Cornea

The cornea plays a vital role in regulating light entering the eye and consists of three main layers: epithelium, stroma, and endothelium [190]. The epithelium is majorly made up of stratified squamous epithelium, which is bound anteriorly to the stroma that makes up 90 % of the corneal thickness. The alignment of collagen in the stroma, along with the extracellular organization on both long and short scales, plays a crucial role in providing the protection, light transmission, and refraction necessary for vision. Beneath the stroma is the non-proliferative endothelium, which is responsible to maintain the corneal transparency through a dehydrating mechanism that dehydrates the stroma. Comprising nonkeratinized, stratified squamous epithelium with approximately 50 μm thickness, it features several cell layers: flat polygonal cells, wing cells, and basal cells adhering to the basement membrane [191]. Originating from the ectoderm's superficial layer of the optical cup, this epithelium serves as a protective barrier against mechanical damage and infection, aided by a tear film that prevents dehydration, supplies nutrients, and acts as a biodefense system [192]. Proliferative basal cells differentiate into wing cells, which migrate to the surface, forming flat cells. Regeneration of the corneal epithelium relies on limbal epithelial stem cells (LSCs) located in the limbus's basal region. These slow-cycling stem cells, do not express differentiation markers (such as cytokeratin 3 (CK3) and 12 (CK12)), become highly proliferative during injury, facilitating epithelial repair [193,194]. Corneal epithelial cells have a unique property of continuous proliferation from the limbus onto the cornea and onto implanted tissue-engineered corneal substitutes [195]. To enhance the surface of constructs and promote cell adherence and migration, coatings with substances like collagen, laminin, fibronectin, or fibrin have been explored [196].

Current clinical approaches for treating epithelial corneal disorders often involve therapies aimed at promoting epithelial healing and regeneration [197]. However, these methods may have limitations, including the risk of scarring and recurrence. Despite progress in research, significant challenges remain, including the need for further optimization of biomaterials to ensure compatibility and functionality with the native corneal epithelium. The corneal stroma, which serves as the basement membrane for the corneal epithelium helps in their polarization. The stroma is made up of aligned arrays of collagen type I/IV (heterotypic and hydrated). These collagen arrays, usually 500–600 units in number, constitute the lamellae, which are parallel to the corneal surface. This stromal arrangement of collagen fibrils and the inability to recapitulate is the major reason for the unsuccessful attempts in engineering corneal equivalents for transplantation. Additionally, the long-term safety and efficacy of bioprinted epithelial corneal constructs require comprehensive evaluation through preclinical studies and clinical trials. Sorkio et al. (2018) demonstrated the feasibility of using LaBB to create cornea-mimicking structures with human stem cells [90]. The study utilized human embryonic stem cell-derived limbal epithelial stem cells (hESC-LESCs) and human adipose tissue-derived stem cells (hASCs) to construct epithelial and stromal layers of the cornea, respectively. By incorporating these cells into bioinks based on human recombinant laminin and collagen type I, they produced constructs with high cell viability and proliferation. Bioprinted structures successfully mimicked the native corneal layers and integrated well with the porcine cornea in culture. Following this study, Campos et al. (2019) demonstrated the feasibility of bioprinting corneal models using DBB, offering promising implications for corneal tissue engineering (Fig. 5A) [133]. Their

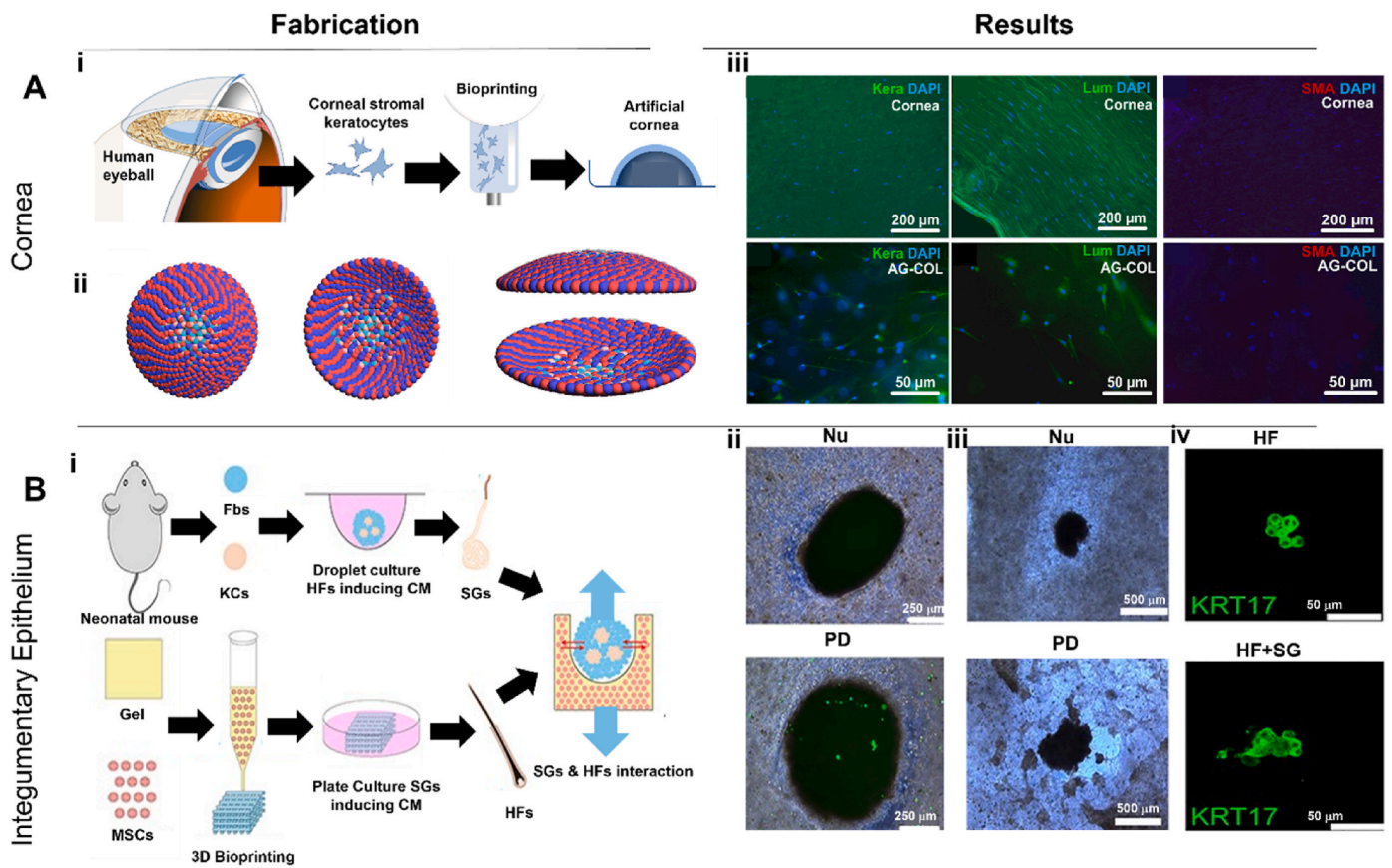


Fig. 5. (A) **i**) Bioprinting a functional and biomimetic 3D corneal model using hydrogels and cultured human corneal stromal keratocytes (CSKs), **ii**) computer-aided design and slicing of 3D models for corneal bioprinting, using customized slicing software compatible with DBB. In the DBB process, drops a and b (blue and red) were bioprinted in an evenly spaced manner in one layer, and the gaps between drops a and b were calculated and filled with additional drops (green and beige), **iii**) Immunohistochemical and immunocytochemical staining of human corneal tissue and CSK-loaded bioprinted samples. Keratocan (Kera) and Lumican (Lum) staining of human corneal tissue slides (5 μm). Kera and Lum staining of CSK-loaded agarose-collagen blends 7 days after bioprinting. Smooth muscle actin (SMA) immunocytochemical stainings of CSK-loaded agarose-collagen blends 7 days after bioprinting and SMA immunohistological stainings of human corneal tissue slides (reproduced with permission from Ref. [133], 1999–2024 John Wiley & Sons). (B) **i**) Diagram illustrating the procedure for creating 3D skin constructs *in vitro*, **ii**) merged brightfield and green fluorescence images of HF spheroids on SG scaffolds after 14 days of culture. Green fluorescence is expressed by GFP-mesenchymal stem cells (MSCs) within the SG scaffolds, **iii**) brightfield images of HF spheroids and the surrounding SG cell mass within SG scaffolds after 14 days of culture (the Nu group refers to SG scaffolds without Plantar dermis homogenate (PD), while the PD group refers to SG scaffolds with PD), **iv**) detection of HF-specific markers in HF spheroids after a 7-day culture period (the HF + SG group refers to HF spheroids seeded on SG scaffolds, while the HF group denotes HF spheroids placed solely in AG scaffolds) (reproduced with permission from Ref. [198], Oxford University Press).

approach yielded translucent corneal stromal equivalents with optical properties comparable to the native tissue, addressing a critical need in corneal transplantation. Additionally, bioprinted corneal stromal keratocytes (CSKs) remained viable and maintained their characteristic phenotypes post-bioprinting, suggesting potential clinical applications for patients with corneal stromal diseases. In a subsequent study, Mahdavi et al. (2020) investigated the use of LiBB (e.g. SLA) with a methacrylated gelatin (GelMA) bioink for creating human corneal stroma equivalents [134]. Their study demonstrated anatomical similarity to the native cornea, with high transparency and water content. Encapsulated corneal stromal cells showed excellent viability, proliferation, and expression of key corneal stroma genes. This approach holds promise for corneal tissue regeneration and transplantation. Most recently, Mörö et al. (2023) developed a hyaluronic acid-based dopamine-containing bioink for bioprinting of corneal equivalents [5]. The bioink exhibited high printability and shape fidelity, and self-healing properties after optimization of the bioink's shear thinning behavior and viscosity for EBB. Human stem cells were bioprinted to create stromal structures, showing tissue formation and integration into *ex vivo* porcine corneas. Moreover, human pluripotent stem cell-derived neurons were bioprinted to the periphery of the corneal structures, demonstrating

innervation. The study highlights the potential of the developed bioink for corneal tissue engineering, offering a promising solution to the scarcity of donor corneas. To address the challenges of obtaining aligned collagen fibrils of the stroma, EBB offers the control of collagen organization by shear flow. Kim et al. (2019) utilized a corneal stroma-derived decellularized atelocollagen based-bioink (encapsulating human keratocytes) to orient collagen fibrils in the direction of applied shear stress using a 25-G nozzle. The printed cornea had transparency comparable to the normal human cornea and helped in the maintenance of keratocyte-specific markers, such as keratocan and aldehyde dehydrogenase [135]. More such smart nozzle designs, which can control the alignment of extruded collagen or other biopolymers can help in overcoming the challenges in bioprinting aligned and transparent cornea conducive for transplantation.

3.3. Integumentary epithelium

The integumentary epithelium, made up of stratified squamous epithelial cells, is typically composed of multiple layers ranging from superficial to deep regions consisting of the primary layers: stratum corneum, stratum granulosum, stratum spinosum, and stratum basale

[199]. The integumentary epithelium forms the crucial barrier between the external environment and the body, and it is majorly constituted by the skin and its associated glands. Skin injuries pose significant challenges in clinical practice, with current treatment methods often facing limitations, such as high costs and lengthy production times. Bioprinting offers a promising solution for skin replacement therapy by precisely depositing cells and biomaterials to recapitulate the stratified hierarchical structure. This technology has the potential to automate and standardize the production of integumentary epithelium, addressing the need for effective wound treatment.

3.3.1. Skin

The skin, the largest organ of the human body, plays a crucial role in protecting the body from external factors and maintaining homeostasis. It comprises multiple layers, each with distinct functions. The outermost layer, the epidermis, provides a protective barrier against pathogens and regulates water loss. The dermis, which contains blood vessels, nerves, hair follicles, and sweat glands, lies beneath the epidermis. The subcutaneous tissue, or hypodermis, is the deepest layer and serves as an insulator [200]. Various bioprinting techniques have been explored to create skin constructs that closely resemble the native skin tissue morphology and function by addressing the challenges, such as the need for suitable skin tissues incorporating essential components like hair follicles (HFs), sweat glands (SGs), and sebaceous glands into bioprinted skin constructs [201]. In addition, *in situ* and *in vitro* bioprinting approaches have been explored in skin bioprinting, each offering unique advantages.

Shi et al. (2018) explored the use of a tyrosinase-doped bioink consisting of GelMA and collagen for EBB of skin [202]. Bioprinted human melanocytes, keratinocytes, and fibroblasts exhibited >90 % cell viability over 2 weeks. Cubo et al. (2017) focused on meticulously depositing bioinks containing human skin fibroblasts and keratinocytes in a fibrin-based bioink layer by layer onto Transwell inserts. Post bioprinting, constructs were matured for 17 days in ALI culture and then transplanted into immunodeficient mice [203]. The bioprinted human skin survived and maintained its native structure as opposed to thin and pinkish mouse skin, while the bioprinted skin also exhibited the right dermo-epidermal junction (confirmed by the presence of human collagen type VII) and protein anchoring fibrils. Additionally, the bioprinted constructs demonstrated precise cell organization, structural integrity resembling intact skin tissue, and the presence of vital skin-specific markers (keratin 10 and filaggrin). Similarly, Pourchet et al. (2017) introduced a scaffold-free technique, utilizing a specialized bioink (gelatin, alginate, and fibrinogen) containing human epidermal keratinocytes onto a biopsied human skin to reconstitute the epidermal layer *in vitro* [136]. The bioprinted skin constructs exhibited attributes resembling natural skin, including precise cell arrangement, structural integrity, and expression of skin-specific markers (collagen type I and V; vimentin, fibrillin, and elastin), showcasing functional proliferation, differentiation, and synthesis of essential ECM components. Lee et al. (2014) investigated the use of DBB in creating human skin equivalents (hSKE), highlighting its superiority compared to EBB in terms of control of cell densities between bioprinted layers [137]. Their research effectively replicated the morphology of native human and mouse skin, demonstrating precise emulation of the keratinization process within the epidermis. Building on these advancements, Jin et al. (2021) successfully developed a full-thickness functional skin model using bioprinting [138]. This model incorporated an acellular dermal matrix (ADM) and GelMA bioinks to create a skin construct that included an epidermal layer, a dermal layer with fibroblasts, and a vascular network with endothelial cells. The bioprinted full-thickness skin not only maintained high cell viability and supported cell proliferation but also facilitated epidermal reconstruction and repair of full thickness wound in Balb/c nude mice model. This highlights the potential of bioprinting in creating full-layer skin substitutes that closely mimic the native skin architecture.

3.3.2. HFs and SGs

The HF epithelium structure is composed of two parts: the epidermal compartment and the dermal compartments. The interaction between these compartments is essential for the development and growth of HFs [204,205]. Effective communication between dermal and epidermal cells is vital for successfully reconstructing HFs for research or therapeutic purposes. The dermal portion of HFs can be further categorized into two compartments: the dermal papilla (DP) and dermal sheath. DP is situated at the base of HFs, while the dermal sheath, also known as the connective tissue sheath, lines the epithelium of HF from the bulge level downwards. The dermal sheath is directly connected to the base of DP through a stalk, with a basement membrane acting as a separator between DP and the dermal sheath in the epithelial segment of HF [206]. In the literature, various models have been established to investigate the interactions between the dermal and epidermal compartments and to reconstitute HFs [207,208]. Most hair reconstitution experiments have been carried out on immunodeficient mice [209,210] or have utilized mouse cells to achieve HF formation. The use of 3D-printed molds has played a significant role in creating a controlled organization and microenvironment conducive to skin recapitulation. For example, Abaci et al. (2018) utilized 3D printed molds to generate microwells to mimic the HF patterns in the collagen-based human skin equivalents, which were also vascularized. Human skin constructs, incorporating fibroblasts, keratinocytes, and DP cells were cultured in collagen type I to promote HF differentiation [211]. The spatial arrangement, mimicking native HF organization, enables the generation of HFs within these skin constructs and successful induction when grafted onto immunodeficient mice. The capability to generate HFs from human cells *in vitro* holds promise for the development of more physiologically relevant skin models and shows potential for applications in regenerative medicine. While these assays have shown success with mouse cells, regenerating human HFs remains a challenging task that requires significant advancements in various areas. Kang et al. (2022) employed EBB to regenerate HFs using a gelatin/alginate scaffold [87]. The bioprinted scaffold, incorporating key cell types, demonstrated cytocompatibility and enhanced dermal papilla cell (DPC) proliferation. Transplantation into mice successfully induced HF-like structures, showing promise for hair loss treatment as it offers precise cell distribution while promoting essential epithelial–mesenchymal interactions for HF formation, making it a promising method for skin tissue engineering. Zhang et al. (2020) developed a bioprinted skin model integrating SGs and HFs, overcoming the challenge of co-regeneration (Fig. 5B) [198]. Their approach combined SG regeneration using 3D bioprinted scaffolds and HF induction through spheroid culture. The study unveiled the interaction between SGs and HFs, showing HF spheroids promoted differentiation of both appendages within SG scaffolds. Additionally, plantar dermis homogenate in SG scaffolds enhanced SG and HF formation in HF spheroids. Wang et al. (2017) explored the influence of a 3D bioprinted SG microenvironment on redirecting mammary progenitor cells (MPCs) towards the SG cell fate [212]. They used gelatin/alginate and mouse SG ECM proteins to create this microenvironment via EBB. Their study demonstrated significant morphological and functional changes in MPCs within the 3D bioprinted SG microenvironment. MPCs predominantly differentiated into luminal epithelial cells of SG, expressing markers like sodium/potassium channel protein ATP1a1 and keratin 8. The study also revealed the involvement of the Shh signaling pathway in guiding MPC differentiation, with its inhibition leading to reduced expression of SG-associated proteins.

3.4. Digestive epithelium

The GI mucosal surface is lined with specialized epithelial cells that form a crucial barrier characterized by intercellular junctions, effectively separating the inner and outer environments to prevent the passage of harmful substances [213]. Despite this barrier function, epithelial cells also facilitate the absorption of essential nutrients and

electrolytes, necessitating a semipermeable structure that selectively permits certain substances while blocking others. This requirement led to the evolution of the intestinal barrier function, a defensive system comprising intra- and extracellular elements that collaboratively hinder the passage of antigens, toxins, and microbial byproducts. Simultaneously, it supports the development of the epithelial barrier, immune system functionality, and tolerance acquisition towards dietary antigens and intestinal microbiota [214].

The esophagus, a muscular tube linking the oral cavity to the stomach, traverses through the neck and thorax, facilitating the transport of ingested materials. It secretes mucus, essential for lubrication and smooth passage of food [215]. The lining epithelium varies across species: it is keratinized in swine, equids, ruminants, rats, and mice, whereas it is nonkeratinized in carnivores and humans. Epithelial cells in the esophagus have a turnover rate of 5–8 days, ensuring continuous renewal and maintenance of the epithelial barrier [216,217].

The intestinal epithelium consists of a single layer of specialized, polarized epithelial cells that undergo continuous renewal every 3–5 days [218,219]. Pluripotent stem cells located deep within the Lieberkühn crypts of the intestine generate progenitor cells that migrate toward the upper villi for final differentiation [220]. Although predominantly composed of enterocytes (approximately 80 %), the diverse functions of the intestinal epithelium are facilitated by specialized cells, such as mucus-secreting Goblet cells, defensin-secreting Paneth cells, hormone and neuropeptide-secreting enterochromaffin cells, and antigen-absorbing M-cells located on lymphoid aggregates at the luminal surface [220–222].

3D Bioprinting offers alternatives to traditional methods for investigating intestinal physiology, diseases, and drug screening. The intestinal epithelium, essential for digestion and immune defense, presents challenges due to its complex microenvironment. However, 3D bioprinting stands out for its ability to recreate key features of the intestinal environment, such as 3D architecture and mechanical stimulation. By precisely depositing bioinks containing intestinal cells and cell-instructive biomaterials, bioprinting enables the fabrication of tissue constructs that mimic the native digestive epithelium [10,223]. These bioengineered models hold promise for advancing our understanding of intestinal or gut function and pathology, providing standardized platforms for drug screening.

3.4.1. Esophagus, stomach, intestine and bile ducts

The human esophagus, a slender hollow tube measuring 18–25 cm in length and spanning three anatomical segments (cervical, thoracic, and abdominal), has gotten attention in the realm of 3D bioprinting [224]. By mimicking the native muscular tube's peristaltic movement, bioprinted esophageal tissues hold promise for efficiently propelling food bolus and liquids toward the stomach. Despite facing challenges, such as achieving the complexity and functionality of native tissue, advancements in bioengineering techniques and regulatory frameworks are driving progress in this field. The integration of 3D bioprinted esophageal tissues into regenerative medicine holds the potential to revolutionize treatment approaches for various medical conditions [225].

Takeoka et al. (2019) utilized a Kengan-method-based bioprinting strategy to create scaffold-free esophageal structures, wherein multicellular spheroids were spatially organized on microneedles [226]. The multicellular spheroids were composed of human dermal fibroblasts, human esophagus smooth muscle cells, and human endothelial cells, and structures with higher proportions of mesenchymal stem cells exhibited greater strength expressing pan-cytokeratin in the lumen recapitulating the esophageal mucosal epithelial polarity. Post-maturation of these structures in a bioreactor, the esophageal structure was studied in a shunt model (between the esophagus and the stomach) in rats for 30 days. The implanted constructs maintained their integrity, with residual food particles noted inside the lumen, and promoted epithelialization *in vivo*. Nam et al. (2020) introduced a dragging technique in EBB, which takes advantage of the viscoelastic nature of the

bioink extruded to stretch it, thus obtaining differential filament width on the fly during bioprinting. This 'dragging' technique helped in making finer pores by altering the filament width, which is difficult to attain in conventional EBB. Moreover, this 'dragging' technique also helped in recapitulating the wrinkled architecture as noted in the native structure of the esophagus (Fig. 6A) [139]. This method utilizes the stretching properties of viscoelastic bioinks when dispensed through a nozzle, where dECM-based bioinks derived from esophageal tissues were used to replicate the complex architecture and biochemical cues essential for regeneration. By controlling parameters like pore size and morphology (compartmentalized pore architecture – inner layers were wrinkled while outer layer was bellows shaped), they achieved improved structural integrity and mechanical flexibility, crucial for mimicking natural peristalsis. *In vitro* studies demonstrated enhanced human esophageal epithelial and human esophageal smooth muscle cell viability and proliferation within porous constructs, showcasing their potential for tissue regeneration. These innovative approaches offer new solutions for reconstructing esophageal defects. In addition to these studies, Farhat et al. (2022) explored the use of methylcellulose/poly (caprolactone)-co-glycolide based bioink using an extrusion-based bioprinter towards a potential esophageal tissue engineering application [140]. The natural/synthetic polymer-based acellular constructs had native-like mechanical properties and exhibited biocompatibility as assessed using fibroblasts. These substitutes foster favorable interactions with endothelial progenitor cells, crucial for tissue integration and vascularization. Moreover, their biodegradability ensures seamless tissue replacement, while their suturability and minimal leakage make them suitable for surgical use.

The stomach and intestines share radial patterns with the esophagus, distinguished by nerve-covered submucosa and mucosa [227]. The stomach boasts an extra muscle layer, particularly an inner oblique layer. Notably, epithelium serves varied functions, with intestinal epithelium focusing on nutrient absorption and waste, while gastric epithelium protects against acid damage and secretes acid [228]. Anatomically, the stomach serves as the widest part of the digestive system, resembling a sac-like structure that connects to the esophagus and duodenum. Functionally, the stomach acts as a reservoir for food, secreting acids and enzymes for digestion, and churning food into chyme [229]. By replicating this complex anatomy and function, 3D bioprinting offers innovative solutions for the reconstitution of the digestive epithelial tissues.

In this regard, Zhao et al. (2020) demonstrated an intraoperative bioprinting concept, specifically targeting gastric wall injuries [230]. Their bioprinting platform, designed for use along with an endoscope, enables precise bioprinting directly within the stomach. Utilizing a gelatin–alginate composite bioink, they successfully bioprinted 2 layers of human gastric epithelial and human gastric smooth muscle cells, where bioprinted constructs maintained ~90 % viability over 10 days *in vitro*. After that, Brassard et al. (2021) introduced 'bioprinting-assisted tissue emergence (BATE),' a novel method focusing on stomach and intestine tissue engineering [231]. BATE enables precise deposition of organoid-forming stem cells in conducive matrices, wherein the deposited cells/organoids spontaneously reorganize leading to interconnected and spatially evolved structures resembling native stomach and intestine tissues. They achieve features like intestinal epithelia with crypts and villus domains, controlled by geometry and cellular density. BATE holds promise for modeling stomach and intestine tissues at various scales, enhancing physiological relevance in drug discovery, diagnostics, and regenerative medicine.

The human intestine serves as a vital organ for digestion, absorption, secretion, and motility, creating a protective barrier between the digestive environment and the body [232]. It plays a key role in systemic physiology by metabolizing drugs, communicating with organs like the liver and pancreas, and hosting an enteric nervous system as a part of the gut-brain axis [233–237]. Additionally, the intestine is a major site for commensal microbes from the gut microbiome, contributing

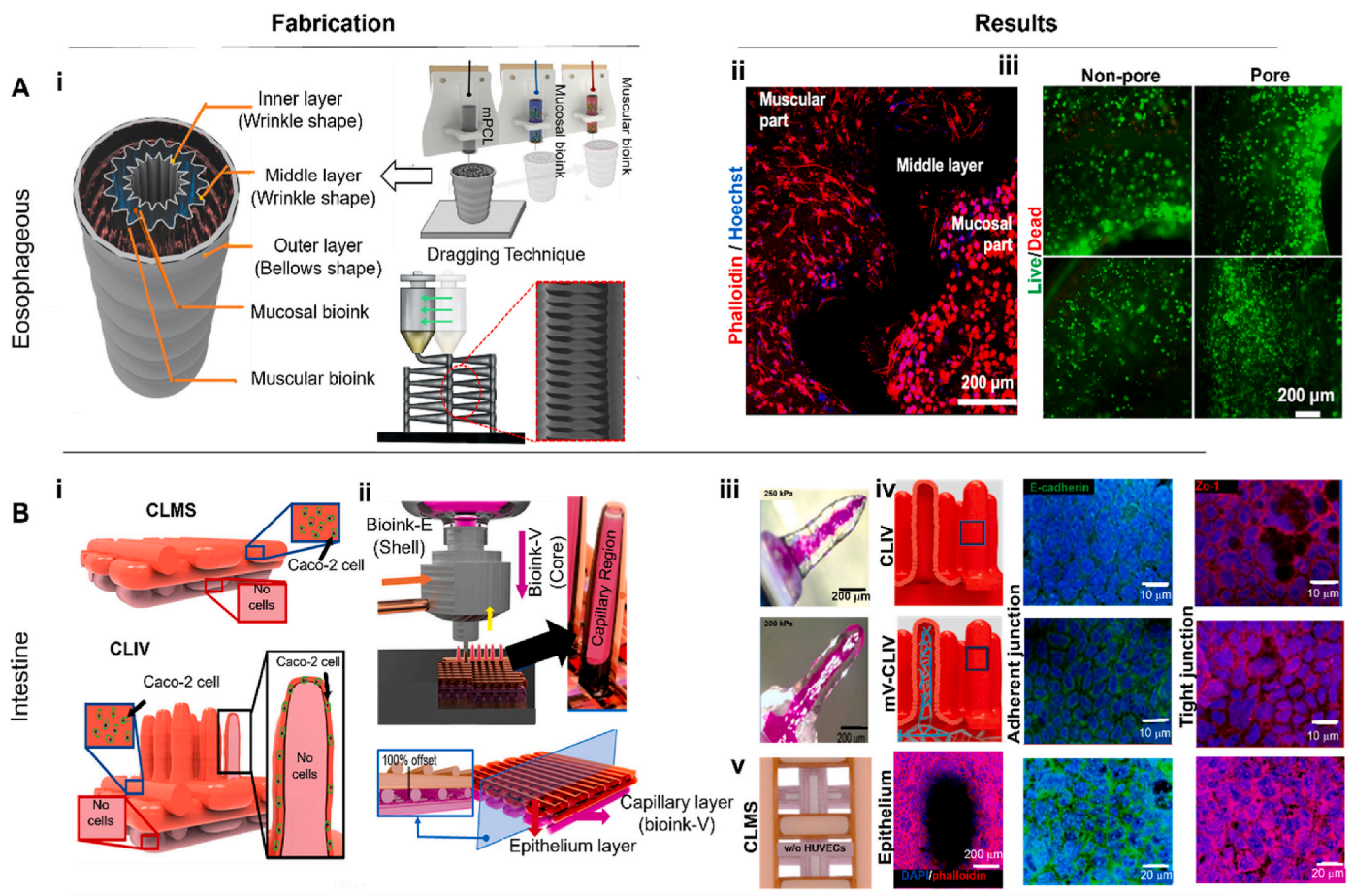


Fig. 6. (A) **i**) Schematic description of a biomimetic esophagegus scaffold. A multilayered, bioprinted tubular construct made using the dragging technique, employing bioinks derived from decellularized inner and outer esophagegus tissues, **ii**) IF staining of the Multi-layered Free-form porous Tubular (MFT) construct, **iii**) LIVE/DEAD assay of the MFT constructs with and without pores at Day 7 (reproduced with permission from Ref. [139], 2024 Springer Nature Limited). (B) **i**) Diagrams of cell-laden mesh structure (CLMS) and cell-laden intestinal villi (CLIV), **ii**) 3D model of the villus region for cell-laden intestinal villi, **iii**) optical images of bioprinted structures at different shell region pressures (200 and 250 kPa), **iv**) IF images showing adherent junctions (E-Cadherin, green) and tight junctions (ZO-1, red) in models cultured for 21 days, **v**) diagram of CLMS along with DAPI/phalloidin fluorescent images and IF staining of E-Cadherin and ZO-1 in models after 21 days (reproduced with permission from Ref. [141], 2024 American Chemical Society).

significantly to intestinal homeostasis [238]. The mucosal lining of the intestine is crucial for nutrient absorption and produces protective mucous and cytokines. The small and large intestines exhibit differences in disease processes, with small intestinal cells showing high resistance to injury, and undergoing rapid apoptosis when damaged [239,240]. In contrast, colon cells may develop mutations post-damage, leading to carcinogenesis [241]. Colon cancer research has led to *in vitro* models for epithelial cells, enhancing our understanding of colon cancer mechanisms, colonic growth, and differentiation [242]. Limited research on the small intestine is attributed to the lack of suitable long-term *in vitro* models. Because of this limitation, bioprinting technology provides a promising approach for fabricating microscale structures that closely resemble the architecture of the intestinal epithelium. Madden et al. (2018) developed a 3D model with distinct layers; human intestinal fibroblasts overlaid with human epithelial cells and the work emphasized on obtaining the apical/basolateral polarity [243]. This bioprinted model mimics human intestine physiology for drug absorption, distribution, metabolism, and excretion (ADME)/Toxicology studies as it exhibited selective permeability with the presence of transporters and key cytochrome P450 (CYP450) enzymes. It outperforms traditional Caco-2 cultures, resembling the native tissue in architecture and functionality. The model assesses metabolic function, barrier integrity, and transporter activity, offering a more physiologically relevant platform for drug development studies. To replicate the functions of the small

intestine, incorporating a capillary system is essential for 3D intestinal villi models. However, creating 3D intestinal villi models with integrated capillary structures is highly challenging using traditional methods, like micromolding, photopolymerization, and direct printing. Kim et al. (2018) addressed this using a core-shell nozzle design to facilitate an EBB-based dual-cell-printing process (Fig. 6B) [141]. This approach allowed the simultaneous bioprinting of the epithelium and vascular network, with Caco-2 cells in the shell region to form the epithelial layer and human umbilical vein endothelial cells (HUVECs) in the core to create the capillary structure. The bioinks used were collagen-based, crosslinked with tannic acid to provide the necessary mechanical stability for maintaining the vertical villus structure during and after bioprinting. The process involved careful optimization of pneumatic pressures (100 kPa for the core and 200 kPa for the shell) to achieve a stable and thin epithelial layer while preserving high cell viability (>90 %). The resulting villus structures (height = ~740 μm ; diameter = ~183 μm ; aspect ratio = ~4.2) closely mimicked the geometry of the native intestinal villi (height = ~721 μm ; diameter = ~151 μm ; aspect ratio = ~4.7), with a high aspect ratio and well-defined separation of the epithelium and capillary network, effectively replicating the complex anatomical features of the human intestine. Following suit to this work, the same research group presented an innovative method for crafting a human intestinal villi model using a collagen bioink and decellularized small intestine submucosa replicating

the microscale villus structure through a three-axis bioprinting system with a pneumatic pressure dispensing system. The incorporation of decellularized small intestine submucosa into the bioink improved the physiological realism, resulting in enhanced cellular activities and improved barrier integrity [244]. The optimized process, involving the tuning of parameters, like nozzle diameter and extrusion time along with tannic acid crosslinking, yielded a villus structure with precise geometry and high initial cell viability. *In vitro* experiments showcased enhanced cellular activities, including proliferation, early differentiation markers, and improved cell-to-cell adhesion compared to control structures. Like decellularized small intestinal mucosa, the use of porcine colon-derived decellularized extracellular matrix (colon dECM) was explored as a viable biomaterial by Han et al. (2022) to guide the maturation of bioprinted intestinal cells [245]. Tubular intestinal constructs were fabricated using a coaxial nozzle with human intestinal epithelial cell-laden in colon dECM and gelatin serving as the sacrificial ink in the core. The colon-dECM helped in maturation of cell aggregates to luminal cysts with enhanced expression of markers, such as LGR5, chromogranin A, and lysozyme relating to enteroendocrine function.

Torras et al. (2023) utilized LiBB (e.g., DLP) and created a gut model with crypt-villus structures [10]. The process exhibited high cell viability (>90 %) and precise spatial resolution, which emphasized the need for a stromal compartment for triggering the epithelial barrier function. Combining fibroblast-laden structures with epithelial cells resulted in a 3D *in vitro* model of the small intestinal mucosa, showcasing improved structural integrity compared to controls owing to the bidirectional crosstalk between fibroblasts and epithelial cells, promoting growth and differentiation. Following suit to this work, the same group continued focusing on this model of the intestinal mucosa, including stromal and epithelial compartments but this time incorporating human intestinal fibroblasts and enterocytes/goblet cells [246]. Using a GelMA- and polyethyleneglycol-diacrylate-based bioink, they successfully fabricated a 3D bioprinted intestinal model featuring proliferating fibroblasts and a well-polarized epithelial layer, resulting in enhanced permeability compared to a 2D model. Drug permeability experiments demonstrated more physiologically relevant results, suggesting the 3D bioprinted model's efficacy for drug absorption studies and highlighting the role of intestinal architecture in transport mechanisms. In another study, Cheng et al. (2023) developed a 3D bioprinted gut model using GelMA-embedded microchannels, which were seeded with Caco-2 cells (intestinal epithelial cells) to study bacteria-host interactions [247]. The model maintained high cell viability under anaerobic conditions, allowing direct coculturing of anaerobic bacteria with epithelial cells. Over 21 days, the model displayed villi-like structures with Caco-2 cells. A centimeter-scale intestinal tissue model, featuring a hollow tubular structure, capillaries, and tightly connected epithelium mimicking the ring-like folds of crypt-villi was developed using embedding bioprinting by Li et al. (2024) [248]. A photocurable bioink composed of GelMA, methacrylated sodium alginate, and poly (ethylene glycol) diacrylate was used for fabricating hollow tubes in a gelatin support bath, which had encapsulated endothelial cells (HUVECs). Caco-2 cells were seeded in the lumen and matured to form the epithelial intestine barrier exhibiting selective absorption function due to its higher transepithelial electrical resistance (TEER, 200–300 Ω).

Bile ducts are essential components of the digestive system as they facilitate the transportation of bile from the liver to the small intestine, aiding in fat digestion [249]. Unlike many other tissues, the bile duct possesses a branching network and a specialized epithelial lining crucial for the regulation and transport of bile [250]. Hence, successful bioprinting of bile ducts necessitates achieving high fidelity and functionality in replicating these complex structures. Bioprinting enables the fabrication of personalized bile ducts tailored to meet the specific requirements of individual patients. The utilization of bioprinting to create bile duct models highlights the potential of this technology in the field of regenerative medicine. Researchers strive to develop functional and biomimetic bile duct structures by employing innovative

biomaterials and advanced bioprinting techniques. As an example, Yan et al. (2018) explored 3D bioprinting of bile ducts by incorporating self-assembling peptide amphiphiles (PAs) into gelatin bioinks [251]. They optimized tissue regeneration by enhancing bioactivity and nanostructure. PAs, particularly (Ile-Lys-Val-Ala-Val) IKVAV-based PAs (mimicking the basement membrane), promote cholangiocyte polarization, maturation, and functional duct formation, potentially via the Notch 2 pathway. This study demonstrated the promise of using PA-containing bioinks for tissue engineering, disease modeling, and drug screening in bile duct regeneration. In addition to the approaches, attempts to create primary intrahepatic bile duct have also been realized. Xue et al. (2023) bioprinted liver tissue, which promoted bile duct morphogenesis and cellular interaction [142]. A polydimethylsiloxane (PDMS) microwell platform (PMP) was used to create uniform hepatic organoid building blocks (HOBB) with controlled cellular density. By combining a temperature-controlled bioprinting system with an alginate-gelatin-collagen-laminin-based bioink, reproducible construction of liver tissues exhibiting enhanced hepatobiliary function and intrahepatic bile duct networks were achieved. This approach is a valuable tool for creating intra-tissue bile ducts with an emphasis on studying liver regeneration and disease modeling.

3.4.2. Salivary glands

Salivary glands produce saliva, a fluid facilitating mouth lubrication, preliminary digestion, and oral infection prevention [252]. Major glands, like the parotid, submandibular, and sublingual, along with minor glands in the mouth, contribute to this process [253]. The gland structure involves acinar cells for fluid secretion, ductal cells for modifying saliva, and myoepithelial cells around acinar units [254]. Supportive tissues include blood vessels and nerves, which are crucial for gland stimulation and nutrient exchange [255].

Recent experiments have exclusively examined the use of magnetic-based bioprinting and bio assembly for producing secretory epithelia in salivary glands studied by Ferreira et al. and Adine et al. First, Ferreira et al. (2019) presented a magnetic 3D levitation (M3DL) method for the efficient generation of scaffold-free salivary gland (SG)-like organoids from porcine primary SG-derived cells [143]. These mini glands, developed within 7 days, demonstrate cellular diversity, proliferation, and functional secretory activity. M3DL offers a promising, scalable, and convenient 3D culture system for potential applications in treating dry mouth conditions. In the second study, Adine et al. (2018) introduced a magnetic 3D bioprinting (M3DB) technique to create innervated SG-like organoids using human dental pulp stem cells (hDPSCs) [256]. In this process, human dental pulp stem cells (hDPSCs) are tagged with magnetic nanoparticles, enabling them to be manipulated using magnetic forces. The magnetized cells are seeded into ultra-low attachment well plates and aggregated using a magnetic pin drive, forming spheroids within hours. These spheroids grow over several days, facilitating essential cell-cell interactions and developing extracellular matrix. After differentiation with fibroblast growth factor 10 (FGF10), the spheroids express SG epithelial and neuronal characteristics. The spheroids, exhibiting high viability, express SG compartments, and respond to neurostimulation. Upon transplantation into an *ex vivo* model, they significantly stimulate epithelial and neuronal growth in a damaged SG, showing promise for SG regeneration and addressing radiotherapy-induced xerostomia. M3DB's success highlights its potential in SG drug screening and regenerative medicine. Alternatively, Charbonneau et al. (2019) explored the feasibility of culturing human salivary cells in cost-effective gelled egg yolk plasma (GEYP) using 3D-Cryo insert wells for 14 days. GEYP, which can be printed with precise geometric shapes, supports cell growth. It served as a simulation for the epithelial-mesenchymal interface, demonstrating reproducible cell positioning [257]. Biofabrication techniques, like magnetic 3D levitation and the use of novel biomaterials, such as with GEYP, present opportunities for consistent organoid formation. In another study, Yin et al. (2023) showcased the potential of 3D bioprinting with the use of a

co-axial nozzle to generate hollow tubes (diameter of 600–2000 μm) to mimic the glandular nature of salivary epithelium [144]. This approach offers the advantage of creating branched structures (with the coaxial nozzle) and allowing cells with multiple cellular densities, which they tested using human patient-specific salivary stem/progenitor cells. The tubes facilitated accurate modeling of physiological processes, advancing our understanding of gland biology and pathology. This study underscores bioprinting's transformative role in salivary gland restoration, promising innovative therapeutic interventions in regenerative medicine.

3.5. Urothelium

The urinary epithelium (urothelium) lining the bladder, urethra, and ureter, is a transitional or distensible epithelium functioning as a barrier between urine and pathogens. It is composed of a superficial layer consisting of a monolayer of umbrella cells, followed by intermediate cells in one or multiple layers, and followed by a single basal layer. In addition to its mechanochemical barrier function, it also communicates changes to underlying nerve fibers and smooth muscle to facilitate ion/water uptake and contraction/expansion of the urinary tract [258]. The urothelium often sustains damage from various factors, such as infection or pathological disposition. Traditional repair methods face limitations but 3D bioprinting offers promising avenues for organ reconstruction. However, challenges such as graft rejection and ethical considerations persist, underscoring the need for continued research in 3D bioprinting of the urinary epithelium.

3.5.1. Urinary bladder

3D Bioprinting holds promise for replicating the complex structure and function of the urinary bladder, which plays a crucial role in storing and voiding urine. Anatomically, the bladder is divided into the apex, body, and base, and its wall consists of four layers: the mucosa, lamina propria, muscular layer, and serosal layer [259]. It is extraperitoneal in humans and intraperitoneal in pigs. The urothelium, consisting of basal, intermediate, and umbrella cells, forms a permeability barrier [260]. The submucosal layer supports urothelium neovascularization. The bladder wall is mostly muscular tissue with inner, middle, and outer layers [261]. Fascicles of longitudinally oriented muscle cells maintain bladder function during filling and emptying [262]. By mimicking this complex anatomy and cellular composition, bioprinting offers exciting possibilities for urinary bladder tissue engineering, including the creation of patient-specific constructs for disease modeling, drug testing, and potentially even bladder replacement therapies.

Imamura et al. (2018) utilized 3D bioprinting (Kenzan method) to create spheroid-based structures made of rat bone marrow-derived cells for regenerating radiation-injured rat urinary bladders [146]. After spheroids fused on a microneedle array (at Day 7), when transplanted, they survived, attracted blood vessels, and differentiated into smooth muscle cells, reducing fibrosis and improving urinary symptoms. Conventional tissue engineered solutions involve the use of mesenchymal stem cell-based cell sheets to reconstruct injured bladders which were very fragile and delicate for suturing. The fused spheroids (with lumen due to the microneedle insertion) enabled replicating the apico-basal polarity of the epithelium and facilitated the migration of neural cells from the host tissue. Multiple studies have contributed to advancing bladder tissue engineering with innovative approaches utilizing 3D bioprinting. For example, Serex et al. (2021) introduced a microfluidic print head for high cell density bioprinting (up to 10 million cells/mL) [263]. The high cell density favored cell-cell interactions and increased the viability of formed bladder organoids (derived from primary mouse bladder epithelial cells). On-demand cell concentration adjustments mimic the native tissue, simplifying organoid production. This technology holds promise for precise bioprinting in studying organogenesis and diseases, offering control for drug testing and organoid research. Furthermore, Chae et al. (2022) used 3D bioprinting and a dynamic

system to create a urinary bladder model with a tissue-specific dECM-based bioink derived from porcine bladder [147]. The platform allowed EBB of human bone marrow-derived stem cells (hBMSCs), supporting cell viability and myogenic differentiation. Their work also integrated a contract-release system (CRS) into the platform to mimic the bladder's mechanical tension, which enhanced stem cell differentiation. Importantly, the addition of dynamic mechanical stimulation significantly enhanced the myogenic differentiation of hBMSCs within tissue constructs. Collectively, these studies highlight the transformative potential of 3D bioprinting in regenerating damaged bladders, offering new avenues for research and therapeutic interventions in bladder-related diseases.

3.5.2. Renal proximal tubules

Renal proximal tubules (PTs) play a pivotal role in kidney function and are often targeted in chronic kidney disease (CKD). Traditional models, such as 2D cultures and *in vivo* animal models, have limitations in accurately recapitulating human renal PT pathology due to their inability to recreate the intricate 3D microenvironment of the kidney. By leveraging 3D bioprinting, bioprinted models provide a more physiologically relevant platform for studying renal and PT pathology, enabling researchers to gain deeper insights into the mechanisms underlying CKD progression and to develop related novel therapeutic interventions.

The field of renal tissue engineering has witnessed significant advancements through the innovative application of 3D bioprinting. Homan et al. (2016) introduced a bioprinting method for constructing 3D human renal proximal tubules on perfusable chips [148]. A sacrificial Pluronic F127 ink was 3D printed onto a gelatin-fibrin-based hydrogel to create a hollow proximal tubule of a nephron. The sacrificial ink was then removed to inject human immortalized proximal tubule epithelial cells (PTECs) into channels, which adhered and formed the engineered tubules. 3D Printed PTs exhibited apical-basolateral polarity as noted by cells resting on the basement membrane (laminin and collagen type IV) and brush border structures (microvilli) on the apical side. The bioprinting process enabled precise control over tubule characteristics, showcasing its potential for creating advanced organ models. The study demonstrated the model's utility in drug toxicity testing, specifically assessing the impact of cyclosporine A on proximal tubules. Building upon this foundation, Singh et al. (2020) used coaxial bioprinting to create advanced renal tissue analogs, addressing the challenge of vascularized and perfusable renal tubule structures [149]. A hybrid bioink of decellularized porcine kidney matrix and sodium alginate-fostered a conducive microenvironment. Coaxial bioprinting yielded stable hollow tubes with HUVECs in the lumen and renal proximal tubule epithelial cells in the shell, mimicking native renal architecture. Bioprinted tubes cultured for 28 days exhibited prominent expression of aquaporin (*AQP1*) and vessel-specific CD31/VE-cadherin markers, suggesting endothelial-epithelial cell interactions, which are necessary for testing drugs for nephrotoxicity. *In vivo* renal sub-capsular transplantation in NOD/SCID mice showcases therapeutic potential, marking a significant stride in bioprinting. Addario et al. (2020) in a similar fashion used a microfluidic platform and bioprinted renal tubules to form core-shell-based tubular structures using an alginate-pectin bioink addressing the need for advanced *in vitro* models to study CKD [264]. By isolating primary renal cells and combining them with polysaccharide bioinks, they successfully fabricated core-shell constructs resembling tubules. Key to their success was optimizing the bioprinting process, focusing on bioink viscosity and process parameters. The study demonstrated high cell viability and metabolic activity in the constructs, offering a promising platform for drug testing and disease modeling. In another study, Tröndle et al. (2021) presented a bioprinting and self-assembly method for the scalable fabrication of renal structures, in order to develop 3D kidney tissue models in pharmaceutical screenings [12]. Using DBB, they achieved defined cell patterns with high viability, allowing customization and hybrid tubule creation.

Advantages include upregulated kidney-specific genes and integration into a microfluidic chip for fluidic access. Challenges involve ensuring long-term stability, which they addressed in their follow-up work by Pichler et al. (2022) by studying directly reprogrammed induced renal tubular epithelial cells (iRECs) in various hydrogels (Matrigel™, fibrin, collagen, and alginate) for their long-term survival [265]. Notably, they found that the choice of hydrogel significantly affected cellular morphology and transcriptional responses, indicating a considerable degree of plasticity in iRECs based on their microenvironment. Furthermore, utilizing a bioprinted tubular model, they were able to characterize the phenotypic alterations associated with PKD, such as disrupted tubular morphology and upregulated expression of certain genes, like *Aldh1a1*. This model provided insights into the early disease manifestations of PKD and highlighted potential targets for therapeutic interventions.

Furthermore, Jin et al. (2020) explored the application of 3D bioprinting in renal tissue engineering [266]. This study integrated microtissues (typically a spheroid obtained through the hanging drop method) derived from human adipose-derived stem cells (hADSCs) into a bioprinted structure, which was then encapsulated and implanted subcutaneously in mice. Key findings revealed enhanced expression of vascular endothelial growth factor A (VEGFA) and tumor necrosis factor-stimulated gene-6 (TSG-6) in bioprinted microtissues compared to hADSCs, indicating improved vascularization and anti-inflammatory potential. Moreover, histological analysis demonstrated that bioprinted structures containing ID-MTs mimicked the smooth muscle layer of the native urinary tract. Notably, seeded urothelial cells formed a protective barrier on the encapsulated structure, suggesting potential for urinary tract patch applications. This study has a promising role in 3D bioprinting in tissue engineering for urinary tract reconstruction. These collective efforts highlight the diverse applications and transformative potential of 3D bioprinting in renal tissue engineering and regenerative medicine.

3.5.3. Ureter and urethra

Abnormalities of the urethra, whether malignant, traumatic, infectious, or developmental, can severely impact an individual's quality of life and incur substantial healthcare costs due to associated complications, such as painful or obstructed urination, urinary tract infections, sexual dysfunction, urinary retention, and even renal failure [267]. Urethroplasty, a surgical procedure aimed at repairing or replacing a section of the urethra, is often necessitated in individuals affected by conditions like hypospadias and urethral stricture disease (narrowing of the urethra). However, conventional approaches to urethroplasty face ongoing challenges, including the need for personalized, multilayered constructs with appropriate mechanical properties and biochemical cues. Herein lies the promise of bioprinting [268]. By leveraging bioprinting, researchers and clinicians can fabricate customized, multilayered urethral constructs with precise control over mechanical properties and spatial distribution of cells. Biomaterials with tunable mechanical characteristics can be utilized as bioinks to mimic the native urethral microenvironment, promoting cellular viability, proliferation, and functional integration within the host tissue upon implantation.

Zhang et al. (2017) achieved success in urethral tissue engineering using PCL/poly(lactide-co-caprolactone) (PLCL) blend and dual autologous cells in fibrin [269]. Their team aimed to mimic the mechanical properties and cell growth environment of native rabbit urethra. The study showed successful bioprinting of a tubular scaffold with a PCL/PLCL (50:50) blend, showing mechanical properties comparable to natural urethra. Urothelial cells (UCs) and smooth muscle cells (SMCs) exhibited over 80 % viability post-bioprinting and maintained proliferation and biomarker expression in the hydrogel. This study lays the groundwork for further exploration of 3D bioprinting's potential in creating biomimetic urethral constructs. Building upon this foundation, Pi et al. (2018) used coaxial bioprinting and a customized bioink consisting of poly (ethylene glycol) (PEG) acrylate with tripentaerythritol

core (PEGOA) in GelMA and alginate for urethral tissue fabrication (Fig. 7A) [270]. This approach enabled the single step bioprinting of multilayered tubular (perfusable) tissues with tunable characteristics, supporting cell viability and proliferation of human urothelial cells and bladder smooth muscle cells.

3.6. Female reproductive epithelium

The ovary and uterus have different epithelial arrangements; however, they share some common features, such as they are mainly composed of microvillated luminal epithelial cells resting on a basement membrane rich in collagen type IV and laminin. In the uterus, columnar luminal epithelial cells are also interspaced by ciliated cells and microvillated secretory cells [271]. One of the hallmarks of this epithelium is its dynamic reorganization with respect to hormonal changes that happen during the reproductive cycle, hence ECM remodeling is very crucial and thus the use of an appropriate bioink is paramount here.

3.6.1. Vaginal and uterine epithelium

Traditional vaginal reconstruction methods often fall short, lacking in functionality and leading to complications [272,273]. While tissue engineering has made strides, it faces challenges like low cell survival rates and lack of personalization. Studies exploring the application of 3D bioprinting for vaginal reconstruction are limited in number and scope. While there has been significant progress in tissue engineering and regenerative medicine, the application of 3D bioprinting to address vaginal reconstruction remains relatively underexplored. Notably, there are limited studies focusing specifically on this area. For example, Hou et al. (2021) explored EBB for vaginal epithelium reconstruction using a pig-derived acellular vagina matrix (AVM) bioink loaded with rat bone marrow-derived mesenchymal stem cells (rBMSCs) [150]. After the decellularization process, AVM exhibited enhanced biocompatibility and mechanical properties when combined with gelatin and alginate. Encapsulating rBMSCs enhanced vascularization and epithelization when bioprinted constructs were placed in rat subcutaneous pockets at Week 4, indicating their potential for effective vaginal epithelial reconstruction. Challenges include the mechanical limitations of ECM-derived bioinks compared to synthetic counterparts highlighting the need for further research.

The uterine integrity is vital for fertility, but injuries can disrupt its structure and function. Current approaches lack homogeneity and fail to replicate the uterine's bilayer structure. In contrast, 3D bioprinting enables precise replication of this structure, with homogeneous cell distribution holding potential for restoring endometrial function and addressing infertility and reproductive health challenges. Souza et al. (2017) utilize magnetic 3D bioprinting to create a 3D *in vitro* model for studying human uterine contractility [151]. By magnetizing myometrial cells with nanoparticles, they successfully bioprinted rings that contracted immediately after bioprinting. This approach allows real-time monitoring of contraction dynamics. The study demonstrates the assay's applicability with both commercially available and patient-derived cells, revealing patient-specific responses to tocolytic drugs. In a complementary effort, Ji et al. (2020) developed a 3D bioprinted construct loaded with human-induced pluripotent stem cell-derived mesenchymal stem cells (hiMSCs) demonstrating promising results for repairing damaged uterine endometrium [274]. The construct enhanced hiMSC survival and significantly improved endometrial tissue regeneration in an animal model. Despite the limited hiMSC differentiation into endometrial cells, the construct, in combination with hiMSCs, positively impacted the endometrial structure and function. Expanding on these advancements, Nie et al. (2023) developed a new approach for treating severe uterine endometrial damage via EBB using an alginate-hyaluronic acid bioink (Fig. 7B) [6]. The study focused on a unique bilayer endometrial construct (EC), where the upper layer consisted of neonatal rat endometrial epithelial cells (EECs) while the lower

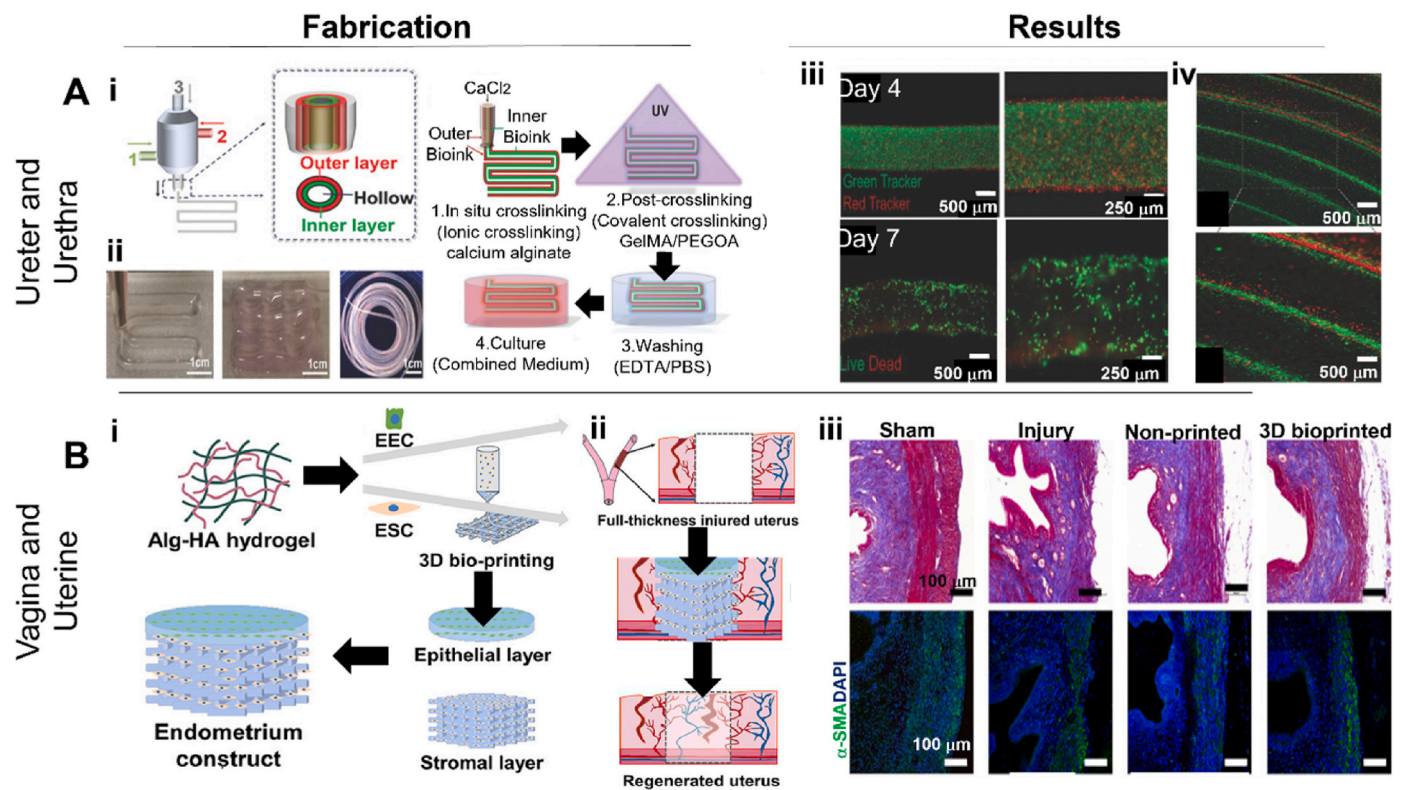


Fig. 7. (A) i) Schematic illustration of coaxial bioprinting generating multilayered hollow tubes, ii) images showing bioprinted perfusable tubes in various shapes, iii) fluorescence images of human urothelial cells labeled with a green cell tracker (inner) and human bladder smooth muscle cells labeled with a red cell tracker (outer) on Days 4 and 7, iv) confocal images showing the gradual transition from a double-layered tube structure (red/green) to a single-layered tube (only green) (reproduced with permission from Ref. [270], 2024 John Wiley & Sons). (B) Schematic representation of a 3D bio-printed endometrial construct, which restores the full-thickness morphology and fertility of an injured uterine endometrium, i) *in vitro*, ii) *in vivo*, iii) Masson's trichrome staining and IF labeling of alpha-smooth muscle actin (α -SMA) (reproduced with permission from Ref. [6], 2024 Elsevier).

layer featured a grid-like microstructure loaded with endometrial stromal cells (ESCs). In a rat model with partial full-thickness uterine excision, 3D bioprinted ECs successfully restored the morphology and structure of the endometrial wall, significantly improving reproductive outcomes. ECs demonstrated biocompatibility, cell survival, and degradation features, making it a promising option for treating severe endometrial injuries.

3.6.2. Mammary glands

The mammary gland's development relies on hormonal cues and interactions within its microenvironment. In contrast to the other vaginal/uterine epithelium, the mammary epithelium is made up of branched ducts ending with glandular structures (acini). This acinus is constituted of double-layered microvillated luminal epithelial cells, encased by contractile myoepithelial cells with the basement membrane surrounding it [271]. In recent years, researchers have been leveraging bioprinting techniques to advance both basic biological understanding and practical applications in mammary tissue engineering. Reid et al. (2018) used bioprinting to achieve precise control over mammary epithelial structures, overcoming variability in traditional methods [275]. Their work demonstrated that a pulled glass microneedle (10–100 μ m in diameter) could be used to dispense cells (in volumes as low as 10 nL) within polymerized collagen without disrupting the matrix structure. In a follow-up study, utilizing the same accessible bioprinting technique, Mollica et al. (2019) investigated the effect of rat and human-derived mammary ECM as a matrix for mammary epithelial organoid development [152]. By meticulously controlling the spatial arrangement of cells, they engineered constructs featuring multiple cell types and growth factors tailored to individual patients. This level of customization not only enhances tissue integration but also ensures

long-term viability after implantation. Overall, this study advances our understanding of developing consistent mammary epithelial organoids through controlled and reproducible 3D structure generation. Building upon this foundation, Swaminathan et al. (2019) demonstrated the EBB of 3D breast epithelial spheroids for drug testing applications [153]. By directly bioprinting pre-formed breast epithelial spheroids in an alginate-based bioink, they tested different breast epithelial cell lines and were able to distinguish between cancerous and non-cancerous cell lines to form spheroids with hollow cores, which recapitulates the glandular structures. Notably, bioprinted breast spheroids exhibited resistance to paclitaxel, a finding influenced by co-culture with endothelial cells [124]. In a recent development by Koskinen et al. (2024), a novel 3D bioprinting approach was developed to engineer normal and cancerous mammary epithelial cultures into a branched Y-shape, closely mimicking the architecture of the mammary ductal network [154]. They found that both normal and cancerous cells proliferate more at the branch tips compared to the trunk region, with the highest proliferation observed further away from the branch point. Interestingly, this proliferation pattern was independent of transforming growth factor beta ($TGF\beta$) signaling. The study also demonstrated that inhibition of $TGF\beta$ signaling reduced the invasion of cancer cells but did not disrupt the spatial control of cell proliferation. Additionally, the proximity of branch points inhibited cell proliferation, mimicking the behavior observed in the mammary gland. This research highlights the importance of tissue geometry and ECM composition in regulating cell behavior in breast morphogenesis and cancer progression.

4. Induced pluripotent stem cells (iPSCs) derived epithelial tissue models: a new direction

iPSCs have revolutionized the field of regenerative medicine and disease modeling due to their ability to differentiate into various cell types. This versatility makes iPSCs a valuable tool for developing complex tissue models and advancing our understanding of various diseases. One of the most promising applications of iPSCs is in 3D bioprinting, where the multipotency of iPSCs and directed control of the physicochemical microenvironment through biomaterials can be harnessed to attain fabricated tissues. Innovative cell culture systems that incorporate these complex 3D structures including epithelial tissues offer new possibilities for developing *in vitro* models with enhanced tissue functionality. Progress in stem cell research has facilitated the creation of organoids that replicate the complex 3D structure and physiological functions observed in living tissues.

A notable advancement in this field was introduced by Brassard et al. (2021), who developed a 3D bioprinting approach called BATE that uses iPSCs to create complex tissue structures (Fig. 8A) [145]. BATE allows for the deposition of iPSCs into hydrogels (i.e., Matrigel™ and collagen) and supports rapid lumen formation and growth, overcoming the

limitations of traditional organoid cultures. BATE enables real-time monitoring and precise cell placement, creating multi-tissue models such as GI tubes while preserving organ-specific identities and functions. Similarly, Lawlor et al. (2021) used an EBB approach that uses human pluripotent stem cells (hPSCs) to create kidney organoids (Fig. 8B) [276]. This method enhances reproducibility and throughput, addressing the limitations of traditional manual processes. The bioprinting approach involves the creation of a cell paste from differentiated hPSCs, which is then precisely deposited to form organoids. This automated process allows for the generation of organoids with highly reproducible cell numbers and viability, significantly increasing nephron yield and maturation compared to manual methods. The bioprinted organoids retain key renal progenitor lineages and exhibit functional markers, making them suitable for drug testing and potential tissue engineering applications. Expanding on the theme of cost-effective bioprinting, Shin et al. (2024) developed a cost-effective and customizable pneumatic force-driven EBB platform for generating kidney organoids from human iPSCs [277]. This platform allows precise and consistent deposition of nephron progenitor cells (NPCs) in a droplet form, enabling high-throughput and reproducible production of organoids. The system demonstrated the capability to bioprint kidney organoids with complex

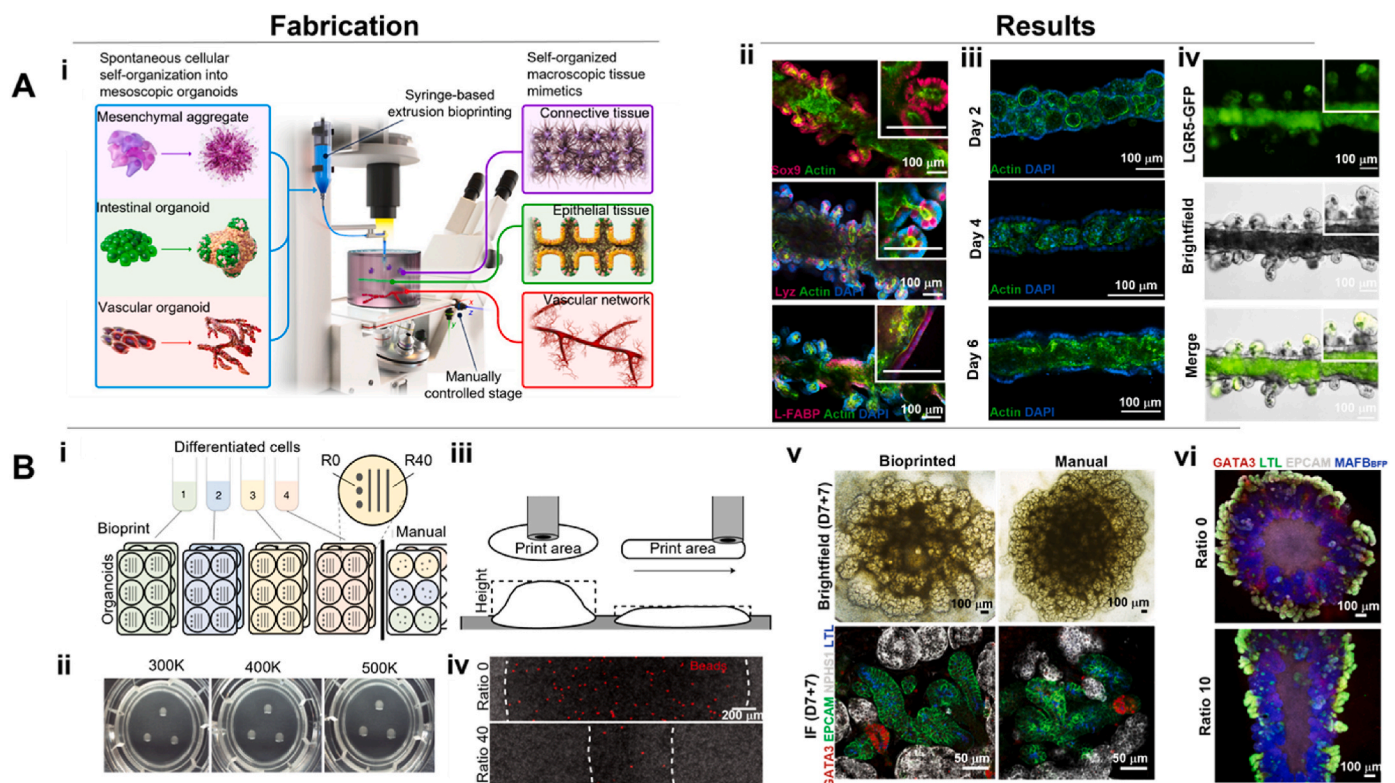


Fig. 8. (A) i) Illustration of the bioprinting concept showcasing the spontaneous self-organization of building blocks to form epithelial tissues, ii) IF images of tubes, displaying both a macroscopic view and higher magnification insets, highlighting stem cells and progenitors, iii) confocal IF images demonstrating the formation of a continuous lumen through colony fusion, iv) IF image of LGR5-eGFP and corresponding bright-field image of a tube after 7 days, showing darker Paneth cells interspersed among stem cells within the crypts (reproduced with permission from Ref. [145], 2024 Springer Nature Limited). (B) i) A single scRNAseq library per condition was created from multiple barcoded organoid sets. For R0 and R40 conditions, 1.1×10^5 cells were used, while manual organoids were generated from 2.3×10^5 cells, ii) the demonstration includes bioprinted kidney organoids with varying cell numbers during bioprinting (500K, 400K, 300K), iii) organoids of increasing length were generated using a consistent initial cell number (1.1×10^5 cells). The diagram shows how the organoid profile and height are affected by bioprinting, changing from a deposition ratio of 0 (no needle movement during extrusion) to 40 (needle movement across the Transwell surface during extrusion). The deposition ratio is defined as the ratio of tip movement to the volume of cell suspension extruded, iv) ratios 0 and 40 cell paste depositions included fluorescent beads to measure cell paste distribution across the Transwell surface. Representative images from the dataset used for quantification are shown, v) brightfield images (Day 7 + 7) and whole-mount IF (Day 7 + 14) of both manual and bioprinted kidney organoids, created from the same batch of iPSC-derived intermediate mesoderm, reveal patterning and segmented nephrons. The IF markers used are EPCAM (epithelium, green), LTL (proximal tubule, blue), NPHS1 (glomeruli, white), and GATA3 (connecting segment/collecting duct, red), vi) IF images of bioprinted organoids from each configuration show MAFBmTagBFP2 (glomeruli, blue fluorescence), EPCAM (epithelium, grey), LTL (proximal tubule, green), and GATA3 (connecting segment/collecting duct, red) (reproduced with permission from Ref. [276], 2024 Springer Nature Limited).

structures, including glomeruli, proximal tubules, distal tubules, and endothelial cells, using as few as 8000 cells. This approach ensures high nutrient accessibility and reduces resource demands, making it suitable for preclinical safety evaluations and nephrotoxicity testing of new drugs.

The epicardium is a crucial epithelial tissue, which still needs remains to be explored. In this regard, Maiullari et al. (2018) engineered vascularized heart tissue using 3D bioprinting, combining HUVECs and iPSCs-derived cardiomyocytes (CMs) [278]. The bioink used here was composed of alginate and polyethylene glycol-fibrinogen (PF) to encapsulate the cells, providing the necessary mechanical support and biocompatibility for cell growth and differentiation. A custom-designed microfluidic printing head (MPH) consisted of a coaxial nozzle system that facilitated immediate gelation of the bioink upon extrusion. The team created multi-cellular constructs with iPSC-derived cardiomyocytes and forming blood vessel-like structures with HUVECs, mimicking the natural cardiac tissue environment. Bioprinted iPSC-derived cardiomyocytes maintained high viability (80–90 %) and demonstrated organized, synchronous contractions, essential for proper heart function. The co-culturing with HUVECs enhanced the formation of vascular networks within the constructs, crucial for nutrient supply and waste removal. When implanted in immunodeficient mice, bioprinted constructs showed improved integration equipped with neo-epicardium and new vasculature, demonstrating the potential for functional vascularized cardiac tissue fabrication.

The rest of the studies discussed below, although not involving 3D bioprinting, underscore the potential of iPSC-derived models to replicate complex epithelial tissue structures and functions. Integrating these iPSC-derived models with 3D bioprinting techniques could further enhance their applications, enabling the creation of more sophisticated and accurate tissue models for disease modelling research and therapeutic development. Furthering the application of iPSCs in disease modeling, Schruf et al. (2020) have developed lung fibrosis model using human (iPSC)-derived ATII-like cells at ALI to study idiopathic pulmonary fibrosis (IPF), a disease characterized by progressive lung fibrosis [279]. This model mimics the *in vivo* lung environment and provides a platform for investigating the differentiation and dysfunction of alveolar epithelial progenitor cells in IPF. By treating iPSC-derived cells with an IPF-relevant cocktail (IPF-RC) that simulates the pro-fibrotic cytokine milieu, the researchers observed an increase in IPF biomarkers and a shift in cell differentiation towards an airway epithelial-like phenotype, resembling the bronchiolization seen in IPF patients. In another study, Abo et al. (2020) demonstrated that iPSC-derived alveolar and airway epithelial cells, cultured in ALI, express key genes necessary for SARS-CoV-2 infection, including ACE2 and TMPRSS2 [280]. These cells maintain their characteristic identity as ATII-like cells (iAT2s) at ALI, expressing lung-specific markers, such as SFTPC and NKX2-1, crucial for modeling lung epithelial interactions with the virus. Transcriptomic analysis revealed that iAT2s closely resemble primary lung epithelial cells both in gene expression profiles and susceptibility to viral infection, highlighting their potential as physiologically relevant models. Alternatively, iPSC-derived iAT2s and airway epithelial cells co-cultured at ALI, researchers can emulate the microenvironment necessary to study viral infections like SARS-CoV-2. The ability to precisely position these cells in a 3D bioprinted structure could facilitate the development of advanced heterocellular models that mimic the cellular architecture and functionality of the human lung.

Apart from the distal lung epithelium, the focus on reconstructing upper airway epithelium using iPSCs has been investigated. For instance, Ikeda et al. (2017) explored the use of iPSCs for regenerating tracheal epithelium, aiming to enhance minimally invasive treatments for tracheal defects [281]. The researchers created tdTomato⁺ mouse iPSCs and differentiated them into tracheal epithelial cells. These differentiated cells were then implanted with artificial tracheas into nude rats with tracheal defects. The key findings indicated that the iPSC-derived tracheal epithelial cells rescued the tracheal defects.

Histological analysis revealed that these cells developed structures resembling the normal tracheal epithelium. Additionally, the differentiated epithelial tissues exhibited ciliated structures and expressed markers, such as β -tubulin IV, ZO-1, and Keratin 5 (KRT5), demonstrating both functional and structural maturity. Differentiated iPSC-derived tracheal epithelial cells can be integrated into a bioprinting workflow to create realistic tracheal models, enhancing drug testing and disease modelling research.

In another application pertaining to digestive epithelium, Gleeson et al. (2020) developed an iPSC-derived model using human intestinal organoids (HIOs) and colonic organoids (HCOs) to study barrier dysfunction in inflammatory bowel disease (IBD) [282]. Their study focused on understanding increased intestinal permeability observed in IBD patients, using iPSCs from healthy controls and different IBD patient groups. HCOs showed distinct gene expression and higher basal TEER compared to HIOs. Under TNF α and IFN γ stimulation, both HIOs and HCOs exhibited significantly increased permeability, with altered localization of tight and adherens junction proteins. In another study, Takayama et al. (2019) successfully generated homogenous and functional human intestinal epithelial cells from iPSCs using CDX2 transduction [283]. These cells closely mimic human small intestinal cells in drug absorption rates and the expression of critical enzymes like CYP3A4. This model surpasses traditional cell lines, such as Caco-2, in predicting intestinal pharmacokinetics and drug responses, making it highly valuable for pharmaceutical research.

Despite recent advances in biofabrication strategies enabling the application of 3D bioprinting to iPSCs, the field is still in its early stages. Challenges, such as the poor survival of iPSCs as single cells, their sensitivity to environmental conditions, and their tendency to form clusters or colonies pose significant hurdles, which still needs to be addressed [284,285]. Moreover, current research is primarily limited to the use of specific iPSC lines for a particular epithelial tissue type, which hinders their translation for personalized medicine applications. Therefore, recent advancements in development of hypoimmunogenic iPSCs will play a key role in the translation of iPSC-based bioprinted epithelial tissues for regenerative medicine applications [286]. While iPSCs have garnered significant attention for their versatility in differentiating into various cell types, the integration of iPSCs with advanced bioprinting strategies offers a promising direction for creation of complex tissue models. For instance, high-resolution bioprinting methods, such as VBP and multiphoton lithography, allow for the precise placement of iPSCs within intricate tissue architectures, facilitating the development of highly detailed organoids and tissue constructs with a resolution range of 0.1–10 μ m [287]. Additionally, the use of bioinks that incorporate ECM components, tailored specifically for iPSCs, can improve the microenvironment, promoting better cell differentiation and maturation. Moreover, scaffold-free bioprinting techniques that enable the self-assembly of stem cell-derived spheroids or organoids into functional tissues, such as aspiration-assisted bioprinting and its derivatives, offer a pathway to creating more physiologically relevant models without the need for synthetic scaffolds [288,289]. These advanced bioprinting strategies not only enhance the potential of iPSCs in tissue engineering but also address key challenges, such as achieving high cell viability, precise spatial organization, and the replication of complex tissue-specific functions. By focusing on these cutting-edge bioprinting techniques, the field can move closer to realizing the full potential of iPSCs in regenerative medicine and disease modeling.

5. Challenges and opportunities in clinical translation – a status Quo

The development of functional epithelial tissue is highly critical for its success in regeneration and serves as an ideal *in vitro* tool for inducing and modeling diseased conditions towards testing/screening potential drug candidates. Though bioprinting has paved the way for advancing our knowledge in generating epithelial tissues, which are more robust

than manual methods, we are still far from translating a bioprinted epithelium to the clinic. In this section, we provide insights on how certain clinical trials are shaping our mechanistic understanding of patient-derived cells to perceive the genomic variations and heterogeneity to design better clinical interventions. Advances in stem cell biology have enabled researchers to generate protocols that recapitulate native tissues in terms of cellular polarity and the use of 3D bioprinting provides unprecedented control in biofabrication workflow while ensuring reproducibility in a high throughput manner. For instance, in a clinical trial (ClinicalTrials.gov identifier number: NCT06265298), the cessation of corneal epithelium renewal due to limbal stem cell deficiency was addressed by transdifferentiating oral mucosa (buccal cells obtained from the same patient) into epithelial cells towards conjunctival reconstruction. Similarly, the use of amniotic epithelial cells (identifier number: NCT00344708), and labial mucosal epithelial cells (identifier number: NCT04995926) have been explored in treating ocular epithelial ulcers associated with limbal stem cell deficiency. Tissue-engineered corneal epithelium is one of the epithelial tissues that has been successfully translated [290]. This bioartificial anterior lamellar cornea consists of nanostructured-fibrin-agarose (fibrin from donor plasma and type 7 agarose) based hydrogel seeded with human allogenic keratocytes and corneal epithelial cells. Though the study adopted a traditional tissue engineering route using Transwell-insert and ALI culture, there is scope here in utilizing bioprinting to incorporate good manufacturing practices (GMP) to improve the reliability and reproducibility of the obtained corneal epithelial transplants.

Apart from corneal epithelium, among the integumentary epithelium, the skin is the only epithelial tissue, which has seen advancement into clinical translation. A GMP-compliant dermo-epidermal substitute (identifier number: NCT04925323) was developed from 25 healthy individuals' isolated fibroblasts and keratocytes, who opted for aesthetic plastic reconstruction. 3D Photogrammetry helps in quick and precise reconstruction of the defect topography (with a resolution of $\sim 30 \mu\text{m}$) [291]. Intraoperative bioprinting has immense scope here as it is easier to access superficial tissues like skin towards treating large surface third-degree burns in a clinical setting. More recently, the COVID pandemic has piqued the interest of researchers in the airway epithelium. Traditionally, chronic obstructive pulmonary disease (COPD) affects millions worldwide and interventions for such pathology necessitate robust humanized models, which do not rely on animals. In this regard, the use of iPSCs to model the bronchial epithelium in severe asthma (due to bronchopulmonary aspergillosis) has been demonstrated (identifier number: NCT05616338). Inflammatory cells and NECs from patients exhibiting type 2 bronchial inflammation were isolated and used as reference controls for modulating the iPSC derived inflamed bronchial epithelium towards devising treatment regimen. The efficacy of prospective drugs can be studied *in vitro* but under clinically relevant conditions by measuring the transepithelial resistance, ciliary beating, and variation in secretion of mucin (MUC5AC and MUC5B). In similar lines, patient-derived BECs have been utilized to study the mean speed of wound closure with respect to COPD stimulants (identifier number: NCT02873988). Bioprinting could help expedite these clinically relevant *in vitro* models, which is gaining interest in developing humanized models as the US Food and Drug Administration (FDA) and European regulatory agencies are trying to phase out animal testing. Though, only a handful of epithelial tissues, such as cornea and skin, have traversed into clinics, the regulatory hurdles for other tissues are impending. Obtaining a 510(K) US FDA clearance for a bioprinted tissue construct is quite cumbersome since these tissue-engineered products do not fall under the minimally manipulated classification (class 1 or 2 device). However, these bioprinted products can avert a more stringent route (Pre-market approval – PMA in US FDA) if they can be demonstrated that they are substantially equivalent to already marketed tissue engineered-substitutes [292]. Poietis™ (France) has a bioprinted full-thickness skin composed of human fibroblasts encapsulated in collagen type I bioink and overlaid with differentiated human

keratinocytes forming the epidermis, which was bioprinted using their proprietary LaBB system. Similarly, such bioprinted skin (integumentary epithelium) can also benefit from existing tissue engineered solutions, such as Epicel™ (Genzyme Biosurgery, USA) (cultured autologous epidermal grafts) and TransCyte™ (Shire Regenerative Medicine, USA) (human fibroblast-based substitute for full thickness burns) [293].

6. Summary and future perspectives

Mimicking epithelial tissue *in vitro* is difficult due to apical-basal polarity, which needs to be achieved to maintain its functionality. Traditional techniques such as ALI have yielded limited success; however, bioprinting has enabled researchers to fabricate epithelial tissues with much more complexities such as the alveolar or renal tubule, as opposed to 2D planar organizations. Impetus can be given in two directions: (i) manufacturing readiness levels (MRL) and (ii) technology readiness levels (TRL). In terms of manufacturing clinically relevant tissues, engineering techniques such as micropatterning, microfluidic-based printing, and DBB confer a greater degree of control over cellular patterning, cell seeding within lumens, and cell density for cell-cell interactions, respectively. Additionally, when such fabricated structures are coupled with dynamic culture conditions (exposure to shear or pulsatile flow) or mechanical loading in bioreactor platforms could further help in generating more organized epithelium, which has not been explored before. The choice of biomaterial to be used as bioinks also plays a crucial role as it dictates the biophysical cue forming the microniche or basement membrane on which these epithelial cells mature. dECM has gained importance because it harbors the essential cell binding motifs and crucial cell signaling factors (extracellular vesicles), which stimulate the differentiation of progenitor cells or help in the maintenance of the phenotype of bioprinted primary cells. Though many of the studies covered in this Review are in the preclinical stage, it becomes essential to define the pharmacological and toxicological effects of fabricated constructs for their safety as a therapeutic product. The regulatory landscape expects that these transplantable grafts be manufactured in GMP-compliant facilities, which would need proper screening of these biomaterials used as bioinks. Sterility tests compliant with to US or EU pharmacopeia ensure that endotoxins, mycoplasma, and adenovirus are absent. Furthermore, cells used also need to be verified by a genetic fingerprint assay and karyotyping to ascertain cell uniformity and the absence of any chromosomal alterations. The biomaterials used must qualify as clinical grade materials complying with ISO 10993 standards, which would help in further translation of these technologies to clinics. Adopting a quality management system (QMS) and establishing the protocols under current good manufacturing practices (cGMP) guidelines is very much essential to improve the efficiency of these therapies while minimizing risks.

In terms of TRL, two important factors play a vital role; (i) scaling up of these constructs and (ii) compatibility in storage and transportation before it can be transplanted. For any technology before it can be commercialized, it has to follow a blueprint involving TRL 1 to 9, a template laid down by NASA (National Aeronautics and Space Administration, USA) [294]. 3D Bioprinting is still in nascent TRL 5 and 6, involving animal testing and preliminary human clinical trials. TRL 8 involves an overall risk-benefit assessment (Phase 3 clinical trial) after which it needs to go through US FDA PMA stage for technology commercialization. Although much of the research discussed here and in the problem definition stage uses lab-grade materials, early adoption of cGMP-related guidelines for biomaterials and cell practices is essential to streamline regulatory clearances. In addition to these regulatory challenges, there are ethical challenges that need to be addressed. Use of bioprinted tissues in clinical trials as a last resort (inclusion criteria) as opposed to healthy individuals is still debatable. Howbeit, bioprinting has proven to be one of the prime technology disruptors in the health-care sector to fabricate tissue constructs in resolution akin to native tissues and holds promise to revolutionize regenerative medicine and

disease modeling for drug testing. With the progress made in the last decade as highlighted in this Review, bioprinting has certainly been very instrumental in replicating complex epithelial tissues and holds precedence in further widening our understanding in epithelial cell biology and pathology.

Funding

Funding was received for this work.

Declaration of competing interest

The authors declare the following financial interests/personal relationships which may be considered as potential competing interests:

Ibrahim Ozbolat reports financial support was provided by National Institute of Allergy and Infectious Diseases. Ibrahim Ozbolat reports was provided by National Institute of Arthritis and Musculoskeletal and Skin Diseases. Ibrahim Ozbolat reports a relationship with Biolife4D that includes: board membership and equity or stocks. Ibrahim Ozbolat reports a relationship with Healshape that includes: board membership. If there are other authors, they declare that they have no known competing financial interests or personal relationships that could have appeared to influence the work reported in this paper.

CRedit authorship contribution statement

Irem Deniz Derman: Writing – review & editing, Writing – original draft, Formal analysis, Data curation, Conceptualization. **Joseph Christakiran Moses:** Writing – review & editing, Writing – original draft, Methodology, Data curation, Conceptualization. **Taino Rivera:** Writing – review & editing, Writing – original draft, Formal analysis, Data curation. **Ibrahim T. Ozbolat:** Writing – review & editing, Writing – original draft, Supervision, Investigation, Funding acquisition, Formal analysis, Conceptualization.

Acknowledgements

This research was supported by National Institute of Allergy and Infectious Diseases Award U19AI142733 (I.T.O.) and the National Institute of Arthritis and Musculoskeletal and Skin Diseases Award R21AR082668 (I.T.O.). Opinions, interpretations, conclusions, and recommendations contained herein are those of the author(s) and are not necessarily endorsed by the National Institute of Allergy and Infectious Diseases and the National Institute of Arthritis and Musculoskeletal and Skin Diseases.

References

- [1] N. Arumugasaamy, J. Navarro, J. Kent Leach, P.C.W. Kim, J.P. Fisher, In vitro models for studying transport across epithelial tissue barriers, *Ann. Biomed. Eng.* 47 (2019), <https://doi.org/10.1007/s10439-018-02124-w>.
- [2] M.-R. Na, *Structure and function of skin*, in: *Toxicology of the Skin*, CRC Press, 2010.
- [3] M. Fuest, G.H.F. Yam, J.S. Mehta, D.F.D. Campos, Prospects and challenges of translational corneal bioprinting, *Bioengineering* 7 (2020), <https://doi.org/10.3390/bioengineering7030071>.
- [4] J. Liu, Z. Zhou, M. Zhang, F. Song, C. Feng, H. Liu, Simple and robust 3D bioprinting of full-thickness human skin tissue, *Bioengineered* 13 (2022), <https://doi.org/10.1080/21655979.2022.2063651>.
- [5] A. Mörö, S. Samanta, L. Honkamäki, V.K. Rangasami, P. Puistola, M. Kauppila, S. Narkilähti, S. Miettinen, O. Oommen, H. Skottman, Hyaluronic acid based next generation bioink for 3D bioprinting of human stem cell derived corneal stromal model with innervation, *Biofabrication* 15 (2023), <https://doi.org/10.1088/1758-5090/acab34>.
- [6] N. Nie, L. Gong, D. Jiang, Y. Liu, J. Zhang, J. Xu, X. Yao, B. Wu, Y. Li, X. Zou, 3D bio-printed endometrial construct restores the full-thickness morphology and fertility of injured uterine endometrium, *Acta Biomater.* 157 (2023), <https://doi.org/10.1016/j.actbio.2022.12.016>.
- [7] L. Shen, Functional morphology of the gastrointestinal tract, *Curr. Top. Microbiol. Immunol.* 337 (2009), https://doi.org/10.1007/978-3-642-01846-6_1.
- [8] K.E. Barrett, Epithelial biology in the gastrointestinal system: insights into normal physiology and disease pathogenesis, *J. Physiol.* 590 (2012), <https://doi.org/10.1113/jphysiol.2011.227058>.
- [9] J. Burclaff, R.J. Bliton, K.A. Breaux, M.T. Ok, I. Gomez-Martinez, J.S. Ranek, A. P. Bhatt, J.E. Purvis, J.T. Woosley, S.T. Magness, A Proximal-To-Distal Survey of Healthy Adult Human Small Intestine and Colon Epithelium by Single-Cell Transcriptomics, *CMGH*, 13, 2022, <https://doi.org/10.1016/j.jcmgh.2022.02.007>.
- [10] N. Torras, J. Zabaló, E. Abril, A. Carré, M. García-Díaz, E. Martínez, A bioprinted 3D gut model with crypt-villus structures to mimic the intestinal epithelial-stromal microenvironment, *Biomater. Adv.* 153 (2023) 213534, <https://doi.org/10.1016/j.bioadv.2023.213534>.
- [11] R.L. Bacon, N.R. Niles, *Epithelium*, in: *Medical Histology*, Springer, New York, 1986, pp. 55–66, https://doi.org/10.1007/978-1-4613-8199-0_3.
- [12] K. Tröndle, L. Rizzo, R. Pichler, F. Koch, A. Itani, R. Zengerle, S.S. Lienkamp, P. Koltay, S. Zimmermann, Scalable fabrication of renal spheroids and nephron-like tubules by bioprinting and controlled self-assembly of epithelial cells, *Biofabrication* 13 (2021), <https://doi.org/10.1088/1758-5090/abe185>.
- [13] C.P. Jayapandian, Y. Chen, A.R. Janowczyk, M.B. Palmer, C.A. Cassol, M. Sekulic, J.B. Hodgins, J. Zee, S.M. Hewitt, J. O'Toole, P. Toro, J.R. Sedor, L. Barisoni, A. Madabhushi, K. Dell, M. Schachere, J. Negrey, K. Lemley, E. Lim, T. Srivastava, F. Kaskel, N. Sethna, K. Laurent, G. Appel, M. Toledo, L. Barisoni, L. Greenbaum, C. Wang, C. Kang, S. Adler, C. Nast, J. LaPage, J.H. Stroger, A. Athavale, M. Itteera, A. Neu, S. Boynton, F. Ferverza, M. Hogan, J. Lieske, V. Chernitskiy, F. Kaskel, N. Kumar, P. Flynn, J. Kopp, J. Blake, H. Trachtman, O. Zhdanova, F. Modersitzki, S. Vento, R. Lafayette, K. Mehta, C. Gadegebeku, D. Johnstone, S. Quinn-Boyle, D. Cattran, M. Hladunewich, H. Reich, P. Ling, M. Romano, A. Fornoni, C. Bidot, M. Kretzler, D. Gipson, A. Williams, J. LaVigne, V. Derebail, K. Gibson, A. Froment, S. Grubbs, L. Holzman, K. Meyers, K. Kalle, J. Lalli, K. Sambandam, Z. Wang, M. Rogers, A. Jefferson, S. Hingorani, K. Tuttle, M. Bray, M. Kelton, A. Cooper, B. Freedman, J.J. Lin, Development and evaluation of deep learning-based segmentation of histologic structures in the kidney cortex with multiple histologic stains, *Kidney Int.* 99 (2021), <https://doi.org/10.1016/j.kint.2020.07.044>.
- [14] N. Kia'i, T. Bajaj, *Histology, Respiratory Epithelium*, in: *StatPearls, StatPearls Publishing, Treasure Island (FL)*, 2023. PMID: 31082105.
- [15] J.A. Whitsett, T. Alenghat, Respiratory epithelial cells orchestrate pulmonary innate immunity, *Nat. Immunol.* 16 (2015), <https://doi.org/10.1038/ni.3045>.
- [16] E.H. Holbrook, E. Wu, W.T. Curry, D.T. Lin, J.E. Schwob, Immunohistochemical characterization of human olfactory tissue, *Laryngoscope* 121 (2011), <https://doi.org/10.1002/lary.21856>.
- [17] I. Deniz Derman, M. Yeo, D.C. Castaneda, M. Callender, M. Horvath, Z. Mo, R. Xiong, E. Fleming, P. Chen, M.E. Peebles, K. Palucka, J. Oh, I.T. Ozbolat, High-throughput bioprinting of the nasal epithelium using patient-derived nasal epithelial cells, *Biofabrication* 15 (2023) 044103, <https://doi.org/10.1088/1758-5090/acced23>.
- [18] N.E. Vrana, P. Lavalle, M.R. Dokmeci, F. Dehghani, A.M. Ghaemmaghami, A. Khademhosseini, Engineering functional epithelium for regenerative medicine and in vitro organ models: a review, *Tissue Eng Part B Rev* 19 (2013), <https://doi.org/10.1089/ten.teb.2012.0603>.
- [19] A.C. Paz, J. Soleas, J.C.H. Poon, D. Trieu, T.K. Waddell, A.P. McGuigan, Challenges and opportunities for tissue-engineering polarized epithelium, *Tissue Eng Part B Rev* 20 (2014), <https://doi.org/10.1089/ten.teb.2013.0144>.
- [20] A. Wanner, M. Salathe, T.G. O'Riordan, Mucociliary clearance in the airways, *Am. J. Respir. Crit. Care Med.* 154 (1996), <https://doi.org/10.1164/ajrccm.154.6.8970383>.
- [21] H. Cui, S. Miao, T. Esworthy, X. Zhou, S. Jun Lee, C. Liu, Z. xi Yu, J.P. Fisher, M. Mohiuddin, L.G. Zhang, 3D bioprinting for cardiovascular regeneration and pharmacology, *Adv. Drug Deliv. Rev.* 132 (2018), <https://doi.org/10.1016/j.addr.2018.07.014>.
- [22] C. Yu, W. Zhu, B. Sun, D. Mei, M. Gou, S. Chen, Modulating physical, chemical, and biological properties in 3D printing for tissue engineering applications, *Appl. Phys. Rev.* 5 (2018), <https://doi.org/10.1063/1.5050245>.
- [23] I.T. Ozbolat, M. Hospodiuk, Current advances and future perspectives in extrusion-based bioprinting, *Biomaterials* 76 (2016), <https://doi.org/10.1016/j.biomaterials.2015.10.076>.
- [24] W.L. Ng, V. Shkolnikov, Jetting-based bioprinting: process, dispense physics, and applications, *BioDes Manuf* (2024), <https://doi.org/10.1007/s42242-024-00285-3>.
- [25] W.L. Ng, J.M. Lee, M. Zhou, Y.W. Chen, K.X.A. Lee, W.Y. Yeong, Y.F. Shen, Vat polymerization-based bioprinting - process, materials, applications and regulatory challenges, *Biofabrication* 12 (2020), <https://doi.org/10.1088/1758-5090/ab6034>.
- [26] J. Karvinen, M. Kellomäki, Design aspects and characterization of hydrogel-based bioinks for extrusion-based bioprinting, *Bioprinting* 32 (2023), <https://doi.org/10.1016/j.bprint.2023.e00274>.
- [27] M.Z. Iqbal, M. Riaz, T. Biedermann, A.S. Klar, Breathing new life into tissue engineering: exploring cutting-edge vascularization strategies for skin substitutes, *Angiogenesis* (2024), <https://doi.org/10.1007/s10456-024-09928-6>.
- [28] S. Boularaoui, G. Al Hussein, K.A. Khan, N. Christoforou, C. Stefanini, An overview of extrusion-based bioprinting with a focus on induced shear stress and its effect on cell viability, *Bioprinting* 20 (2020), <https://doi.org/10.1016/j.bprint.2020.e00093>.
- [29] Z. Ataie, S. Kheirabadi, J.W. Zhang, A. Kedzierski, C. Petrosky, R. Jiang, C. Vollberg, A. Sheikhi, Nanoengineered granular hydrogel bioinks with

- preserved interconnected microporosity for extrusion bioprinting, *Small* 18 (2022), <https://doi.org/10.1002/smll.202202390>.
- [30] L. Ouyang, R. Yao, Y. Zhao, W. Sun, Effect of bioink properties on printability and cell viability for 3D bioplotting of embryonic stem cells, *Biofabrication* 8 (2016), <https://doi.org/10.1088/1758-5090/8/3/035020>.
- [31] A. Blaeser, D.F. Duarte Campos, U. Puster, W. Richtering, M.M. Stevens, H. Fischer, Controlling shear stress in 3D bioprinting is a key factor to balance printing resolution and stem cell integrity, *Adv. Healthcare Mater.* 5 (2016), <https://doi.org/10.1002/adhm.201500677>.
- [32] S. Emebu, R.O. Ogunleye, E. Achbergerová, L. Vítková, P. Ponížil, C.M. Martinez, Review and proposition for model-based multivariable-multiobjective optimisation of extrusion-based bioprinting, *Appl. Mater. Today* 34 (2023), <https://doi.org/10.1016/j.adma.2023.101914>.
- [33] P.A. Amorim, M.A. d'Ávila, R. Anand, P. Moldenaers, P. Van Puyvelde, V. Bloemen, Insights on shear rheology of inks for extrusion-based 3D bioprinting, *Bioprinting* 22 (2021), <https://doi.org/10.1016/j.bprint.2021.e00129>.
- [34] T. Schuller, P. Fanzio, F.J. Galindo-Rosales, Analysis of the importance of shear-induced elastic stresses in material extrusion, *Addit. Manuf.* 57 (2022), <https://doi.org/10.1016/j.addma.2022.102952>.
- [35] T. Schuller, M. Jalaal, P. Fanzio, F.J. Galindo-Rosales, *Optimal Shape Design of Printing Nozzles for Extrusion-Based Additive Manufacturing*, 2024.
- [36] Y. Wu, X. Yang, D. Gupta, M.A. Alioglu, M. Qin, V. Ozbolat, Y. Li, I.T. Ozbolat, Dissecting the interplay mechanism among process parameters toward the biofabrication of high-quality shapes in embedded bioprinting, *Adv. Funct. Mater.* 34 (2024), <https://doi.org/10.1002/adfm.202313088>.
- [37] L.G. Brunel, S.M. Hull, S.C. Heilshorn, Engineered assistive materials for 3D bioprinting: support baths and sacrificial inks, *Biofabrication* 14 (2022), <https://doi.org/10.1088/1758-5090/ac6bbe>.
- [38] E. Reina-Romo, S. Mandal, P. Amorim, V. Bloemen, E. Ferraris, L. Geris, Towards the experimentally-informed in silico nozzle design optimization for extrusion-based bioprinting of shear-thinning hydrogels, *Front. Bioeng. Biotechnol.* 9 (2021), <https://doi.org/10.3389/fbioe.2021.701778>.
- [39] S. Song, Y. Li, J. Huang, Z. Zhang, Development and characterization of complementary polymer network bioinks for 3D bioprinting of soft tissue constructs, *Macromol. Biosci.* 22 (2022), <https://doi.org/10.1002/mabi.202200181>.
- [40] L. Ouyang, C.B. Highley, C.B. Rodell, W. Sun, J.A. Burdick, 3D printing of shear-thinning hyaluronic acid hydrogels with secondary cross-linking, *ACS Biomater. Sci. Eng.* 2 (2016), <https://doi.org/10.1021/acsbiomaterials.6b00158>.
- [41] H. Gudapati, M. Dey, I. Ozbolat, A comprehensive review on droplet-based bioprinting: past, present and future, *Biomaterials* 102 (2016), <https://doi.org/10.1016/j.biomaterials.2016.06.012>.
- [42] K.W. Binder, A.J. Allen, J.J. Yoo, A. Atala, Drop-on-demand inkjet bioprinting: a primer, *Gene Ther. Regul.* 6 (2011), <https://doi.org/10.1142/S1568558611000258>.
- [43] C. Xu, M. Zhang, Y. Huang, A. Ogale, J. Fu, R.R. Markwald, Study of droplet formation process during drop-on-demand inkjetting of living cell-laden bioink, *Langmuir* 30 (2014), <https://doi.org/10.1021/la501430x>.
- [44] J. Adhikari, A. Roy, A. Das, M. Ghosh, S. Thomas, A. Sinha, J. Kim, P. Saha, Effects of processing parameters of 3D bioprinting on the cellular activity of bioinks, *Macromol. Biosci.* 21 (2021), <https://doi.org/10.1002/mabi.202000179>.
- [45] W. Meng, W. Zhihai, W. Can, W. Fei, C. Xi, Bioprinting: the influence of pneumatic microdrop-on-demand printing process on cell viability, in: *ACM International Conference Proceeding Series*, 2018, <https://doi.org/10.1145/3208955.3208963>.
- [46] W.L. Ng, X. Huang, V. Shkolnikov, R. Sutorrnmond, W.Y. Yeong, Polyvinylpyrrolidone-based bioink: influence of bioink properties on printing performance and cell proliferation during inkjet-based bioprinting, *Biodes Manuf* 6 (2023), <https://doi.org/10.1007/s42242-023-00245-3>.
- [47] W.L. Ng, X. Huang, V. Shkolnikov, G.L. Goh, R. Sutorrnmond, W.Y. Yeong, Controlling droplet impact velocity and droplet volume: key factors to achieving high cell viability in sub-nanoliter droplet-based bioprinting, *Int J Bioprint* 8 (2022), <https://doi.org/10.18063/IJB.V8I1.424>.
- [48] M. Nooranidoost, D. Izbassarov, S. Tasoglu, M. Muradoglu, A computational study of droplet-based bioprinting: effects of viscoelasticity, *Phys. Fluids* 31 (2019), <https://doi.org/10.1063/1.5108824>.
- [49] E. Brouzes, M. Medkova, N. Savenelli, D. Marran, M. Twardowski, J.B. Hutchison, J.M. Rothberg, D.R. Link, N. Perrimon, M.L. Samuels, Droplet microfluidic technology for single-cell high-throughput screening, *Proc. Natl. Acad. Sci. U.S.A.* 106 (2009), <https://doi.org/10.1073/pnas.0903542106>.
- [50] J. Hendriks, C. Willem Visser, S. Henke, J. Leijten, D.B.F. Saris, C. Sun, D. Lohse, M. Karperien, Optimizing cell viability in droplet-based cell deposition, *Sci. Rep.* 5 (2015), <https://doi.org/10.1038/srep11304>.
- [51] J. Chang, X. Sun, Laser-induced forward transfer based laser bioprinting in biomedical applications, *Front. Bioeng. Biotechnol.* 11 (2023), <https://doi.org/10.3389/fbioe.2023.1255782>.
- [52] S. Santoni, S.G. Gugliandolo, M. Sponchioni, D. Moscatelli, B.M. Colosimo, 3D bioprinting: current status and trends—a guide to the literature and industrial practice, *Biodes Manuf* 5 (2022), <https://doi.org/10.1007/s42242-021-00165-0>.
- [53] C. Mandrycky, Z. Wang, K. Kim, D.H. Kim, 3D bioprinting for engineering complex tissues, *Biotechnol. Adv.* 34 (2016) 422–434, <https://doi.org/10.1016/j.biotechadv.2015.12.011>.
- [54] O. Kérouédan, M. Rémy, H. Oliveira, F. Guillemot, R. Devillard, Laser-assisted bioprinting of cells for tissue engineering, in: *Laser Printing of Functional Materials*, 2018, <https://doi.org/10.1002/9783527805105.ch15>.
- [55] A. Zennifer, A. Subramanian, S. Sethuraman, Design considerations of bioinks for laser bioprinting technique towards tissue regenerative applications, *Bioprinting* 27 (2022), <https://doi.org/10.1016/j.bprint.2022.e00205>.
- [56] S. Chameettachal, S. Yeleswarapu, S. Sasikumar, P. Shukla, P. Hibare, A.K. Bera, S.S.R. Bojedla, F. Pati, 3D bioprinting: recent trends and challenges, *J. Indian Inst. Sci.* 99 (2019), <https://doi.org/10.1007/s41745-019-00113-z>.
- [57] A. Ovsianikov, M. Gruene, M. Pflaum, L. Koch, F. Maiorana, M. Wilhelm, A. Haverich, B. Chichkov, Laser printing of cells into 3D scaffolds, *Biofabrication* 2 (2010), <https://doi.org/10.1088/1758-5082/2/1/014104>.
- [58] P.N. Bernal, P. Delrot, D. Loterie, Y. Li, J. Malda, C. Moser, R. Levato, Volumetric bioprinting of complex living-tissue constructs within seconds, *Adv. Mater.* 31 (2019), <https://doi.org/10.1002/adma.201904209>.
- [59] Y. Wu, H. Su, M. Li, H. Xing, Digital light processing-based multi-material bioprinting: processes, applications, and perspectives, *J. Biomed. Mater. Res.* 111 (2023), <https://doi.org/10.1002/jbm.a.37473>.
- [60] R. Raman, R. Bashir, Stereolithographic 3D bioprinting for biomedical applications, in: *Essentials of 3D Biofabrication and Translation*, 2015, <https://doi.org/10.1016/B978-0-12-800972-7.00006-2>.
- [61] R. Levato, O. Dudaryeva, C.E. Garciamendez-Mijares, B.E. Kirkpatrick, R. Rizzo, J. Schimelman, K.S. Anseth, S. Chen, M. Zenobi-Wong, Y.S. Zhang, Light-based vat-polymerization bioprinting, *Nature Reviews Methods Primers* 3 (2023), <https://doi.org/10.1038/s43586-023-00231-0>.
- [62] Z. Zheng, D. Eglin, M. Alini, G.R. Richards, L. Qin, Y. Lai, Visible light-induced 3D bioprinting technologies and corresponding bioink materials for tissue engineering: a review, *Engineering* 7 (2021), <https://doi.org/10.1016/j.eng.2020.05.021>.
- [63] J. Zhang, Q. Hu, S. Wang, J. Tao, M. Gou, Digital light processing based three-dimensional printing for medical applications, *Int J Bioprint* 6 (2020), <https://doi.org/10.18063/ijb.v6i1.242>.
- [64] G. Lu, R. Tang, J. Nie, X. Zhu, Photocuring 3D printing of hydrogels: techniques, materials, and applications in tissue engineering and flexible devices, *Macromol. Rapid Commun.* 45 (2024), <https://doi.org/10.1002/marc.202300661>.
- [65] I. Chiulan, E.B. Heggset, Ş.I. Voicu, G. Chinga-Carrasco, Photopolymerization of bio-based polymers in a biomedical engineering perspective, *Biomacromolecules* 22 (2021), <https://doi.org/10.1021/acs.biomac.0c01745>.
- [66] G.C.J. Lindberg, K.S. Lim, B.G. Soliman, A. Nguyen, G.J. Hooper, R.J. Narayan, T. B.F. Woodfield, Biological function following radical photo-polymerization of biomedical polymers and surrounding tissues: design considerations and cellular risk factors, *Appl. Phys. Rev.* 8 (2021), <https://doi.org/10.1063/5.0015093>.
- [67] M.M. Stanford, *3D Printing with Photopolymerizable Polyester Resins for Resorbable Medical Device Applications*, Clemson University, 2023.
- [68] J.P. Fouassier, X. Allonas, J. Lalevéé, C. Dietlin, Photoinitiators for free radical polymerization reactions, in: *Photochemistry and Photophysics of Polymer Materials*, 2010, <https://doi.org/10.1002/9780470594179.ch10>.
- [69] A. Kowalska, J. Sokolowski, K. Bociog, The photoinitiators used in resin based dental composite—a review and future perspectives, *Polymers (Basel)* 13 (2021), <https://doi.org/10.3390/polym13030470>.
- [70] G. Burke, D.M. Devine, I. Major, Effect of stereolithography 3d printing on the properties of pgedma hydrogels, *Polymers (Basel)* 12 (2020), <https://doi.org/10.3390/polym12092015>.
- [71] J. Kiefer, Effects of ultraviolet radiation on DNA, in: *Chromosomal Alterations: Methods, Results and Importance in Human Health*, 2007, https://doi.org/10.1007/978-3-540-71414-9_3.
- [72] G.Y. Fraikin, N.S. Belenikina, A.B. Rubin, Photochemical processes of cell DNA damage by UV radiation of various wavelengths: biological consequences, *Mol. Biol.* 58 (2024), <https://doi.org/10.1134/S0026893324010047>.
- [73] K.S. Lim, B.J. Klotz, G.C.J. Lindberg, F.P.W. Melchels, G.J. Hooper, J. Malda, D. Gawliitta, T.B.F. Woodfield, Visible light cross-linking of gelatin hydrogels offers an enhanced cell microenvironment with improved light penetration depth, *Macromol. Biosci.* 19 (2019), <https://doi.org/10.1002/mabi.201900098>.
- [74] I. Mironi-Harpaz, D.Y. Wang, S. Venkatraman, D. Selihtar, Photopolymerization of cell-encapsulating hydrogels: crosslinking efficiency versus cytotoxicity, *Acta Biomater.* 8 (2012), <https://doi.org/10.1016/j.actbio.2011.12.034>.
- [75] X. Kuang, Q. Rong, S. Belal, T. Vu, A.M. López López, N. Wang, M.O. Arican, C. E. Garciamendez-Mijares, M. Chen, J. Yao, Y.S. Zhang, Self-enhancing sono-inks enable deep-penetration acoustic volumetric printing, *Science* 382 (2023), <https://doi.org/10.1126/science.ad1563> (1979).
- [76] C. Yu, J. Schimelman, P. Wang, K.L. Miller, X. Ma, S. You, J. Guan, B. Sun, W. Zhu, S. Chen, Photopolymerizable biomaterials and light-based 3D printing strategies for biomedical applications, *Chem. Rev.* 120 (2020), <https://doi.org/10.1021/acs.chemrev.9b00810>.
- [77] Q. Zhang, H.P. Bei, M. Zhao, Z. Dong, X. Zhao, Shedding light on 3D printing: printing photo-crosslinkable constructs for tissue engineering, *Biomaterials* 286 (2022), <https://doi.org/10.1016/j.biomaterials.2022.121566>.
- [78] S.M. King, S.C. Presnell, D.G. Nguyen, Abstract 2034: development of 3D bioprinted human breast cancer for in vitro drug screening, *Cancer Res.* 74 (2014), <https://doi.org/10.1158/1538-7445.am2014-2034>.
- [79] N.S. Bhise, V. Manoharan, S. Massa, A. Tamayol, M. Ghaderi, M. Miscuglio, Q. Lang, Y.S. Zhang, S.R. Shin, G. Calzone, N. Annabi, T.D. Shupe, C.E. Bishop, A. Atala, M.R. Dokmeci, A. Khademhosseini, A liver-on-a-chip platform with bioprinted hepatic spheroids, *Biofabrication* 8 (2016), <https://doi.org/10.1088/1758-5090/8/1/014101>.
- [80] J.E. Snyder, Q. Hamid, C. Wang, R. Chang, K. Emami, H. Wu, W. Sun, Bioprinting cell-laden matrigel for radioprotection study of liver by pro-drug conversion in a dual-tissue microfluidic chip, *Biofabrication* 3 (2011), <https://doi.org/10.1088/1758-5082/3/3/034112>.

- [81] T. Xu, J. Jin, C. Gregory, J.J. Hickman, T. Boland, Inkjet printing of viable mammalian cells, *Biomaterials* 26 (2005), <https://doi.org/10.1016/j.biomaterials.2004.04.011>.
- [82] R.E. Saunders, B. Derby, Inkjet printing biomaterials for tissue engineering: bioprinting, *Int. Mater. Rev.* 59 (2014), <https://doi.org/10.1179/1743280414Y.0000000040>.
- [83] J.I. Rodríguez-Dévara, B. Zhang, D. Reyna, Z.D. Shi, T. Xu, High throughput miniature drug-screening platform using bioprinting technology, *Biofabrication* 4 (2012), <https://doi.org/10.1088/1758-5082/4/3/035001>.
- [84] H. Yang, K.H. Yang, R.J. Narayan, S. Ma, Laser-based bioprinting for multilayer cell patterning in tissue engineering and cancer research, *Essays Biochem.* 65 (2021), <https://doi.org/10.1042/EBC20200093>.
- [85] I.T. Ozbolat, W. Peng, V. Ozbolat, Application areas of 3D bioprinting, *Drug Discov. Today* 21 (2016) 1257–1271, <https://doi.org/10.1016/j.drudis.2016.04.006>.
- [86] M. Wang, W. Li, L.S. Mille, T. Ching, Z. Luo, G. Tang, C.E. Garciamendez, A. Lesha, M. Hashimoto, Y.S. Zhang, Digital light processing based bioprinting with composable gradients, *Adv. Mater.* 34 (2022), <https://doi.org/10.1002/adma.202107038>.
- [87] D. Kang, Z. Liu, C. Qian, J. Huang, Y. Zhou, X. Mao, Q. Qu, B. Liu, J. Wang, Z. Hu, Y. Miao, 3D bioprinting of a gelatin-alginate hydrogel for tissue-engineered hair follicle regeneration, *Acta Biomater.* (2022), <https://doi.org/10.1016/j.actbio.2022.03.011>.
- [88] J.H. Park, J.K. Yoon, J.B. Lee, Y.M. Shin, K.W. Lee, S.W. Bae, J.H. Lee, J.J. Yu, C. R. Jung, Y.N. Youn, H.Y. Kim, D.H. Kim, Experimental tracheal replacement using 3-dimensional bioprinted artificial trachea with autologous epithelial cells and chondrocytes, *Sci. Rep.* 9 (2019) 2103, <https://doi.org/10.1038/s41598-019-38565-z>.
- [89] L. Horvath, Y. Umehara, C. Jud, F. Blank, A. Petri-Fink, B. Rothen-Rutishauser, Engineering an in vitro air-blood barrier by 3D bioprinting, *Sci. Rep.* 5 (2015) 7974, <https://doi.org/10.1038/srep07974>.
- [90] A. Sorkio, L. Koch, L. Koivusalo, A. Deiwick, S. Miittinen, B. Chichkov, H. Skottman, Human stem cell based corneal tissue mimicking structures using laser-assisted 3D bioprinting and functional bioinks, *Biomaterials* 171 (2018), <https://doi.org/10.1016/j.biomaterials.2018.04.034>.
- [91] J.M. Mullin, Epithelial barriers, compartmentation, and cancer, *Sci. STKE* 2004 (2004), <https://doi.org/10.1126/stke.2162004pe2>.
- [92] G.K. Kumaran, I. Hanukoglu, Identification and classification of epithelial cells in nephron segments by actin cytoskeleton patterns, *FEBS J.* 287 (2020), <https://doi.org/10.1111/febs.15088>.
- [93] K. Chopra, D. Calva, M. Sosin, K.K. Tadisina, A. Banda, C. De La Cruz, M. R. Chaudhry, T. Legesse, C.B. Drachenberg, P.N. Manson, M.R. Christy, A comprehensive examination of topographic thickness of skin in the human face, *Aesthetic Surg. J.* 35 (2015), <https://doi.org/10.1093/asj/sjv079>.
- [94] N. Ehlers, S. Heegaard, J. Hjortdal, A. Ivarsen, K. Nielsen, J.U. Prause, Morphological evaluation of normal human corneal epithelium, *Acta Ophthalmol.* 88 (2010), <https://doi.org/10.1111/j.1755-3768.2009.01610.x>.
- [95] T.R. Ruch, J.N. Engel, Targeting the mucosal barrier: how pathogens modulate the cellular polarity network, *Cold Spring Harbor Perspect. Biol.* 9 (2017), <https://doi.org/10.1101/cshperspect.a027953>.
- [96] M. Lee, V. Vasioukhin, Cell polarity and cancer - cell and tissue polarity as a non-canonical tumor suppressor, *J. Cell Sci.* 121 (2008), <https://doi.org/10.1242/jcs.016634>.
- [97] S. Eaton, K. Simons, Apical, basal, and lateral cues for epithelial polarization, *Cell* 82 (1995), [https://doi.org/10.1016/0092-8674\(95\)90045-4](https://doi.org/10.1016/0092-8674(95)90045-4).
- [98] M. Cerejido, R.G. Contreras, L. Shoshani, D. Flores-Benitez, I. Larre, Tight junction and polarity interaction in the transporting epithelial phenotype, *Biochim. Biophys. Acta Biomembr.* 1778 (2008), <https://doi.org/10.1016/j.bbmem.2007.09.001>.
- [99] H.-J. Merker, Morphology of the basement membrane, *Microsc. Res. Tech.* 28 (1994), <https://doi.org/10.1002/jemt.1070280203>.
- [100] Q. Wang, B. Margolis, Apical junctional complexes and cell polarity, *Kidney Int.* 72 (2007), <https://doi.org/10.1038/sj.ki.5002579>.
- [101] B. Schlingmann, S.A. Molina, M. Koval, Claudins: gatekeepers of lung epithelial function, *Semin. Cell Dev. Biol.* 42 (2015), <https://doi.org/10.1016/j.semcdb.2015.04.009>.
- [102] S. Mana-Capelli, D. McCollum, Angiotensin stimulate LATS kinase autophosphorylation and act as scaffolds that promote Hippo signaling, *J. Biol. Chem.* 293 (2018), <https://doi.org/10.1074/jbc.RA118.004187>.
- [103] W. Tang, M. Li, X. Yangzhong, X. Zhang, A. Zu, Y. Hou, L. Li, S. Sun, Hippo signaling pathway and respiratory diseases, *Cell Death Dis.* 8 (2022), <https://doi.org/10.1038/s41420-022-01020-6>.
- [104] F.X. Yu, B. Zhao, K.L. Guan, Hippo pathway in organ size control, tissue homeostasis, and cancer, *Cell* 163 (2015), <https://doi.org/10.1016/j.cell.2015.10.044>.
- [105] D. Wang, Y. Cong, Q. Deng, X. Han, S. Zhang, L. Zhao, Y. Luo, X. Zhang, Physiological and disease models of respiratory system based on organ-on-a-chip technology, *Micromachines (Basel)* 12 (2021), <https://doi.org/10.3390/mi12091106>.
- [106] M. Mukherjee, M.L. Latif, D.I. Pritchard, C. Bosquillon, In-cell WesternTM detection of organic cation transporters in bronchial epithelial cell layers cultured at an air-liquid interface on Transwell® inserts, *J. Pharmacol. Toxicol. Methods* 68 (2013), <https://doi.org/10.1016/j.vascn.2013.05.007>.
- [107] H. Lin, H. Li, H.J. Cho, S. Bian, H.J. Roh, M.K. Lee, S.K. Jung, S.J. Chung, C. K. Shim, D.D. Kim, Air-Liquid Interface (ALI) culture of human bronchial epithelial cell monolayers as an in vitro model for airway drug transport studies, *J. Pharmaceut. Sci.* 96 (2007), <https://doi.org/10.1002/jps.20803>.
- [108] L. Müller, L.E. Brighton, J.L. Carson, W.A. Fischer, I. Jaspers, Culturing of human nasal epithelial cells at the air liquid interface, *JoVE* 80 (2013) e50646, <https://doi.org/10.3791/50646>.
- [109] M. Chi, B. Yi, S. Oh, D.J. Park, J.H. Sung, S. Park, A microfluidic cell culture device (μFCCD) to culture epithelial cells with physiological and morphological properties that mimic those of the human intestine, *Biomed. Microdevices* 17 (2015), <https://doi.org/10.1007/s10544-015-9966-5>.
- [110] W. Yu, A. Datta, P. Leroy, L.E. O'Brien, G. Mak, T.S. Jou, K.S. Matlin, K.E. Mostov, M.M.P. Zegers, β1-integrin orients epithelial polarity via Rac1 and laminin, *Mol. Biol. Cell* 16 (2005), <https://doi.org/10.1091/mbc.E04-05-0435>.
- [111] N. Akhtar, C.H. Streuli, An integrin-ILK-microtubule network orients cell polarity and lumen formation in glandular epithelium, *Nat. Cell Biol.* 15 (2013), <https://doi.org/10.1038/ncb2646>.
- [112] C. Leung, S.J. Wadsworth, S. Jasmine Yang, D.R. Dorscheid, Structural and functional variations in human bronchial epithelial cells cultured in air-liquid interface using different growth media, *Am. J. Physiol. Lung Cell Mol. Physiol.* 318 (2020), <https://doi.org/10.1152/AJPLUNG.00190.2019>.
- [113] L.E. Cote, J.L. Feldman, Won't you be my neighbor: how epithelial cells connect together to build global tissue polarity, *Front. Cell Dev. Biol.* 10 (2022), <https://doi.org/10.3389/fcell.2022.887107>.
- [114] D. Fan, U. Stauffer, A. Accardo, Engineered 3d polymer and hydrogel microenvironments for cell culture applications, *Bioengineering* 6 (2019), <https://doi.org/10.3390/bioengineering6040113>.
- [115] S. Maji, H. Lee, Engineering hydrogels for the development of three-dimensional in vitro models, *Int. J. Mol. Sci.* 23 (2022), <https://doi.org/10.3390/ijms23052662>.
- [116] J. Park, J.E. Schwarzbauer, Mammary epithelial cell interactions with fibronectin stimulate epithelial-mesenchymal transition, *Oncogene* 33 (2014), <https://doi.org/10.1038/ncr.2013.118>.
- [117] I.C. Teller, J.F. Beaulieu, Interactions between laminin and epithelial cells in intestinal health and disease, *Expet Rev. Mol. Med.* 3 (2001), <https://doi.org/10.1017/S1462399401003623>.
- [118] M.A. Karasek, M.E. Charlton, Growth of postembryonic skin epithelial cells on collagen gels, *J. Invest. Dermatol.* 56 (1971), <https://doi.org/10.1111/1523-1747.ep12260838>.
- [119] T.R. Sodunke, K.K. Turner, S.A. Caldwell, K.W. McBride, M.J. Reginato, H. M. Noh, Micropatterns of Matrigel for three-dimensional epithelial cultures, *Biomaterials* 28 (2007), <https://doi.org/10.1016/j.biomaterials.2007.05.021>.
- [120] J. Temple, E. Velliou, M. Shehata, R. Lévy, Current strategies with implementation of three-dimensional cell culture: the challenge of quantification, *Interface Focus* 12 (2022), <https://doi.org/10.1098/rsfs.2022.0019>.
- [121] N. Davidenko, C.F. Schuster, D.V. Bax, N. Raynal, R.W. Farndale, S.M. Best, R. E. Cameron, Control of crosslinking for tailoring collagen-based scaffolds stability and mechanics, *Acta Biomater.* 25 (2015), <https://doi.org/10.1016/j.actbio.2015.07.034>.
- [122] K.L. Billiar, The mechanical environment of cells in collagen gel models: global and local effects in three-dimensional biological hydrogels, in: *Studies in Mechanobiology, Tissue Engineering and Biomaterials*, 2011, https://doi.org/10.1007/8415_2010_30.
- [123] T. Ozdemir, E.W. Fowler, S. Liu, D.A. Harrington, R.L. Witt, M.C. Farach-Carson, S. Pradhan-Bhatt, X. Jia, Tuning hydrogel properties to promote the assembly of salivary gland spheroids in 3D, *ACS Biomater. Sci. Eng.* 2 (2016), <https://doi.org/10.1021/acsbomaterials.6b00419>.
- [124] Q. Guo, B. Xia, S. Moshiah, C. Xu, Y. Jiang, Y. Chen, Y. Sun, J.M. Lahti, X. A. Zhang, The microenvironmental determinants for kidney epithelial cyst morphogenesis, *Eur. J. Cell Biol.* 87 (2008), <https://doi.org/10.1016/j.ejcb.2007.11.004>.
- [125] A. Jacinto, A. Martínez-Arias, P. Martín, Mechanisms of epithelial fusion and repair, *Nat. Cell Biol.* 3 (2001), <https://doi.org/10.1038/35074643>.
- [126] S.W. Kang, J. Mueller, Multiscale 3D printing via active nozzle size and shape control, *Sci. Adv.* 10 (2024), <https://doi.org/10.1126/sciadv.adn7772>.
- [127] D.E. Ingber, Human organs-on-chips for disease modelling, drug development and personalized medicine, *Nat. Rev. Genet.* 23 (2022), <https://doi.org/10.1038/s41576-022-00466-9>.
- [128] G. Urkasemsin, S. Rungarunlert, J.N. Ferreira, Bioprinting strategies for secretory epithelial organoids, in: *Methods in Molecular Biology*, 2020, https://doi.org/10.1007/978-1-0716-0520-2_16.
- [129] J.H. Park, M. Ahn, S.H. Park, H. Kim, M. Bae, W. Park, S.J. Hollister, S.W. Kim, D. W. Cho, 3D bioprinting of a trachea-mimetic cellular construct of a clinically relevant size, *Biomaterials* 279 (2021), <https://doi.org/10.1016/j.biomaterials.2021.121246>.
- [130] M. Torsello, A. Salvati, L. Borro, D. Meucci, M.L. Tropiano, F. Cialente, A. Secinaro, A. Del Fattore, C.M. Emiliana, P. Francalanci, G. Battafarano, I. Cacciotti, M. Trozzi, 3D bioprinting in airway reconstructive surgery: a pilot study, *Int. J. Pediatr. Otorhinolaryngol.* 161 (2022), <https://doi.org/10.1016/j.ijporl.2022.111253>.
- [131] J. Berg, Z. Weber, M. Fechner-Bitteti, A.C. Hocke, S. Hippenstiel, L. Elomaa, M. Weinhardt, J. Kurreck, Bioprinted multi-cell type lung model for the study of viral inhibitors, *Viruses* 13 (2021) 1590, <https://doi.org/10.3390/v13081590>.
- [132] M. Estermann, C. Bisig, D. Septiadi, A. Petri-Fink, B. Rothen-Rutishauser, Bioprinting for human respiratory and gastrointestinal in vitro models, in: *Methods in Molecular Biology*, 2020, https://doi.org/10.1007/978-1-0716-0520-2_13.

- [133] D.F. Duarte Campos, M. Rohde, M. Ross, P. Anvari, A. Blaeser, M. Vogt, C. Panfil, G.H.F. Yam, J.S. Mehta, H. Fischer, P. Walter, M. Fuest, Corneal bioprinting utilizing collagen-based bioinks and primary human keratocytes, *J. Biomed. Mater. Res.* 107 (2019), <https://doi.org/10.1002/jbm.a.36702>.
- [134] S.S. Mahdavi, M.J. Abdekhoodaie, H. Kumar, S. Mashayekhan, A. Baradaran-Rafii, K. Kim, Stereolithography 3D bioprinting method for fabrication of human corneal stroma equivalent, *Ann. Biomed. Eng.* 48 (2020), <https://doi.org/10.1007/s10439-020-02537-6>.
- [135] H. Kim, J. Jang, J. Park, K.P. Lee, S. Lee, D.M. Lee, K.H. Kim, H.K. Kim, D.W. Cho, Shear-induced alignment of collagen fibrils using 3D cell printing for corneal stroma tissue engineering, *Biofabrication* 11 (2019), <https://doi.org/10.1088/1758-5090/ab1a8b>.
- [136] L.J. Pourchet, A. Thepot, M. Albouy, E.J. Courtial, A. Boher, L.J. Blum, C. A. Marquette, Human skin 3D bioprinting using scaffold-free approach, *Adv. Healthcare Mater.* 6 (2017), <https://doi.org/10.1002/adhm.201601101>.
- [137] V. Lee, G. Singh, J.P. Trasatti, C. Bjornsson, X. Xu, T.N. Tran, S.S. Yoo, G. Dai, P. Karande, Design and fabrication of human skin by three-dimensional bioprinting, *Tissue Eng. C Methods* 20 (2014), <https://doi.org/10.1089/ten.tec.2013.0335>.
- [138] R. Jin, Y. Cui, H. Chen, Z. Zhang, T. Weng, S. Xia, M. Yu, W. Zhang, J. Shao, M. Yang, C. Han, X. Wang, Three-dimensional bioprinting of a full-thickness functional skin model using acellular dermal matrix and gelatin methacrylamide bioink, *Acta Biomater.* 131 (2021) 248–261, <https://doi.org/10.1016/j.actbio.2021.07.012>.
- [139] H. Nam, H.J. Jeong, Y. Jo, J.Y. Lee, D.H. Ha, J.H. Kim, J.H. Chung, Y.S. Cho, D. W. Cho, S.J. Lee, J. Jang, Multi-layered free-form 3D cell-printed tubular construct with decellularized inner and outer esophageal tissue-derived bioinks, *Sci. Rep.* 10 (2020), <https://doi.org/10.1038/s41598-020-64049-6>.
- [140] W. Farhat, D. Ayollo, L. Arakelian, B. Thierry, E. Mazari-Arighi, V. Caputo, L. Faivre, P. Cattani, J. Larghero, F. Chatelain, A. Fuchs, Biofabrication of an esophageal tissue construct from a polymer blend using 3D extrusion-based printing, *Adv. Eng. Mater.* (2022), <https://doi.org/10.1002/adem.202200096>.
- [141] W. Kim, G. Kim, Intestinal villi model with blood capillaries fabricated using collagen-based bioink and dual-cell-printing process, *ACS Appl. Mater. Interfaces* 10 (2018) 41185–41196, <https://doi.org/10.1021/acsami.8b17410>.
- [142] S. Xue, Y. Su, C. Xu, M. Xu, R. Yao, Heterogeneous liver tissues with multicellular stromal and bile duct morphogenesis through organoid bioprinting, *Research Square Platform LLC* (2023) 1–29, <https://doi.org/10.21203/rs.3.rs-2727920/v1>.
- [143] J.N. Ferreira, R. Hasan, G. Urkasemsin, K.K. Ng, C. Adine, S. Muthumariappan, G. R. Souza, A magnetic three-dimensional levitated primary cell culture system for the development of secretory salivary gland-like organoids, *J. Tissue Eng Regen Med* 13 (2019), <https://doi.org/10.1002/term.2809>.
- [144] Y. Yin, E.J. Vázquez-Rosado, D. Wu, V. Viswanathan, A. Farach, M.C. Farach-Carson, D.A. Harrington, Microfluidic coaxial 3D bioprinting of cell-laden microfibers and microtubes for salivary gland tissue engineering, *Biomater. Adv.* 154 (2023), <https://doi.org/10.1016/j.bioadv.2023.213588>.
- [145] J.A. Brassard, M. Nikolaev, T. Hübscher, M. Hofer, M.P. Lutolf, Recapitulating macro-scale tissue self-organization through organoid bioprinting, *Nat. Mater.* 20 (2021), <https://doi.org/10.1038/s41563-020-00803-5>.
- [146] T. Imamura, M. Shimamura, T. Ogawa, T. Minagawa, T. Nagai, S. Silwal Gautam, O. Ishizuka, Biofabricated structures reconstruct functional urinary bladders in radiation-injured rat bladders, *Tissue Eng.* 24 (2018), <https://doi.org/10.1089/ten.tea.2017.0533>.
- [147] S. Chae, J. Kim, H.G. Yi, D.W. Cho, 3D bioprinting of an in vitro model of a biomimetic urinary bladder with a contract-release system, *Micromachines* (Basel) 13 (2022), <https://doi.org/10.3390/mi13020277>.
- [148] K.A. Homan, D.B. Kolesky, J.A. Skylar-Scott, J. Herrmann, H. Obuobi, A. Moisan, J.A. Lewis, Bioprinting of 3D convoluted renal proximal tubules on perfusable chips, *Sci. Rep.* 6 (2016), <https://doi.org/10.1038/srep34845>.
- [149] N.K. Singh, W. Han, S.A. Nam, J.W. Kim, J.Y. Kim, Y.K. Kim, D.W. Cho, Three-dimensional cell-printing of advanced renal tubular tissue analogue, *Biomaterials* 232 (2020), <https://doi.org/10.1016/j.biomaterials.2019.119734>.
- [150] C. Hou, J. Zheng, Z. Li, X. Qi, Y. Tian, M. Zhang, J. Zhang, X. Huang, Printing 3D vagina tissue analogues with vagina decellularized extracellular matrix bioink, *Int. J. Biol. Macromol.* 180 (2021), <https://doi.org/10.1016/j.ijbiomac.2021.03.070>.
- [151] G.R. Souza, H. Tseng, J.A. Gage, A. Mani, P. Desai, F. Leonard, A. Liao, M. Longo, J.S. Refuerzo, B. Godin, Magnetically bioprinted human myometrial 3D cell rings as a model for uterine contractility, *Int. J. Mol. Sci.* 18 (2017), <https://doi.org/10.3390/ijms18040683>.
- [152] P.A. Mollica, E.N. Booth-Creech, J.A. Reid, M. Zamponi, S.M. Sullivan, X. L. Palmer, P.C. Sachs, R.D. Bruno, 3D bioprinted mammary organoids and tumoroids in human mammary derived ECM hydrogels, *Acta Biomater.* 95 (2019), <https://doi.org/10.1016/j.actbio.2019.06.017>.
- [153] S. Swaminathan, Q. Hamid, W. Sun, A.M. Clyne, Bioprinting of 3D breast epithelial spheroids for human cancer models, *Biofabrication* 11 (2019), <https://doi.org/10.1088/1758-5090/aaf49>.
- [154] L.M. Koskinen, L. Nieminen, A. Arjonen, C. Guzmán, M. Peurla, E. Peuhu, Spatial engineering of mammary epithelial cell cultures with 3D bioprinting reveals growth control by branch point proximity, *J. Mammary Gland Biol. Neoplasia* 29 (2024), <https://doi.org/10.1007/s10911-024-09557-1>.
- [155] B. Xie, B. Laxman, S. Hashemifar, R. Stern, T.C. Gilliam, N. Maltsev, S.R. White, Chemokine expression in the early response to injury in human airway epithelial cells, *PLoS One* 13 (2018), <https://doi.org/10.1371/journal.pone.0193334>.
- [156] A. Laitinen, L.A. Laitinen, Airway morphology: epithelium/basement membrane, *Am. J. Respir. Crit. Care Med.* (1994), https://doi.org/10.1164/ajrccm.150.5_pt_2.814.
- [157] M. Wu, X. Zhang, Y. Lin, Y. Zeng, Roles of airway basal stem cells in lung homeostasis and regenerative medicine, *Respir. Res.* 23 (2022), <https://doi.org/10.1186/s12931-022-02042-5>.
- [158] J.E. Boers, A.W. Ambergen, F.B.J.M. Thunnissen, Number and proliferation of basal and parabasal cells in normal human airway epithelium, *Am. J. Respir. Crit. Care Med.* 157 (1998), <https://doi.org/10.1164/ajrccm.157.6.9707011>.
- [159] Bijou Thomas, Ciliated Epithelium in Respiratory Diseases, Doctoral Dissertation, University of Leicester, 2011.
- [160] P.C. Avila, Plasticity of airway epithelial cells, *J. Allergy Clin. Immunol.* 128 (2011), <https://doi.org/10.1016/j.jaci.2011.10.006>.
- [161] D.F. Rogers, Airway goblet cells: responsive and adaptable frontline defenders, *Eur. Respir. J.* 7 (1994), <https://doi.org/10.1183/09031936.94.07091690>.
- [162] V. Cortez, S. Schultz-Cherry, The role of goblet cells in viral pathogenesis, *FEBS J.* 288 (2021), <https://doi.org/10.1111/febs.15731>.
- [163] C.G. Plopper, Comparative morphologic features of bronchiolar epithelial cells, in: *The Clara Cell, American Review of Respiratory Disease*, 128, 1983.
- [164] T. Kawai, S. Akira, The role of pattern-recognition receptors in innate immunity: update on toll-like receptors, *Nat. Immunol.* 11 (2010), <https://doi.org/10.1038/ni.1863>.
- [165] D. Li, M. Wu, Pattern recognition receptors in health and diseases, *Signal Transduct. Targeted Ther.* 6 (2021), <https://doi.org/10.1038/s41392-021-00687-0>.
- [166] M. Ball, M. Hossain, D. Padalia, *Anatomy Airway*, StatPearls Publishing, 2022.
- [167] Qutayba Hamid, Joanne Shannon, James Martin, Histology and gross anatomy of the respiratory tract, *Physiologic Basis of Respiratory*, [edited by] Qutayba Hamid, Joanne Shannon, James Martin. Published by Hamilton : BC Decker, Inc., (2005). pp 429-453.
- [168] S. Pai, V. Muruganandah, A. Kupz, What lies beneath the airway mucosal barrier? Throwing the spotlight on antigen-presenting cell function in the lower respiratory tract, *Clin Transl Immunology* 9 (2020), <https://doi.org/10.1002/cti2.1158>.
- [169] R.G. Crystal, S.H. Randell, J.F. Engelhardt, J. Voynov, M.E. Sunday, Airway epithelial cells: current concepts and challenges, *Proc. Am. Thorac. Soc.* (2008), <https://doi.org/10.1513/pats.200805-041HR>.
- [170] R.J. Hewitt, C.M. Lloyd, Regulation of immune responses by the airway epithelial cell landscape, *Nat. Rev. Immunol.* 21 (2021), <https://doi.org/10.1038/s41577-020-00477-9>.
- [171] J.D. Davis, T.P. Wypych, Cellular and functional heterogeneity of the airway epithelium, *Mucosal Immunol.* 14 (2021), <https://doi.org/10.1038/s41385-020-00370-7>.
- [172] M.C. McElroy, M. Kasper, The use of alveolar epithelial type I cell-selective markers to investigate lung injury and repair, *Eur. Respir. J.* 24 (2004), <https://doi.org/10.1183/09031936.04.00096003>.
- [173] D.L. Laskin, J.D. Laskin, Macrophages, inflammatory mediators, and lung injury, *Methods: A Companion to Methods in Enzymology* 10 (1996), <https://doi.org/10.1006/meth.1996.0079>.
- [174] M.F. Beers, Y. Moodley, When Is an alveolar type 2 cell an alveolar type 2 cell?: a conundrum for lung stem cell biology and regenerative medicine, *Am. J. Respir. Cell Mol. Biol.* 57 (2017), <https://doi.org/10.1165/rcmb.2016-0426PS>.
- [175] B. Ruardo, F. Salton, L. Braga, B. Wade, P. Confalonieri, M.C. Volpe, E. Barattella, S. Maiocchi, M. Confalonieri, The history and mystery of alveolar epithelial type ii cells: focus on their physiologic and pathologic role in lung, *Int. J. Mol. Sci.* 22 (2021), <https://doi.org/10.3390/ijms22052566>.
- [176] K. Shin, V.C. Fogg, B. Margolis, Tight junctions and cell polarity, *Annu. Rev. Cell Dev. Biol.* 22 (2006), <https://doi.org/10.1146/annurev.cellbio.22.010305.104219>.
- [177] A.V. Andreeva, M.A. Kutuzov, T.A. Voynov-Yasenetskaya, Regulation of surfactant secretion in alveolar type II cells, *Am. J. Physiol. Lung Cell Mol. Physiol.* 293 (2007), <https://doi.org/10.1152/ajplung.00112.2007>.
- [178] J.M. Lee, W.Y. Yeong, Design and printing strategies in 3D bioprinting of cell-hydrogels: a review, *Adv. Healthcare Mater.* 5 (2016), <https://doi.org/10.1002/adhm.201600435>.
- [179] S.A. Irvine, S.S. Venkatraman, Bioprinting and differentiation of stem cells, *Molecules* 21 (2016), <https://doi.org/10.3390/molecules21091188>.
- [180] M.M. De Santis, Next Generation Bioengineering of Lung Tissue for Transplantation, Lund University, Faculty of Medicine Doctoral Dissertation Series, Lund University, 2021. <https://portal.research.lu.se/en/publications/next-generation-bioengineering-of-lung-tissue-for-transplantation>. (Accessed 11 April 2024).
- [181] M. Barreiro Carpio, M. Dabaghi, J. Ungureanu, M.R. Kolb, J.A. Hirota, J. M. Moran-Mirabal, 3D bioprinting strategies, challenges, and opportunities to model the lung tissue microenvironment and its function, *Front. Bioeng. Biotechnol.* 9 (2021), <https://doi.org/10.3389/fbioe.2021.773511>.
- [182] B.A.G. de Melo, J.C. Benincasa, E.M. Cruz, J.T. Maricato, M.A. Porcionatto, 3D culture models to study SARS-CoV-2 infectivity and antiviral candidates: from spheroids to bioprinting, *Biomed. J.* 44 (2021), <https://doi.org/10.1016/j.bj.2020.11.009>.
- [183] J.Y. Park, H. Ryu, B. Lee, D.H. Ha, M. Ahn, S. Kim, J.Y. Kim, N.L. Jeon, D.W. Cho, Development of a functional airway-on-a-chip by 3D cell printing, *Biofabrication* 11 (2019), <https://doi.org/10.1088/1758-5090/aae545>.
- [184] S. Shakir, T.L. Hackett, L.B. Mostaço-Guidolin, Bioengineering lungs: an overview of current methods, requirements, and challenges for constructing scaffolds,

- Front. Bioeng. Biotechnol. 10 (2022), <https://doi.org/10.3389/fbioe.2022.1011800>.
- [185] J.F. Tomashefski, C.F. Farver, Anatomy and histology of the lung, in: Dail and Hammar's Pulmonary Pathology, 2008, https://doi.org/10.1007/978-0-387-68792-6_2.
- [186] N. Kanaji, M. Yokohira, Y. Nakano-Narusawa, N. Watanabe, K. Imaida, N. Kadowaki, S. Bandoh, Hepatocyte growth factor produced in lung fibroblasts enhances non-small cell lung cancer cell survival and tumor progression, *Respir. Res.* 18 (2017), <https://doi.org/10.1186/s12931-017-0604-z>.
- [187] R.A.M. Panganiban, R.M. Day, Hepatocyte growth factor in lung repair and pulmonary fibrosis, *Acta Pharmacol. Sin.* 32 (2011), <https://doi.org/10.1038/aps.2010.90>.
- [188] Y. Ito, K. Correll, J.A. Schiel, J.H. Finigan, R. Prekeris, R.J. Mason, Lung fibroblasts accelerate wound closure in human alveolar epithelial cells through hepatocyte growth factor/c-Met signaling, *Am. J. Physiol. Lung Cell Mol. Physiol.* 307 (2014), <https://doi.org/10.1152/ajplung.00233.2013>.
- [189] W.L. Ng, T.C. Ayi, Y.C. Liu, S.L. Sing, W.Y. Yeong, B.H. Tan, Fabrication and characterization of 3D bioprinted triple-layered human alveolar lung models, *Int J Bioprint* 7 (2021) 332, <https://doi.org/10.18063/ijb.v7i2.332>.
- [190] A.O. Eghrari, S.A. Riazuddin, J.D. Gottsch, Overview of the cornea: structure, function, and development, *Prog Mol Biol Transl Sci* (2015), <https://doi.org/10.1016/bs.pmbts.2015.04.001>.
- [191] H.S. Dua, D.G. Said, Ocular surface epithelium: applied anatomy, https://doi.org/10.1007/978-3-030-01304-2_12, 2019.
- [192] J.S. Ng, Adler's physiology of the eye, in: *Optometry and Vision Science*, eleventh ed., 89, 2012, <https://doi.org/10.1097/0px.0b013e318253c8a6>.
- [193] T.T. Sun, R.M. Lavker, Corneal epithelial stem cells: past, present, and future, in: *Journal of Investigative Dermatology Symposium Proceedings*, 2004, <https://doi.org/10.1111/j.1087-0024.2004.09311.x>.
- [194] Y. Sasamoto, B.R. Ksander, M.H. Frank, N.Y. Frank, Repairing the corneal epithelium using limbal stem cells or alternative cell-based therapies, *Expet Opin. Biol. Ther.* 18 (2018), <https://doi.org/10.1080/14712598.2018.1443442>.
- [195] T. Nakamura, T. Inatomi, C. Sotozono, N. Koizumi, S. Kinoshita, Ocular surface reconstruction using stem cell and tissue engineering, *Prog. Retin. Eye Res.* 51 (2016), <https://doi.org/10.1016/j.preteyeres.2015.07.003>.
- [196] Y. Feng, M. Borrelli, S. Reichl, S. Schrader, G. Geerling, Review of alternative carrier materials for ocular surface reconstruction, *Curr. Eye Res.* 39 (2014), <https://doi.org/10.3109/02713683.2013.853803>.
- [197] E.Yu Zernii, V.E. Baksheeva, E.V. Yani, P.P. Philippov, I.I. Senin, Therapeutic proteins for treatment of corneal epithelial defects, *Curr. Med. Chem.* 26 (2019), <https://doi.org/10.2174/0929867324666170609080920>.
- [198] Y. Zhang, Enhejirigala, B. Yao, Z. Li, W. Song, J. Li, D. Zhu, Y. Wang, X. Duan, X. Yuan, S. Huang, X. Fu, Using bioprinting and spheroid culture to create a skin model with sweat glands and hair follicles, *Burns Trauma* 9 (2021), <https://doi.org/10.1093/burnst/tkab013>.
- [199] J.Y. Kim, H. Dao, *Physiology, Integument*. In: *StatPearls*. StatPearls Publishing, Treasure Island (FL) (2023). PMID:32119273.
- [200] J.A. McGrath, J. Uitto, Anatomy and organization of human skin, in: *Rook's Textbook of Dermatology*, eighth ed., 2010, <https://doi.org/10.1002/9781444317633.ch3>.
- [201] P. He, J. Zhao, J. Zhang, B. Li, Z. Gou, M. Gou, X. Li, Bioprinting of skin constructs for wound healing, *Burns Trauma* 6 (2018), <https://doi.org/10.1186/s41038-017-0104-x>.
- [202] Y. Shi, T.L. Xing, H.B. Zhang, R.X. Yin, S.M. Yang, J. Wei, W.J. Zhang, Tyrosinase-derived bioink for 3D bioprinting of living skin constructs, *Biomed. Mater.* 13 (2018), <https://doi.org/10.1088/1748-605X/aaa5b6>.
- [203] N. Cubo, M. Garcia, J.F. Del Cañizo, D. Velasco, J.L. Jorcano, 3D bioprinting of functional human skin: production and in vivo analysis, *Biofabrication* 9 (2017), <https://doi.org/10.1088/1758-5090/9/1/015006>.
- [204] S.E. Millar, Molecular mechanisms regulating hair follicle development, *J. Invest. Dermatol.* 118 (2002), <https://doi.org/10.1046/j.0022-202x.2001.01670.x>.
- [205] G. Cotsarelis, Epithelial stem cells: a folliculocentric view, *J. Invest. Dermatol.* 126 (2006), <https://doi.org/10.1038/sj.jid.5700376>.
- [206] A. Madaan, R. Verma, A.T. Singh, M. Jaggi, Review of Hair Follicle Dermal Papilla cells as in vitro screening model for hair growth, *Int. J. Cosmet. Sci.* 40 (2018), <https://doi.org/10.1111/ics.12489>.
- [207] W.C. Weinberg, L.V. Goodman, C. George, D.L. Morgan, S. Ledbetter, S.H. Yuspa, U. Lichti, Reconstitution of hair follicle development in vivo: determination of follicle formation, hair growth, and hair quality by dermal cells, *J. Invest. Dermatol.* 100 (1993), <https://doi.org/10.1111/1523-1747.ep12468971>.
- [208] J. Lee, R. Böske, P.C. Tang, B.H. Hartman, S. Heller, K.R. Koehler, Hair follicle development in mouse pluripotent stem cell-derived skin organoids, *Cell Rep.* 22 (2018), <https://doi.org/10.1016/j.celrep.2017.12.007>.
- [209] H. Aoki, A. Hara, T. Motohashi, M. Osawa, T. Kunisada, Functionally distinct melanocyte populations revealed by reconstitution of hair follicles in mice, *Pigment Cell Melanoma Res* 24 (2011), <https://doi.org/10.1111/j.1755-148X.2010.00801.x>.
- [210] S.E. Xiao, Y. Miao, J. Wang, W. Jiang, Z.X. Fan, X.M. Liu, Z.Q. Hu, As a carrier-Transporter for hair follicle reconstitution, platelet-rich plasma promotes proliferation and induction of mouse dermal papilla cells, *Sci. Rep.* 7 (2017), <https://doi.org/10.1038/s41598-017-01105-8>.
- [211] H.E. Abaci, A. Coffman, Y. Doucet, J. Chen, J. Jacków, E. Wang, Z. Guo, J.U. Shin, C.A. Jahoda, A.M. Christiano, Tissue engineering of human hair follicles using a biomimetic developmental approach, *Nat. Commun.* 9 (2018), <https://doi.org/10.1038/s41467-018-07579-y>.
- [212] R. Wang, Y. Wang, B. Yao, T. Hu, Z. Li, Y. Liu, X. Cui, L. Cheng, W. Song, S. Huang, X. Fu, Redirecting differentiation of mammary progenitor cells by 3D bioprinted sweat gland microenvironment, *Burns Trauma* 7 (2019), <https://doi.org/10.1186/s41038-019-0167-y>.
- [213] H.N. Shi, W.A. Walker, Development and physiology of the intestinal mucosal defense, in: *Mucosal Immunology*, Fourth Edition, 2015, <https://doi.org/10.1016/B978-0-12-415847-4.00002-1>.
- [214] R.G. Carroll, *Elsevier's Integrated Physiology, Elsevier's Integrated Physiology*, 2007.
- [215] M. Gavaghan, Anatomy and physiology of the esophagus, *AORN J.* 69 (1999), [https://doi.org/10.1016/s0001-2092\(06\)62494-0](https://doi.org/10.1016/s0001-2092(06)62494-0).
- [216] B. Creamer, R.G. Shorter, J. Bamforth, The turnover and shedding of epithelial cells. I. The turnover in the gastro-intestinal tract, *Gut* 2 (1961), <https://doi.org/10.1136/gut.2.2.110>.
- [217] C. Günther, H. Neumann, M. Vieth, Esophageal epithelial resistance, *Dig. Dis.* 32 (2014), <https://doi.org/10.1159/000357001>.
- [218] J.P. Kraehenbuhl, E. Pringault, M.R. Neutra, Review article: intestinal epithelia and barrier functions, *Aliment Pharmacol. Therapeut.* 11 (1997), <https://doi.org/10.1111/j.1365-2036.1997.tb00803.x>. Supplement.
- [219] L.G. Van Der Flier, H. Clevers, Stem cells, self-renewal, and differentiation in the intestinal epithelium, *Annu. Rev. Physiol.* 71 (2009), <https://doi.org/10.1146/annurev.physiol.010908.163145>.
- [220] M. Bjerknes, H. Cheng, Intestinal epithelial stem cells and progenitors, in: *Methods Enzymol*, 2006, [https://doi.org/10.1016/S0076-6879\(06\)19014-X](https://doi.org/10.1016/S0076-6879(06)19014-X).
- [221] L.V. Hooper, Epithelial cell contributions to intestinal immunity, in: *Adv Immunol*, 2015, <https://doi.org/10.1016/bs.ai.2014.11.003>.
- [222] A. Iftekhar, M. Sigal, Defence and adaptation mechanisms of the intestinal epithelium upon infection, *International Journal of Medical Microbiology* 311 (2021), <https://doi.org/10.1016/j.ijmm.2021.151486>.
- [223] T. Agarwal, V. Onesto, L. Lamboni, A. Ansari, T.K. Maiti, P. Makvandi, M. Yosough, G. Yang, Engineering biomimetic intestinal topological features in 3D tissue models: retrospects and prospects, *Biodes Manuf* 4 (2021), <https://doi.org/10.1007/s42242-020-00120-5>.
- [224] B. Kuo, D. Urma, *Esophagus - anatomy and development* : GI Motility online, Nature Publishing Group (, 2006, <https://doi.org/10.1038/gim06>.
- [225] K.S. Vasanthan, V. Srinivasan, V. Mathur, P. Agarwal, N. Negi, S. Kumari, 3D Bioprinting for esophageal tissue regeneration: a review, *J. Mater. Res.* 37 (2022), <https://doi.org/10.1557/s43578-021-00409-w>.
- [226] Y. Takeoka, K. Matsumoto, D. Taniguchi, T. Tsuchiya, R. Machino, M. Moriyama, S. Oyama, T. Tetsuo, Y. Taura, K. Takagi, T. Yoshida, A. Elgalad, N. Matsuo, M. Kunizaki, S. Tobinaga, T. Nonaka, S. Hidaka, N. Yamasaki, K. Nakayama, T. Nagayasu, Regeneration of esophagus using a scaffoldfree biomimetic structure created with biothree- dimensional printing, *PLoS One* 14 (2019), <https://doi.org/10.1371/journal.pone.0211339>.
- [227] R.K. Buddington, V. Kuz'mina, *Digestive system, in: The Laboratory Fish*, Elsevier, 2000, pp. 379–384, <https://doi.org/10.1016/B978-012529650-2/50029-9>.
- [228] S. Kong, Y.H. Zhang, W. Zhang, Regulation of intestinal epithelial cells properties and functions by amino acids, *BioMed Res. Int.* 2018 (2018), <https://doi.org/10.1155/2018/2819154>.
- [229] V. Mahadevan, Anatomy of the stomach, *Surgery* 38 (2020), <https://doi.org/10.1016/j.mpsur.2020.08.005>.
- [230] W. Zhao, T. Xu, Preliminary engineering for in situ in vivo bioprinting: a novel micro bioprinting platform for in situ in vivo bioprinting at a gastric wound site, *Biofabrication* 12 (2020), <https://doi.org/10.1088/1758-5090/aba4ff>.
- [231] J.A. Brassard, M. Nikolaev, T. Hübscher, M. Hofer, M.P. Lutolf, Recapitulating macro-scale tissue self-organization through organoid bioprinting, *Nat. Mater.* 20 (2021), <https://doi.org/10.1038/s41563-020-00803-5>.
- [232] D.U. Silverthorn, *Human Physiology: an Integrated Approach*, 4 ed, 2009. Regulation.
- [233] S.M. Jandhyala, A. Madhulika, G. Deepika, G.V. Rao, D.N. Reddy, C. Subramanyam, M. Sasikala, R. Talukdar, Altered intestinal microbiota in patients with chronic pancreatitis: implications in diabetes and metabolic abnormalities, *Sci. Rep.* 7 (2017), <https://doi.org/10.1038/srep43640>.
- [234] F. Frost, T. Kacprowski, M. Rühlmann, R. Bülow, J.P. Kühn, A. Franke, F. A. Heinsen, M. Pietzner, M. Nauck, U. Völker, H. Völzke, A.A. Aghdassi, M. Sendler, J. Mayerle, F.U. Weiss, G. Homuth, M.M. Lerch, Impaired exocrine pancreatic function associates with changes in intestinal microbiota composition and diversity, *Gastroenterology* 156 (2019), <https://doi.org/10.1053/j.gastro.2018.10.047>.
- [235] J.F. Cryan, T.G. Dinan, Mind-altering microorganisms: the impact of the gut microbiota on brain and behaviour, *Nat. Rev. Neurosci.* 13 (2012), <https://doi.org/10.1038/nrn3346>.
- [236] F.A. Moore, E.E. Moore, R. Poggetti, O.J. McAnena, V.M. Peterson, C. M. Abernathy, P.E. Parsons, Gut bacterial translocation via the portal vein: a clinical perspective with major torso trauma, *J. Trauma Inj. Infect. Crit. Care* 31 (1991), <https://doi.org/10.1097/00005373-199105000-00006>.
- [237] L.Z. Benet, C.Y. Wu, M.F. Hebert, V.J. Wachter, Intestinal drug metabolism and antitransport processes: a potential paradigm shift in oral drug delivery, *J. Contr. Release* (1996), [https://doi.org/10.1016/0168-3659\(95\)00147-6](https://doi.org/10.1016/0168-3659(95)00147-6).
- [238] L.V. Hooper, A.J. MacPherson, Immune adaptations that maintain homeostasis with the intestinal microbiota, *Nat. Rev. Immunol.* 10 (2010), <https://doi.org/10.1038/nri2710>.
- [239] P. De Santa Barbara, G.R. Van Den Brink, D.J. Roberts, Development and differentiation of the intestinal epithelium, *Cell. Mol. Life Sci.* 60 (2003), <https://doi.org/10.1007/s00018-003-2289-3>.

- [240] J.M. Allaire, S.M. Crowley, H.T. Law, S.Y. Chang, H.J. Ko, B.A. Vallance, The intestinal epithelium: central coordinator of mucosal immunity, *Trends Immunol.* 39 (2018), <https://doi.org/10.1016/j.it.2018.04.002>.
- [241] P.R. Gibson, R.P. Anderson, J.M. Mariadason, A.J. Wilson, Protective role of the epithelium of the small intestine and colon, *Inflamm. Bowel Dis.* 2 (1996), <https://doi.org/10.1002/ibd.3780020412>.
- [242] I.H. Hundscheid, J. Grootjans, K. Lenaerts, D.H. Schellekens, J.P. Derikx, B. T. Boonen, M.F. Von Meyenfeldt, G.L. Beets, W.A. Buurman, C.H. Dejong, The human colon is more resistant to ischemia-reperfusion-induced tissue damage than the small intestine: an observational study, *Ann. Surg.* 262 (2015), <https://doi.org/10.1097/SLA.0000000000001131>.
- [243] L.R. Madden, T.V. Nguyen, S. Garcia-Mojica, V. Shah, A.V. Le, A. Peier, R. Visconti, E.M. Parker, S.C. Presnell, D.G. Nguyen, K.N. Retting, Bioprinted 3D primary human intestinal tissues model aspects of native physiology and ADME/toxic functions, *iScience* 2 (2018) 156–167, <https://doi.org/10.1016/j.isci.2018.03.015>.
- [244] W.J. Kim, G.H. Kim, An intestinal model with a finger-like villus structure fabricated using a bioprinting process and collagen/SIS-based cell-laden bioink, *Theranostics* 10 (2020) 2495, <https://doi.org/10.7150/tno.41225>.
- [245] H. Han, Y. Park, Y. mi Choi, U. Yong, B. Kang, W. Shin, S. Min, H.J. Kim, J. Jang, A bioprinted tubular intestine model using a colon-specific extracellular matrix bioink, *Adv. Healthcare Mater.* 11 (2022), <https://doi.org/10.1002/adhm.202101768>.
- [246] M.H. Macedo, N. Torras, M. García-Díaz, C. Barrias, B. Sarmento, E. Martínez, The shape of our gut: dissecting its impact on drug absorption in a 3D bioprinted intestinal model, *Biomater. Adv.* 153 (2023) 213564, <https://doi.org/10.1016/j.bioadv.2023.213564>.
- [247] L. Cheng, T. Liu, Q. Liu, L. Lian, G. Tang, L.S. Mille, F.R. García, L. Engstrand, Y. S. Zhang, J. Du, A 3D bioprinted gut anaerobic model for studying bacteria–host interactions, *Research* 6 (2023), <https://doi.org/10.34133/research.0058>.
- [248] Y. Li, S. Cheng, H. Shi, R. Yuan, C. Gao, Y. Wang, Z. Zhang, Z. Deng, J. Huang, 3D embedded bioprinting of large-scale intestine with complex structural organization and blood capillaries, *Biofabrication* 16 (2024) 045001, <https://doi.org/10.1088/1758-5090/ad5b1b>.
- [249] M. Strazzabosco, L. Fabris, Functional anatomy of normal bile ducts, *Anat. Rec.* 291 (2008), <https://doi.org/10.1002/ar.20664>.
- [250] A.L. Jones, D.L. Schmucker, R.H. Renston, T. Murakami, The architecture of bile secretion - a morphological perspective of physiology, *Dig. Dis. Sci.* 25 (1980), <https://doi.org/10.1007/BF01318875>.
- [251] M. Yan, P.L. Lewis, R.N. Shah, Tailoring nanostructure and bioactivity of 3D-printable hydrogels with self-assemble peptides amphiphile (PA) for promoting bile duct formation, *Biofabrication* 10 (2018), <https://doi.org/10.1088/1758-5090/aac902>.
- [252] C. Porcheri, T.A. Mitsiadis, Physiology, pathology and regeneration of salivary glands, *Cells* 8 (2019), <https://doi.org/10.3390/cells8090976>.
- [253] A. Famuyide, T.F. Massoud, G. Moonis, Oral cavity and salivary glands anatomy, *Neuroimaging Clin.* 32 (2022), <https://doi.org/10.1016/j.nic.2022.07.021>.
- [254] M.G. Ghannam, P. Singh, *Anatomy, Head, Neck, Salivary Glands.* In: *StatPearls.* StatPearls Publishing, Treasure Island (FL) (2023). PMID:30855909.
- [255] J.E. Beare, L. Curtis-Whitchurch, A.J. LeBlanc, J.B. Hoying, Microvasculature in health and disease, in: *Encyclopedia of Cardiovascular Research and Medicine*, 2017, <https://doi.org/10.1016/B978-0-12-809657-4.99820-X>.
- [256] C. Adine, K.K. Ng, S. Rungarunlert, G.R. Souza, J.N. Ferreira, Engineering innervated secretory epithelial organoids by magnetic three-dimensional bioprinting for stimulating epithelial growth in salivary glands, *Biomaterials* 180 (2018), <https://doi.org/10.1016/j.biomaterials.2018.06.011>.
- [257] A.M. Charbonneau, J.M. Kinsella, S.D. Tran, 3D cultures of salivary gland cells in native or gelled egg yolk plasma, combined with egg white and 3D-printing of gelled egg yolk plasma, *Materials* 12 (2019), <https://doi.org/10.3390/ma12213480>.
- [258] M.G. Dalghi, N. Montalbetti, M.D. Carattino, G. Apodaca, The urothelium: life in a liquid environment, *Physiol. Rev.* 100 (2020), <https://doi.org/10.1152/physrev.00041.2019>.
- [259] E.S. Shermadou, S.W. Leslie, *Anatomy, Abdomen and Pelvis, Bladder*, 2018.
- [260] M. Lazerri, The physiological function of the urothelium - more than a simple barrier, *Urol. Int.* 76 (2006), <https://doi.org/10.1159/000092049>.
- [261] R.T. Woodburne, Anatomy of the bladder and bladder outlet, *J. Urol.* 100 (1968), [https://doi.org/10.1016/S0022-5347\(17\)62556-4](https://doi.org/10.1016/S0022-5347(17)62556-4).
- [262] R.N. Miftahof, H.G. Nam, The bladder as a dynamic system, in: *Biomechanics of the Human Urinary Bladder*, Springer Berlin Heidelberg, Berlin, Heidelberg, 2013, pp. 1–23, https://doi.org/10.1007/978-3-642-36146-3_1.
- [263] L. Serex, K. Sharma, V. Rizov, A. Bertsch, J.D. McKinney, P. Renaud, Microfluidic-assisted bioprinting of tissues and organoids at high cell concentrations, *Biofabrication* 13 (2021), <https://doi.org/10.1088/1758-5090/abca80>.
- [264] G. Addario, S. Djudjaj, S. Farè, P. Boor, L. Moroni, C. Mota, Microfluidic bioprinting towards a renal in vitro model, *Bioprinting* 20 (2020), <https://doi.org/10.1016/j.bprint.2020.e01008>.
- [265] R. Pichler, L. Rizzo, K. Tröndle, M. Bühler, H. Brucker, A.L. Müller, K. Grand, S. Farè, A. Viau, M.M. Kaminski, E.W. Kuehn, F. Koch, S. Zimmermann, P. Koltay, S.S. Lienkamp, Tuning the 3D microenvironment of reprogrammed tubule cells enhances biomimetic modeling of polycystic kidney disease, *Biomaterials* 291 (2022), <https://doi.org/10.1016/j.biomaterials.2022.121910>.
- [266] Y.P. Jin, C. Shi, Y.Y. Wu, J.L. Sun, J.P. Gao, Y. Yang, Encapsulated three-dimensional bioprinted structure seeded with urothelial cells: a new construction technique for tissue-engineered urinary tract patch, *Chin Med J (Engl)* 133 (2020), <https://doi.org/10.1097/CM9.0000000000000654>.
- [267] S.R. Chowdhury, N. Keshavan, B. Basu, Urinary bladder and urethral tissue engineering, and 3D bioprinting approaches for urological reconstruction, *J. Mater. Res.* 36 (2021), <https://doi.org/10.1557/s43578-021-00255-w>.
- [268] D. Booter, R. Afshari, M. Ghovvati, K. Shariati, R. Sturm, N. Annabi, Advances in 3D bioprinting for urethral tissue reconstruction, *Trends Biotechnol.* (2023), <https://doi.org/10.1016/j.tibtech.2023.10.009>.
- [269] K. Zhang, Q. Fu, J. Yoo, X. Chen, P. Chandra, X. Mo, L. Song, A. Atala, W. Zhao, 3D bioprinting of urethra with PCL/PLCL blend and dual autologous cells in fibrin hydrogel: an in vitro evaluation of biomimetic mechanical property and cell growth environment, *Acta Biomater.* 50 (2017), <https://doi.org/10.1016/j.actbio.2016.12.008>.
- [270] Q. Pi, S. Maharjan, X. Yan, X. Liu, B. Singh, A.M. van Genderen, F. Robledo-Padilla, R. Parra-Saldivar, N. Hu, W. Jia, C. Xu, J. Kang, S. Hassan, H. Cheng, X. Hou, A. Khademhosseini, Y.S. Zhang, Digitally tunable microfluidic bioprinting of multilayered cannular tissues, *Adv. Mater.* 30 (2018), <https://doi.org/10.1002/adma.201706913>.
- [271] H.A. Adissu, E.K. Asem, S.A. Lelievre, Three-Dimensional cell culture to model epithelia in the female reproductive system, *Reprod. Sci.* 14 (2007), <https://doi.org/10.1177/1933719107310872>.
- [272] N. Callens, G. De Cuyper, P. De Sutter, S. Monstrey, S. Weyers, P. Hoebeke, M. Cools, An update on surgical and non-surgical treatments for vaginal hypoplasia, *Hum. Reprod. Update* 20 (2014), <https://doi.org/10.1093/humupd/dmu024>.
- [273] R.W. Cali, J.H. Pratt, Congenital absence of the vagina. Long-term results of vaginal reconstruction in 175 cases, *Am. J. Obstet. Gynecol.* 100 (1968), [https://doi.org/10.1016/S0002-9378\(15\)33575-4](https://doi.org/10.1016/S0002-9378(15)33575-4).
- [274] W. Ji, B. Hou, W. Lin, L. Wang, W. Zheng, W. Li, J. Zheng, X. Wen, P. He, 3D Bioprinting a human iPSC-derived MSC-loaded scaffold for repair of the uterine endometrium, *Acta Biomater.* 116 (2020), <https://doi.org/10.1016/j.actbio.2020.09.012>.
- [275] J.A. Reid, P.M. Mollica, R.D. Bruno, P.C. Sachs, Consistent and reproducible cultures of large-scale 3D mammary epithelial structures using an accessible bioprinting platform, *Breast Cancer Res.* 20 (2018), <https://doi.org/10.1186/s13058-018-1045-4>.
- [276] K.T. Lawlor, J.M. Vanslambrouck, J.W. Higgins, A. Chambon, K. Bishard, D. Arndt, P.X. Er, S.B. Wilson, S.E. Howden, K.S. Tan, F. Li, L.J. Hale, B. Shepherd, S. Pentoney, S.C. Presnell, A.E. Chen, M.H. Little, Cellular extrusion bioprinting improves kidney organoid reproducibility and conformation, *Nat. Mater.* 20 (2021), <https://doi.org/10.1038/s41563-020-00853-9>.
- [277] J. Shin, H. Chung, H. Kumar, K. Meadows, S. Park, J. Chun, K. Kim, 3D bioprinting of human iPSC-Derived kidney organoids using a low-cost, high-throughput customizable 3D bioprinting system, *Bioprinting* 38 (2024), <https://doi.org/10.1016/j.bprint.2024.e00337>.
- [278] F. Maiullari, M. Costantini, M. Milan, V. Pace, M. Chirivì, S. Maiullari, A. Rainer, D. Baci, H.E.S. Marei, D. Seliktar, C. Gargioli, C. Bearzi, R. Rizzi, A multi-cellular 3D bioprinting approach for vascularized heart tissue engineering based on HUVECs and iPSC-derived cardiomyocytes, *Sci. Rep.* 8 (2018), <https://doi.org/10.1038/s41598-018-31848-x>.
- [279] E. Schruf, V. Schroeder, H.Q. Le, T. Schönberger, D. Raedel, E.L. Stewart, K. Fundel-Clemens, T. Bluhmki, S. Weigle, M. Schuler, M.J. Thomas, R. Heilker, M.J. Webster, M. Dass, M. Frick, B. Stierstorfer, K. Quast, J.P. Garnett, Recapitulating idiopathic pulmonary fibrosis related alveolar epithelial dysfunction in a human iPSC-derived air-liquid interface model, *FASEB (Fed. Am. Soc. Exp. Biol.) J.* 34 (2020), <https://doi.org/10.1096/fj.201902926R>.
- [280] K.M. Abo, L. Ma, T. Matte, J. Huang, K.D. Alysandratos, R.B. Werder, A. Mithal, M. Lou Beermann, J. Lindstrom-Vautrin, G. Mostoslavsky, L. Ikonomou, D. N. Kotton, F. Hawkins, A. Wilson, C. Villacorta-Martin, Human iPSC-derived alveolar and airway epithelial cells can be cultured at air-liquid interface and express SARS-CoV-2 host factors, *bioRxiv* (2020), <https://doi.org/10.1101/2020.06.03.132639>.
- [281] M. Ikeda, M. Imaizumi, S. Yoshie, R. Nakamura, K. Otsuki, S. Murono, K. Omori, Implantation of induced pluripotent stem cell-derived tracheal epithelial cells, *Annals of Otolaryngology and Laryngology* 126 (2017), <https://doi.org/10.1177/0003489417713504>.
- [282] J.P. Gleeson, H.Q. Estrada, M. Yamashita, C.N. Svendsen, S.R. Targan, R. J. Barrett, Development of physiologically responsive human iPSC-derived intestinal epithelium to study barrier dysfunction in IBD, *Int. J. Mol. Sci.* 21 (2020), <https://doi.org/10.3390/ijms21041438>.
- [283] K. Takayama, R. Negoro, T. Yamashita, K. Kawai, M. Ichikawa, T. Mori, N. Nakatsu, K. Harada, S. Ito, H. Yamada, Y. Yamaura, K. Hirata, S. Ishida, H. Mizuguchi, Generation of human iPSC-derived intestinal epithelial cell monolayers by CDX2 transduction, *CM* 8 (2019), <https://doi.org/10.1016/j.jcmgh.2019.06.004>.
- [284] D. Henriques, R. Moreira, J. Schwamborn, L. Pereira de Almeida, L.S. Mendonça, Successes and hurdles in stem cells application and production for brain transplantation, *Front. Neurosci.* 13 (2019), <https://doi.org/10.3389/fnins.2019.01194>.
- [285] Z.R. Lim, S. Vassilev, Y.W. Leong, J.W. Hang, L. Rénia, B. Malleret, S.K.W. Oh, Industrially compatible transfusable iPSC-derived RBCs: progress, challenges and prospective solutions, *Int. J. Mol. Sci.* 22 (2021), <https://doi.org/10.3390/ijms22189808>.
- [286] X. Hu, K. White, A.G. Olroyd, R. DeJesus, A.A. Dominguez, W.E. Dowdle, A. M. Friera, C. Young, F. Wells, E.Y. Chu, C.E. Ito, H. Krishnapura, S. Jain, R. Ankala, T.J. McGill, A. Lin, K. Egenberger, A. Gagnon, J. Michael Rukstalis, N. J. Hogrebe, C. Gattis, R. Basco, J.R. Millman, P. Kievit, M.M. Davis, L.L. Lanier, A. J. Connolly, T. Deuse, S. Schrepfer, Hypoimmune induced pluripotent stem cells

- survive long term in fully immunocompetent, allogeneic rhesus macaques, *Nat. Biotechnol.* 42 (2024), <https://doi.org/10.1038/s41587-023-01784-x>.
- [287] L. Tytgat, A. Dobos, M. Markovic, L. Van Damme, J. Van Hoorick, F. Bray, H. Thienpont, H. Ottevaere, P. Dubruel, A. Ovsianikov, S. Van Vlierberghe, High-resolution 3D bioprinting of photo-cross-linkable recombinant collagen to serve tissue engineering applications, *Biomacromolecules* 21 (2020), <https://doi.org/10.1021/acs.biomac.0c00386>.
- [288] B. Ayan, D.N. Heo, Z. Zhang, M. Dey, A. Povilianskas, C. Drapaca, I.T. Ozbolat, Aspiration-assisted bioprinting for precise positioning of biologics, *Sci. Adv.* 6 (2020) eaaw5111, <https://doi.org/10.1126/sciadv.aaw5111>.
- [289] J.G. Roth, L.G. Brunel, M.S. Huang, Y. Liu, B. Cai, S. Sinha, F. Yang, S.P. Paçca, S. Shin, S.C. Heilshorn, Spatially controlled construction of assembloids using bioprinting, *Nat. Commun.* 14 (2023), <https://doi.org/10.1038/s41467-023-40006-5>.
- [290] L. Rico-Sánchez, I. Garzón, M. González-Andrades, A. Ruíz-García, M. Punzano, A. Lizana-Moreno, J.I. Muñoz-Ávila, M. del C. Sánchez-Quevedo, J. Martínez-Atienza, L. Lopez-Navas, R. Sanchez-Pernaute, R.I. Oruezabal, S. Medialdea, M. del C. Gonzalez-Gallardo, G. Carmona, S. Sanbonmatsu-Gámez, M. Perez, P. Jimenez, N. Cuende, A. Campos, M. Alaminos, Successful development and clinical translation of a novel anterior lamellar artificial cornea, *J Tissue Eng Regen Med* 13 (2019), <https://doi.org/10.1002/term.2951>.
- [291] Y. Wu, D.J. Ravnic, I.T. Ozbolat, Intraoperative bioprinting: repairing tissues and organs in a surgical setting, *Trends Biotechnol.* 38 (2020), <https://doi.org/10.1016/j.tibtech.2020.01.004>.
- [292] K. Belsky, J. Smiell, Navigating the regulatory pathways and requirements for tissue-engineered products in the treatment of burns in the United States, *J. Burn Care Res.* 42 (2021), <https://doi.org/10.1093/jbcr/iraa210>.
- [293] J.M. Bliley, D.J. Shiwarski, A.W. Feinberg, 3D-bioprinted human tissue and the path toward clinical translation, *Sci. Transl. Med.* 14 (2022), <https://doi.org/10.1126/scitranslmed.abo7047>.
- [294] C.D. O'Connell, P.D. Dalton, D.W. Hutmacher, Why bioprinting in regenerative medicine should adopt a rational technology readiness assessment, *Trends Biotechnol.* (2024), <https://doi.org/10.1016/j.tibtech.2024.03.006>.